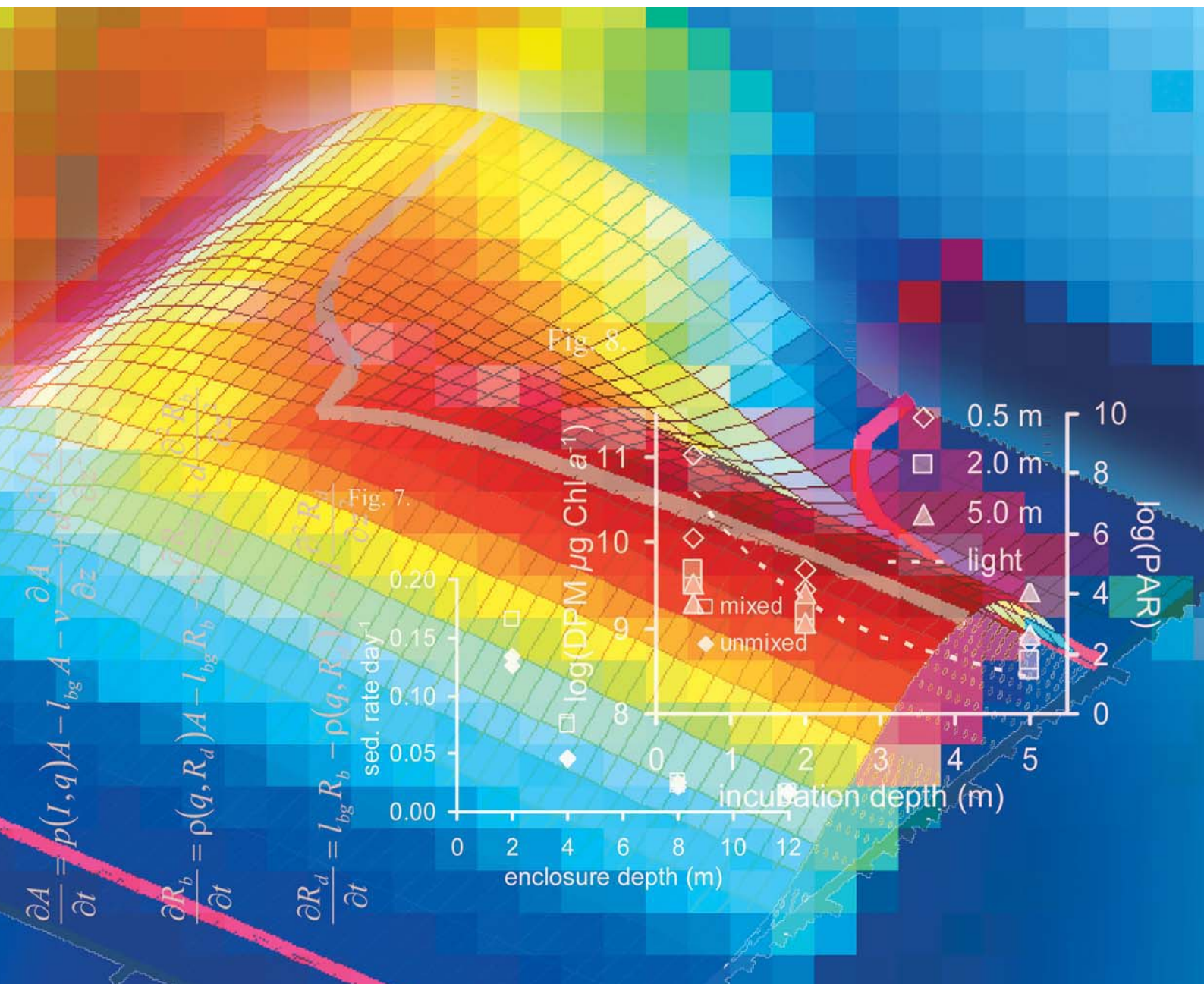


The influence of light, nutrients and mixing on pelagic communities and ecosystem dynamics

Christoph G. Jäger

Dissertation zur Erlangung des Doktorgrades
 an der Fakultät für Biologie der Ludwig-Maximilians-Universität München
 April 2008



Erstgutachter: Prof. Dr. Sebastian Diehl

Zweitgutachter: Prof. Dr. Wilfried Gabriel

Tag der mündlichen Prüfung: 14.07.2008

Erklärung

Diese Promotion wurde im Sinne § 12 der Promotionsordnung von Prof. Dr. Sebastian Diehl betreut. Ich erkläre hiermit, dass die Dissertation keiner anderen Prüfungskommission vorgelegt worden ist, und dass ich mich nicht anderweitig einer Doktorprüfung ohne Erfolg unterzogen habe.

Ehrenwörtliche Versicherung

Ich versichere hiermit, dass die vorgelegte Dissertation von mir selbstständig, ohne unerlaubte Hilfe angefertigt wurde.

München, den 29.04.2008

Christoph Jäger

Beitrag der Koautoren und eigener Beitrag:

Kapitel 1 bis 3 bilden den Kern meiner Dissertation. Hier beschreibe ich den Beitrag der Koautoren. An Kapitel 4 habe ich nur eine beitragende Rolle gespielt. Hier beschreibe ich meinen eigenen Beitrag.

Kapitel 1:

Maximilian Emans war mir bei der Programmierung von COMSOL und bei der Lösung numerischer Probleme behilflich.

Kapitel 2:

Gertraud Schmidt war als Diplomandin an der Durchführung des Freilandversuchs beteiligt und half beim Auszählen der Phytoplanktonproben.

Kapitel 3:

Christian Matauschek war als Diplomand an der Durchführung des Freilandversuchs beteiligt und half beim Auszählen der Phytoplanktonproben. Chris Klausmeier schlug den Vergleich der numerischen Simulationen mit ‚analytical correlates‘ vor (Appendix C und D). Herwig Stibor leistete Betreuungsarbeit während der experimentellen Phase des Projektes.

Kapitel 4:

Ich half bei Aufbau und Durchführung des Freilandversuchs, beriet die beteiligten Diplomandinnen bei den Auswertungen der Proben und war an der Diskussion der Daten beteiligt.

Sebastian Diehl unterstützte mich bei der Konzipierung der Studien und beim Schreiben der Kapitel 1 bis 3.

Contents

Contents.....	02
Zusammenfassung.....	03
Summary.....	05
General Introduction.....	07
Chapter 1:	
Physical determinants of phytoplankton production, algal stoichiometry, and vertical nutrient fluxes.....	12
Chapter 2:	
Influence of water column depth and mixing on phytoplankton biomass, community composition, and nutrients.....	37
Chapter 3:	
Transient dynamics of pelagic producer-grazer systems in a gradient of nutrients and mixing depths.....	60
Chapter 4:	
Water temperature and mixing depth affect timing and magnitude of events during spring succession of the plankton.....	93
General Discussion and Research Outlook.....	109
References.....	113
Danksagung.....	122
Curriculum Vitae.....	123

Zusammenfassung

Phototrophe Primärproduzenten benötigen zwei unterschiedliche Arten von essentiellen Ressourcen: Licht und Nährstoffe. Die Verfügbarkeit dieser Ressourcen für pelagische Produzenten ist stark von Umweltfaktoren beeinflusst, wie z.B. Nährstoffangebot, Wassertrübe, Tiefe der durchmischten Wassersäule und Durchmischungsintensität. Die Tiefe der durchmischten Wassersäule und deren Durchmischungsintensität beeinflussen vor allem das relative Angebot an Licht und Nährstoffen und dadurch die Produktion der Algen und deren Bindung von Kohlenstoff und Nährstoffen, was die Kohlenstoff-zu-Nährstoff-Stöchiometrie der Algenbiomasse bestimmt. Die Biomasse und Stöchiometrie der Algen bestimmen wiederum deren Futterquantität und -qualität für Grazer. Weiterhin beeinflussen die Tiefe einer Wassersäule und deren Durchmischungsintensität auch die Sedimentationsverluste, da die meisten Algentaxa zum Aussinken tendieren. In dieser Dissertation untersuchte ich verschiedene Aspekte des Einflusses von Umweltfaktoren auf pelagische Gemeinschaften, mit einem Schwerpunkt auf der Rolle von Wassersäulentiefe und Durchmischungsintensität.

In Kapitel 1, untersuchte ich die interaktiven Effekte der Tiefe einer Wassersäule und ihrer Durchmischungsintensität auf die Biomasse und auf die vertikale Verteilung einer Population sinkender Algen mit einer flexiblen Kohlenstoff-zu-Nährstoff-Stöchiometrie. Dies geschah anhand eines Modells, das die zeitliche und räumliche Dynamik von Licht, gelösten und sedimentierten Nährstoffen, Produktion und Sedimentation des Phytoplanktons und der Biomasse und Stöchiometrie der Algen beschreibt. Es zeigte sich, dass die Gesamtbioasse in einer Wassersäule von drei Prozessen limitiert werden kann: Der vertikalen Lichtattenuation, Sedimentationsverlusten und dem Recycling aussinkender Nährstoffe. In sehr flachen Wassersäulen wird die Algenbiomasse bei allen Durchmischungsintensitäten durch Sedimentationsverluste stark limitiert. Im Gegensatz dazu ist es in tiefen Wassersäulen von der Durchmischungsintensität abhängig welcher Faktor limitierend ist. Bei starker Turbulenz ist Licht limitierend, bei schwacher Turbulenz hingegen wird die Algenbiomasse durch einen geringen Nährstofftransport vom Sediment zur Oberfläche limitiert. Die höchste Gesamtbioasse kann folglich in tiefen Wassersäulen bei mittlerer Turbulenzstärke erreicht werden, in denen weder Sinkverluste noch Licht und Nährstoffe stark limitierend sind.

In Kapitel 2 beschreibe ich ein Freiland-Enclosure-Experiment, in dem in einem faktoriellen Design vier unterschiedliche Enclosurestiefen (2, 4, 8 und 12 m) mit zwei Durchmischungsintensitäten (starke künstliche Durchmischung, Hintergrundturbulenz) gekreuzt wurden. Nach einer anfänglichen Phosphordüngung zeigte das Phytoplankton ein vorübergehendes Maximum und eine Änderung der Artenzusammensetzung, mit einer ansteigenden Dominanz pennaler Diatomeen in den voll durchmischten Enclosures und einer Dominanz beweglicher Arten (Flagellaten) in den Enclosures mit schwacher Durchmischung. In den Enclosures mit schwacher Durchmischung entwickelten sich vertikale Gradienten der Algenbiomasse und der gelösten mineralischen Nährstoffe bei einer Enclosurestiefe von mehr als 4 m. Die Diversität war in den voll durchmischten Enclosures niedriger als in den schwach durchmischten, was auf eine mögliche vertikale Nischendifferenzierung bei schwacher Durchmischung hindeutet. Diese Hypothese wird durch eine Primärproduktionsmessung unterstützt, bei der Phytoplanktongemeinschaften verschiedener Herkunftstiefen aus den schwach durchmischten Enclosures jeweils dann die relativ höchste Produktion zeigten, wenn sie in ihrer Herkunftstiefe inkubiert wurden.

In Kapitel 3 untersuchte ich den Einfluss von Nährstoffangebot und Wassersäulentiefe (bei homogener Durchmischung) auf die transiente Dynamik von pelagischen Produzenten-Konsumenten Systemen anhand von Modellanalysen und eines Freiland-Enclosure-Experiments. Im Modell, das für Grazer der Gattung *Daphnia* parametrisiert wurde, ist die Kopplung zwischen der Algen- und der Grazerdynamik bei mittleren Wassersäulentiefen am stärksten, d.h. die Periode der entstehenden Algen-Grazer Oszillationen ist am kürzesten und ihre Amplitude am höchsten. Diese Kopplung ist bei geringen Wassersäulentiefen aufgrund einer geringeren Futterqualität (= geringer Nährstoffgehalt der Algen) und bei großen Wassersäulentiefen aufgrund einer geringeren Primärproduktion weniger stark. Eine Nährstoffanreicherung verbessert die Futterqualität der Algen und verstärkt somit die Kopplung bei geringen bis mittleren Wassersäulentiefen, nicht aber in großen Wassersäulentiefen, in denen die Algenproduktion stark lichtlimitiert ist. Diese Vorhersagen verglich ich mit den Ergebnissen des Freilandexperiments, in dem ich das Nährstoffangebot (im Bereich von 10-60 μg Gesamtphosphor L^{-1}) und die Wassersäulentiefe (1, 3, 6 und 12 m) einer natürlichen Phytoplanktongemeinschaft bei Anwesenheit von *Daphnia hyalina* unabhängig voneinander manipulierte. Dabei stimmten die Ergebnisse qualitativ mit den meisten Erwartungen aus dem Modell gut überein.

In beschreibenden Datensätzen sind Schichtungstiefe und Oberflächentemperatur von Seen im Allgemeinen invers miteinander korreliert. Kapitel 4 beschreibt ein Freilandexperiment, in dem die Effekte dieser beiden Faktoren auf Höhe und Zeitpunkt verschiedener Ereignisse der Frühjarssukzession des Planktons (d.h. Phytoplanktonblüte, Maximum der Grazerdichte und Klarwasserstadium) untersucht wurden. Die unabhängige Manipulation von Wassersäulentiefe und Wassertemperatur ergab, dass eine tiefere Durchmischung die Geschwindigkeit der Sukzessionsabfolge verlangsamte und die Höhe der Phytoplanktonblüte und des folgenden Grazermaximums reduzierte. Tiefere Temperaturen verzögerten das Klarwasserstadium und das folgende Grazermaximum, wohingegen der Zeitpunkt der Phytoplanktonblüte nicht durch die Temperatur beeinflusst wurde.

Summary

Phototrophic primary producers need two different kinds of essential resources: light and nutrients. The availability of these resources for pelagic producers is highly influenced by environmental factors such as nutrient supply, water turbidity, the depth of the mixed water column, and mixing intensity. Water column depth and mixing intensity, in particular, influence the relative supply with light and nutrients, and, consequently, algal production and their sequestration of carbon and nutrients, affecting algal biomass and carbon to nutrient stoichiometry. Algal biomass and stoichiometry, in turn, determine food quantity and quality for grazers. Because most algal taxa tend to sink, the depth of a water column and the intensity of its mixing also affect sedimentation losses. In this thesis I have investigated the influence of the physical environment on pelagic community and ecosystem dynamics, with an emphasis on the roles of water column depth and mixing intensity.

In chapter 1 I used a model which describes the temporal and spatial dynamics of light, dissolved and sedimented nutrients, algal production and sedimentation, and algal biomass and carbon to nutrient stoichiometry to theoretically investigate the interactive effects of the depth of a water column and the intensity of its mixing on the biomass and vertical distribution of a population of sinking algae with a flexible carbon to nutrient stoichiometry. In the model total water column biomass is limited by three processes: vertical light attenuation, sedimentation losses, and nutrient recycling from sinking algae. In very shallow water columns, algal biomass is always strongly limited by sedimentation losses. In contrast, in deep water columns the limiting factor depends on turbulence, with light being most strongly limiting at high and nutrient transport being most strongly limiting at low turbulences. Consequently, the highest depth-integrated biomasses are attained in deep water columns at intermediate turbulences, where none of sinking, light attenuation, and nutrient recycling is particularly strongly limiting.

In chapter 2 I examined the effects of water column depth and mixing intensity on a natural lake phytoplankton community in a field enclosure experiment. I crossed four different water column depths (2, 4, 8, and 12 m) with two mixing intensities (strong artificial mixing vs. background turbulence) in a factorial design. After an initial phosphorus pulse, phytoplankton went through a transient peak and a change in species composition, with an increasing dominance of pennate diatoms in well-mixed enclosures and a dominance of motile taxa (flagellates) in low turbulence enclosures. Low turbulence enclosures developed opposite vertical gradients in algal biomass (highest near the surface) and dissolved mineral nutrients (highest near the bottom) in water columns > 4 m. Diversity was lower in mixed than in low turbulence enclosures, suggesting vertical niche partitioning at low turbulence. The latter hypothesis was supported by a primary production assay in low turbulence treatments, in which phytoplankton originating from different water depths had the relatively highest primary productivity when incubated at their respective depths of origin.

In chapter 3 I examined the effects of nutrient supply and water column depth in perfectly well-mixed systems on the transient dynamics of a pelagic producer-grazer system starting from low initial population densities, such as at the end of winter in temperate lakes. I adopted a combined approach using model analyses and a field enclosure experiment. In the model system, which was parameterized for a grazer of the genus *Daphnia*, the coupling between algal and grazer dynamics is tightest (i.e. the period of the algae-grazer oscillation is shortest and the amplitude largest) at intermediate water column

depths. The coupling is looser at both shallow and deep water column depths, because of reduced food quality (= low algal nutrient content) and reduced algal production, respectively. Nutrient enrichment improves algal quality and tightens the algae-grazer coupling at shallow and intermediate water column depths, but not at deep water column depths, where algal production is strongly light limited. I compared these predictions with the results of the field-experiment, in which I manipulated nutrient supply (range 10-60 μg total Phosphorus L^{-1}) and mixing depth (1, 3, 6, and 12 m) independently in a natural phytoplankton community in the presence of *Daphnia hyalina*. The results were in good qualitative agreement with most model expectations.

In comparative lake data, depth of stratification and water temperature are usually inversely correlated. Chapter 4 describes a field enclosure experiment, which was conducted to disentangle the separate impacts of these two factors on the magnitude and timing of spring successional events in the plankton (i.e. phytoplankton bloom, grazer population peak, clearwater phase). Independent manipulation of water column depth and water temperature showed that deeper mixing delayed the timing of all spring seasonal events and reduced the magnitude of the phytoplankton bloom and the subsequent grazer peak. Lower temperatures retarded the timing of the clear-water-phase and the subsequent grazer peak, whereas the timing of the phytoplankton peak was unrelated to temperature.

General Introduction

Background

Primary production depends critically on the supply with two fundamentally different types of essential resources, i.e. light and mineral nutrients. Photosynthetically active radiation is always supplied externally and cannot be stored. Photons can only be absorbed once and have to be instantaneously transformed into chemically bound energy. In contrast nutrients can be stored and recycled within and among organisms and ecosystems. The different nature of these essential resources poses a challenge for primary producers in pelagic habitats. Here, gravity often leads to a spatial separation of the zones where detrital nutrients are recycled and where they are needed for primary production. Because light is always supplied from the surface and is vertically attenuated by water molecules, dissolved and suspended organic matter (i.e. background attenuation) and phytoplankton itself, primary production is restricted to an upper surface layer, the euphotic zone (Kirk and Tyler 1986; Coker 1987; Guildford et al. 1987; Kirk 1994). Most living algal cells and essentially all detrital material have, however, a higher specific density than water (Smayda 1969; Reynolds 1984). Consequently, in sufficiently deep water bodies both living algae and detritus tend to sink out of the euphotic zone and a large proportion of their nutrient content is eventually mineralized in the sediment or in deep water layers (Wetzel 1983; Antia 2005; Peterson et al. 2005). Turbulent mixing is then required to transport recycled nutrients back from below into the euphotic zone, to which light and nutrients are therefore supplied from opposite directions (Klausmeier and Litchman 2001; Huisman et al. 2006).

Physical characteristics of the water column, most notably its depth and the degree of turbulent mixing, are key factors influencing population dynamics of pelagic primary producers by affecting the average light climate, sedimentation losses, and the availability of nutrients (Visser et al. 1996; Diehl 2002; Huisman et al. 2002; 2006). For example, under well-mixed conditions phytoplankton are passively entrained in the entire water column and, over time, each algal cell experiences the depth-averaged light intensity, which is a decreasing function of water column depth (cf. Fig. 1a-c). Consequently, depth-averaged specific primary production decreases with increasing water column depth (Huisman 1999; Diehl et al. 2002; 2005) and will become insufficient for the maintenance of a viable population when the mixed water column exceeds a 'critical depth' (Sverdrup 1953). In contrast, in a weakly mixed water column the speed of entrainment will often be slower than the speed of algal reproduction. Consequently, algal cells can remain in the well-lit upper part of the water column for long enough to maintain a population even if the water column exceeds the 'critical depth' (Huisman et al. 1999) (cf. Fig. 1c vs. d).

Water column depth and mixing intensity also affect algal sedimentation losses. The probability of an individual algal cell or colony to sink out of the water column increases with increasing sinking velocity and decreasing water column depth (Visser et al. 1996; Ptacnik et al. 2003) (cf. Fig. 1a-c). Sinking velocities vary among different species, depending mainly on density and cell (or colony) size and shape, and cell alignment in e.g. colonies (Reynolds 1984). Algal sinking velocities range for most taxa under most conditions from 0 to 1 m day⁻¹, but sinking velocities of up to 7 m day⁻¹ have been observed in fast sinking diatoms (Wetzel 1983; Reynolds 1984). While there are some taxa which overcome sinking by active movement (e.g. autotrophic flagellates) or by buoyancy regulation [mainly cyanobacteria (Reynolds 1984)], sinking taxa have to be entrained within the water column to counteract their down-flux. Enhanced

entrainment of algal cells by turbulent mixing has been observed to reduce sedimentation losses of fast sinking taxa (Visser et al. 1996; Condie and Bormans 1997; Huisman et al. 2002; O'Brien et al. 2003). Overall, sinking losses should thus be most severe for fast sinking algae in shallow and stagnant water columns (Diehl 2002; Huisman et al. 2002).

Algal sedimentation constantly removes particular nutrients from the water column, which are subsequently mineralized and recycled back into the water column from below. In sufficiently deep and weakly mixed water columns nutrients may therefore become strongly limiting close to the surface but be available in excess in deeper layers, creating a vertical gradient in mineral nutrient concentration (Klausmeier and Litchman 2001; Huisman et al. 2006) (cf. Fig. 1d). In well-mixed water columns vertical gradients are absent and nutrient availability is expected to depend exclusively on total water column depth. Nutrient concentrations should be low in shallow water columns, where algal sinking removes particulate nutrients at high rates, and high in deep water columns, where algal production and nutrient use is strongly light limited (Huisman and Weissing 1995; Diehl 2002) (cf. Fig. 1a-c).

By mediating light and nutrient availability, water column depth and mixing intensity may also profoundly affect the outcome of competition among planktonic algae. Strong mixing minimizes the possibilities for spatial niche differentiation. Under constant environmental conditions, those taxa that reduce the light intensity at the bottom of the water column to the lowest level and the limiting nutrients to the lowest concentrations will then displace all other competitors, allowing at best a few species to persist in the long run (Sommer 1985; Huisman and Weissing 1995; Passarge et al. 2006). In contrast, coexistence by means of vertical niche separation is possible in weakly mixed systems (Reynolds 1992). For example, a superior competitor for light may coexist with a superior competitor for nutrients, with the former dominating at deeper and the latter at shallower depths within the water column (Huisman et al. 2006).

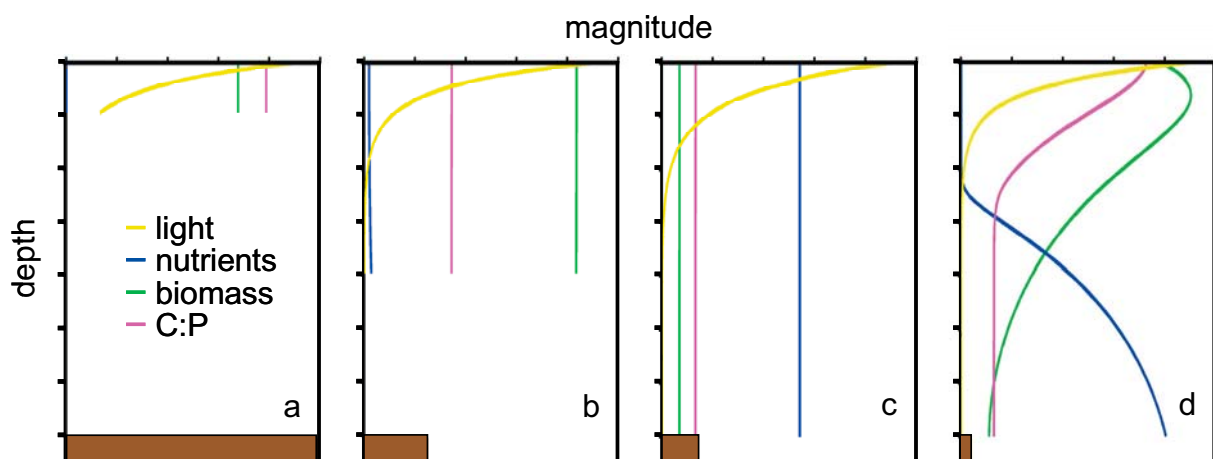


Fig. 1. Schematic diagram of the equilibrium vertical distributions of light, dissolved nutrient concentration, algal biomass, and algal C:P ratio (as indicated by legend) in water columns of different depth and turbulence. Brown bars at the bottom show the magnitude of specific algal sedimentation rates. Panels a-c show well-mixed water columns of increasing total depth, panel d shows a deep, weakly mixed water column. Incident radiation and total initial nutrient content per volume are the same in all panels.

The outcome of algal competition in response to mixing intensity and water column depth depends, however, not only on algal traits related to resource use but also on buoyancy. Several studies have reported that systems could be moved back and forth from dominance of buoyant taxa in weakly or shallowly mixed water columns to dominance of fast sinking taxa in deeply mixed water columns by turning off and on artificial mixing (Reynolds et al. 1983; 1984; Visser et al. 1996; Huisman et al. 2004). Buoyancy may also enable coexistence of a weaker competitor for an essential resource with a superior one (Litchman 2003). In particular, motile taxa may benefit from weak mixing intensity, because low turbulence enables them to move to depths with optimal growth conditions (Klausmeier and Litchman 2001). Such habitat choice could accentuate vertical niche separation of different taxa (Elliott et al. 2002; Clegg et al. 2007). Thus, if weak mixing leads to the development of multiple gradients of growth enhancing and inhibiting environmental parameters, this could enable substantial vertical niche partitioning and enhance diversity compared to a well-mixed system of the same overall depth.

Nutrient and light supply do, however, not only affect algal growth and competition between different taxa, but also algal physiology, e.g. the carbon to nutrient stoichiometry of algal biomass (cf. Fig. 1). For example, when light supply is high relative to phosphorus availability, phytoplankton biomass tends to be carbon rich and phosphorus poor (Fig. 1a). In contrast, when light supply is low relative to phosphorus availability, 'excess' nutrients may be taken up (and stored) by phytoplankton (Sterner et al. 1997; Berger et al. 2006) (Fig. 1c). In particular, across a range of well-mixed water columns of different depths this leads to pronounced differences in algal carbon to phosphorus (= C:P) ratio - and less pronounced differences in mineral nutrient concentration (Diehl et al. 2005; Berger et al. 2006). Similarly, because of the opposite supply directions of light and nutrients, profiles of vertically decreasing seston C:P ratios can be observed within weakly mixed water columns (Rothhaupt 1991; Elser and George 1993; Park et al. 2004) (Fig. 1d).

Various influences of flexible producer stoichiometry on ecosystem processes have been studied in the last decade such as sequestration and storage of atmospheric carbon dioxide, the transfer of energy and matter within a food web, and the transport, storage, and recycling of nutrients within and among ecosystems and their components (e.g. Andersen 1997; Sterner and Elser 2002; Hessen et al. 2004; Diehl 2007; Riebesell et al. 2007). One example is the influence of producer stoichiometry on the coupling of producer-grazer interactions. The flexibility of producer stoichiometry may create a mismatch with the nutritional needs of grazers such as *Daphnia* spp., whose body composition is characterized by a relatively low C:P ratio (Andersen and Hessen 1991; Sterner et al. 1993). An increase in light supply may therefore decrease grazer production if the benefits of increased food quantity (increased algal carbon fixation) are outweighed by decreased food quality (increased algal C:P ratio) and, thus, decreased conversion efficiency of algal into *Daphnia* biomass [reviewed in Andersen et al. (2004)]. Flexible algal C:P stoichiometry is therefore likely to affect the timing and magnitude of consumer-resource oscillations, because phytoplankton peaks should often be associated with high C:P ratios (i.e., low quality) of algal biomass. Long delays in the build-up of *Daphnia* population peaks have indeed been observed in the presence of high biomasses of low quality (high C:P) algal food (Sommer 1992; Urabe et al. 2002).

Transient oscillatory dynamics of pelagic producer-grazer systems are a common phenomenon in seasonal environments such as temperate lakes. These systems typically show a seasonal succession of the plankton, which is usually initiated by spring circulation bringing nutrients to the water surface and subsequent thermal stratification creating a well-lit mixed surface layer, both of which stimulate planktonic primary production (Sommer et al. 1986). The resulting phytoplankton spring bloom is frequently terminated by the grazing activity of a growing crustacean zooplankton population producing the ‘clearwater phase’, a period of low phytoplankton biomass; the latter, in turn, is often followed by a crash of the crustacean population that has temporally overexploited its resource base (Lampert et al. 1986; Sarnelle 1993; Talling 2003). Empirical evidence suggests that the magnitude and timing of such transient producer-grazer oscillations depend on the nutrient and light regime, with more nutrient rich and more shallow systems experiencing earlier and more pronounced phytoplankton and zooplankton peaks and troughs (Sommer et al. 1986). The onset and depth of water column stratification, and consequently the starting point of spring succession, depends on regional weather conditions such as air temperature and wind speed. In particular, low wind speeds during winter and early spring promote an early onset of stratification, the depth of which is modulated by ambient temperature (Gaedke et al. 1998a, b; Winder and Schindler 2004a, Peeters et al. 2007a).

Specific thesis goals

In this thesis I present theoretical and experimental research on the influence of several physical environmental factors on planktonic systems. The first chapter describes theoretical investigations of the interactive effects of water column depth and turbulence on the biomass and vertical distribution of a population of negatively buoyant algae with flexible nutrient to carbon stoichiometry. To this end, I performed numerical model analyses describing the temporal and spatial dynamics of light intensity, dissolved and sedimented nutrients, algal production and sedimentation, algal biomass, and algal carbon to nutrient stoichiometry in a 1-dimensional water column. I explored algal sinking losses and the vertical distribution of light, dissolved nutrients, specific primary production, phytoplankton biomass, and algal C:P ratio for a wide range of water column depths (1-50 m) and mixing intensities (turbulent diffusion spanning 5 orders of magnitude). I furthermore determined the depth-integrated values of these variables. I analyzed the influence of several potentially limiting processes on total algal biomass in the water column, with an emphasis on vertical light attenuation, sedimentation losses, and the recycling and transport of nutrients from sedimented algae back to the euphotic zone. I investigated the conditions in the depth-turbulence space under which the highest depth-integrated phytoplankton biomass can be supported by a given incident radiation. I explored the robustness of the resulting qualitative model predictions to changes in nutrient and light supply. Additionally, I analyzed the influence of a flexible algal carbon to nutrient stoichiometry on the model results by comparing them with results of a model with a fixed algal stoichiometry. All analyses were restricted to equilibrium conditions.

In the second chapter I empirically investigated the influence of the depth of a water column and the intensity of its mixing on the dynamics of a natural lake phytoplankton community. To this end, I conducted a field enclosure experiment in which water column depth and mixing intensity were manipulated independently. I present the temporal development of algal biovolume, the functional composition and diversity of the phytoplankton community, the concentration of mineral nutrients, and

the algal C:P ratio over a period of five weeks. Also algal sedimentation rate was estimated during the experiment. Vertical profiles of algal biomass and nutrients were measured weekly and the possibility of vertical niche partitioning at weak mixing intensity was explored in a primary production assay.

In the third chapter a second trophic level (grazers) was added to the study system. In this chapter the focus is set on the exploration of transient dynamics of pelagic producer-grazer systems and how they are influenced by environmental factors. Because producer-grazer oscillations, which are typically observed in temperate lakes at the beginning of seasonal succession, should be strongly influenced by nutrient supply and mixed water column depth, the study focused on these factors in a coupled theoretical and experimental investigation. I explored how nutrient supply and water column depth affect the transient dynamics of a phytoplankton-grazer system starting from low population densities until the end of the first grazer peak, when natural phytoplankton communities often shift towards less edible taxa (Sommer et al. 1986; Sarnelle 1993). In the first part of chapter 3 I used a producer-grazer model parameterized for *Daphnia* feeding on edible algae to explore how the timing and magnitudes of transient population peaks and troughs are affected by nutrient supply and water column depth. I examined the potential importance of variable algal carbon to nutrient stoichiometry to these dynamics by investigating two variants of the model, one with fixed and one with flexible algal C:P ratio. The outputs of the two models were then compared with the results of a field enclosure experiment in which I manipulated nutrient supply and water column depth in a factorial design, and followed the dynamics of phytoplankton and a population of *Daphnia hyalina* over a period of 7 weeks.

In chapter 4 the effects of stratification depth and water temperature on the magnitude and timing of spring successional events of the plankton are analyzed. In natural lakes stratification depth and water temperature usually covary negatively. To disentangle their separate and combined effects a field enclosure experiment was conducted in which enclosure depth and water temperature were manipulated independently. The resulting transient dynamics of phytoplankton biomass and *Daphnia hyalina* abundance (the native crustacean grazer in the experimental lake) are presented. The data analysis focuses on treatment effects on the magnitude of the phytoplankton and grazer peaks, and on the timing of the phytoplankton and grazer peaks and of the clearwater phase.

Chapter 1

Physical determinants of phytoplankton production, algal stoichiometry, and vertical nutrient fluxes

Christoph G. Jäger,
Sebastian Diehl,
and Maximilian Emans*

*AVL List GmbH, Hans-List-Platz 1, 8020 Graz, Austria

Abstract

Pelagic aquatic primary producers often face opposite vertical gradients in supply with essential resources (i.e. light vs. nutrients). We numerically explore a dynamical model of a population of light and nutrient limited, negatively buoyant algae inhabiting a 1-dimensional water column to ask how water column depth, gravity and turbulence affect the vertical distributions of phytoplankton, dissolved, suspended and sedimented nutrients, and how physical constraints on the vertical fluxes of light, nutrients and algae limit the biomass of pelagic primary producers. We show that total water column biomass is limited by three processes: vertical light attenuation, sedimentation losses, and nutrient recycling from sinking algae. In very shallow water columns, algal biomass is always strongly limited by sedimentation losses. In contrast, in deep water columns the limiting factor depends on turbulence, with light being most strongly limiting at high and nutrient transport being most strongly limiting at low turbulences. Consequently, the highest depth-integrated biomasses are attained in deep water columns at intermediate turbulences, where none of sinking, light attenuation, and nutrient recycling is particularly strongly limiting. These qualitative patterns arise under a broad range of nutrient and light supply scenarios and are insensitive to the assumption of fixed vs. flexible algal stoichiometry.

Introduction

Primary production depends critically on the supply with two fundamentally different types of resources, i.e. light and mineral nutrients. While photosynthetically active radiation is always supplied externally and cannot be stored, sustained nutrient supply requires efficient storage and recycling of nutrients within the ecosystem. In terrestrial systems primary production is dominated by vascular plants using separate, specialized organs for nutrient uptake and light harvesting. Gravity insures that nutrients stored in the light harvesting above-ground canopy eventually return to the soil in the form of detritus where they are resupplied to the root system after mineralization. Nutrient uptake by plants and nutrient recycling thus take place in close proximity.

In contrast, primary production in pelagic aquatic habitats is dominated by planktonic microorganisms facing very different environmental challenges. Here, gravity often leads to a spatial separation of the zones where detrital nutrients are recycled and where they are needed for primary production. Because light is vertically attenuated by water molecules and dissolved and suspended materials, primary production is restricted to an upper surface layer, the euphotic zone (Kirk 1994). Most living algal cells and essentially all detrital material have, however, a higher specific density than water (Smayda 1969; Reynolds 1984). Consequently, in sufficiently deep water bodies both living algae and detritus tend to sink out of the euphotic zone and a large proportion of their nutrient content is eventually mineralized in deep water layers or in the sediment (Wetzel 1983; Antia 2005; Peterson et al. 2005). Turbulent mixing is then required to transport recycled nutrients back into the euphotic zone. Thus, physical characteristics of the water column, most notably its depth and the degree of turbulent mixing, are key factors influencing the spatial separation of the zones of nutrient recycling and of nutrient use by primary producers, and the vertical transport between these zones (Klausmeier and Litchman 2001; Diehl 2002; Huisman et al. 2006).

That water column depth and mixing intensity are crucial determinants of phytoplankton production has been known for a long time (Riley et al. 1949; Sverdrup 1953). Recently, this topic has received renewed interest. All else equal, increased water column depth decreases specific sedimentation losses, but also decreases depth-averaged light availability (Visser et al. 1996; Huisman 1999; Diehl et al. 2002; Ptacnik et al. 2003). Similarly, enhanced turbulence reduces sedimentation losses but increases downward mixing of algae to more light limited depths (Condie and Bormans 1997; Huisman et al. 1999; O'Brien et al. 2003). Consequently, phytoplankton population growth can be strongly limited by sinking losses in shallow, weakly mixed water columns and by light in deep, turbulent water columns. To maintain a population of negatively buoyant algae therefore requires a minimal water column depth and a minimal turbulence to counteract sinking losses (Diehl 2002; Huisman and Sommeijer 2002). Conversely, the maintenance of populations of both negatively and positively buoyant algae requires that the water column does not exceed a maximal depth and that mixing intensity remains below a threshold of maximal turbulence to counteract entrainment below the euphotic depth (Sverdrup 1953; Huisman et al. 1999; Huisman et al. 2002; Peeters et al. 2007b).

While the influences of water column depth and turbulence on the potential limitation of algal production by sinking vs. vertical light attenuation are fairly well understood in theory, a similarly comprehensive picture of their influences on nutrient limitation of algal production is still lacking. So far the influence of water column depth on nutrient dynamics has been theoretically explored primarily for

well-mixed systems. In such systems phytoplankton production tends again to be limited by sinking losses in shallow water columns and by low average light levels in deep water columns, whereas at intermediate water column depths algal production is limited by nutrient availability (Huisman and Weissing 1995; Diehl 2002; Diehl et al. 2005; Berger et al. 2006). It seems plausible to expect that reduced turbulence may alter this pattern by changing vertical nutrient fluxes, but this important aspect remains largely unexplored [but see Huisman et al. (2006)].

Pelagic algal and nutrient dynamics may be further complicated by variability in the elemental composition of phytoplankton in response to the relative supplies with light and nutrients, as influenced by e.g. water column depth or vertical position in the water column (Sterner et al. 1997; Bertilsson et al. 2003; Berger et al. 2006). Algal stoichiometry, in turn, feeds back on the nutrient-dependence of algal growth rates, the amount of algal self shading produced per unit assimilated nutrient, and the nutrient fluxes associated with algal sinking (Rothhaupt 1991; Elser and George 1993; Geider et al. 1998; Park et al. 2004; Diehl et al. 2005; Christian 2005). Clearly, a comprehensive analysis of the influences of water column depth and turbulence on phytoplankton dynamics must consider nutrient dynamics and algal nutrient limitation and should include flexible algal nutrient to carbon stoichiometry.

The purpose of this study was to theoretically investigate the interactive effects of water column depth and turbulence on the biomass and vertical distribution of a population of potentially nutrient limited, negatively buoyant algae with flexible nutrient to carbon stoichiometry. We performed extensive numerical analyses of a model describing the temporal and spatial dynamics of light intensity, dissolved and sedimented nutrients, algal production and sedimentation, algal biomass, and algal carbon to nutrient stoichiometry in a 1-dimensional water column. We show that total water column biomass is limited by three processes, vertical light attenuation, sedimentation losses, and nutrient recycling from sinking algae, the relative importance of which varies depending on water column depth and turbulence. Additional analyses show that these qualitative patterns are insensitive to the assumption of fixed vs. flexible algal carbon to nutrient stoichiometry and are qualitatively robust against changes in environmental conditions affecting the overall light and nutrient availability.

The Model

Basic model structure and boundary fluxes

The basic model (subsequently called the ‘standard’ model) consists of a 1-dimensional water column and a sediment layer. We assume that algal production is limited by the supplies with light and a single mineral nutrient and that the system is closed for nutrients. A system of three partial differential equations, one ordinary differential equation and one algebraic equation describes the dynamics of the concentrations of algal carbon biomass (A), particulate nutrients bound in algae (R_b) and dissolved mineral nutrients (R_d) in the water column, of light intensity (I) in the water column, and of the pool of sedimented nutrients (R_s):

$$\frac{\partial A}{\partial t} = p(I, q)A - l_{bg}A - v \frac{\partial A}{\partial z} + d \frac{\partial^2 A}{\partial z^2} \quad (1)$$

$$\frac{\partial R_b}{\partial t} = \rho(q, R_d)A - l_{bg}R_b - v \frac{\partial R_b}{\partial z} + d \frac{\partial^2 R_b}{\partial z^2} \quad (2)$$

$$\frac{\partial R_d}{\partial t} = l_{bg}R_b - \rho(q, R_d)A + d \frac{\partial^2 R_d}{\partial z^2} \quad (3)$$

$$I_{(z,t)} = I_0 \cdot e^{-\left(\int_0^z k \cdot A dz + k_{bg} \cdot z \right)} \quad (4)$$

$$\frac{dR_s}{dt} = vR_b(z_{\max}) - rR_s \quad (5)$$

In all numerical simulations the limiting nutrient was assumed to be phosphorus. All state variables and parameters with definitions and units are listed in Table 1. The water column runs from depth 0 at the surface to z_{\max} at the bottom. Mixing of water, suspended algae and dissolved nutrients is described by the turbulent diffusion coefficient d , which is assumed to be constant over depth z . Phytoplankton sink through the water column with velocity v and have constant specific maintenance losses l_{bg} . Specific algal growth rate p is an increasing, saturating function of light intensity I and algal nutrient quota q (= nutrient content per carbon biomass)

$$p(I, q) = \mu_{\max} \left(1 - \frac{q_{\min}}{q} \right) \frac{I}{h + I}, \quad (6)$$

where μ_{\max} is the ‘nominal’ maximum specific production rate (theoretically attained when $q \rightarrow \infty$), q_{\min} is the algal nutrient quota at which growth ceases, and h is the half-saturation constant of light-dependent production. We assume that the vertical light gradient follows Lambert-Beer’s law. Light intensity at depth z then depends on surface light intensity I_0 and on the integral of light attenuation by algal biomass (with specific attenuation coefficient k) and by nonalgal components k_{bg} above depth z (eq. 4).

For computational convenience, we describe algal carbon biomass A and particulate nutrients R_b with separate dynamic equations. Algal nutrient quota q is then calculated as

$$q = \frac{R_b}{A}. \quad (7)$$

This procedure assumes that all algae at a given depth have the average cell quota of that depth and, thus, ignores that sinking and turbulence blend algae from neighboring depth strata potentially differing in q . Because p increases nonlinearly with q , the use of average q in eq. 6 slightly overestimates true production rate. The error introduced by this procedure is, however, negligible because algae from neighboring depth strata have similar cell quotas and quickly adapt their cell quota to local light-nutrient conditions.

Algae take up dissolved nutrients and transform them into particulate nutrients at rate

$$\rho(q, R_d) = \rho_{\max} \left(1 - \frac{q - q_{\min}}{q_{\max} - q_{\min}} \right) \frac{R_d}{m + R_d}, \quad (8)$$

where ρ_{\max} is the maximum specific uptake rate, m is the half-saturation constant of nutrient uptake, and q_{\max} is the algal nutrient quota at which uptake ceases. At a given dissolved nutrient concentration nutrient uptake is thus a linear function of q , with no uptake at q_{\max} and maximum uptake at q_{\min} . We assume that algae excrete mineral nutrients and respire carbon at the same specific rate l_{bg} . At the other extreme, one could assume that maintenance involves only carbon respiration but no nutrient losses (Diehl et al. 2005). Because excreted nutrients are almost instantly taken up by the algae excreting them (except when q is close to q_{\max}), results are not sensitive to this assumption.

The boundary conditions are set such that algal biomass and particulate nutrients neither leave nor enter the system at the surface ('no flux' at $z = 0$), but sink out at the bottom of the water column ('convective flux' at $z = z_{\max}$). The latter implies that the fluxes of particulate carbon and nutrients into the sediment are $-vA(z_{\max})$ and $-vR_b(z_{\max})$, respectively. Particulate nutrients are mineralized in the sediment and returned to the water column in dissolved mineral form at rate r . Dissolved nutrients therefore have an influx of mineralized nutrients rR_d at the bottom and 'no flux' conditions at the surface of the water column. A table with the boundary conditions is given in Appendix A (Table A1).

For computational convenience, we calculated the temporal dynamics of the vertical light gradient and of sedimented nutrients not with eqs. 4 and 5, but used the equations shown in Appendix A, where also the technical details of our numerical approach are described.

Model analyses

We performed extensive numerical simulations to explore how water column depth, turbulence, and other environmental factors influence the dynamics of our model system. All parameter values not varied among simulations are representative of a generic temperate lake inhabited by phytoplankton with average traits [see e.g. Andersen (1997), chapter 3.5] and are identical or similar to the ones used in Diehl et al. (2005) (Table 1). Simulations were performed with COMSOL 3.2 with a vertical grid of 0.02 m and an automatic time step and were run to equilibrium.

In a first set of baseline simulations, we investigated how five different levels of turbulence ($d = 0.1, 1, 10, 100, 1000 \text{ m}^2 \text{ day}^{-1}$) cross-classified with fifty different water column depths (1-50 m, evenly spaced at 1-m intervals) affect equilibrium patterns of phytoplankton biomass, production and sedimentation, algal nutrient quota, and dissolved and sedimented nutrients in the 'standard' model. These analyses were performed with a fairly low background light attenuation coefficient k_{bg} of 0.4 m^{-1} and initially homogeneous vertical distributions of algal biomass and dissolved nutrients of 100 mg C m^{-3} and 30 mg P m^{-3} , respectively. The initial pool of sedimented nutrients was assumed to be zero, and the initial concentration of particulate nutrients was 2.2 mg P m^{-3} , yielding an initial algal nutrient quota of $0.022 \text{ mg P mg C}^{-1}$ (close to the Redfield ratio) and a total nutrient concentration ($R_d + R_b$) of 32.2 mg P m^{-3} . We subsequently explored the robustness of the observed patterns to changes in environmental conditions affecting the light and nutrient supplies by running simulations at different levels of background turbidity and initial dissolved nutrient concentration.

Table 1.
Definitions and units of parameters and variables and basic set of parameter values and initial conditions

Parameter	Value	Definition and Units
d	0.01 – 1000 ¹⁾	turbulent diffusion [$\text{m}^2 \text{day}^{-1}$]
d_s	1000	turbulent diffusion in the sediment layer [$\text{m}^2 \text{day}^{-1}$]
h	120	half saturation constant for light-dependent algal production [$\mu\text{mol photons m}^{-2} \text{s}^{-1}$]
I_0	300	light intensity at the surface [$\mu\text{mol photons m}^{-2} \text{s}^{-1}$]
k	0.0003	specific light attenuation coefficient of algal biomass [$\text{m}^2 \text{mg C}^{-1}$]
k_{bg}	0.2, 0.4, 0.8 ¹⁾	background light attenuation coefficient [m^{-1}]
l_{bg}	0.1	specific algal maintenance respiration losses [day^{-1}]
m	1.5	half saturation of algal nutrient uptake [mg P m^{-3}]
μ'_{\max}	1.08	maximum specific algal production rate in the 'light limitation' model [day^{-1}]
μ_{\max}	1.2	maximum specific algal production rate in all models except the 'light limitation' model [day^{-1}]
q_{fix}	0.0244	algal nutrient quota in the fixed stoichiometry model [mg P mg C^{-1}]
q_{max}	0.04	algal maximum nutrient quota [mg P mg C^{-1}]
q_{min}	0.004	algal minimum nutrient quota [mg P mg C^{-1}]
r	0.02	specific mineralization rate of sedimented nutrients [day^{-1}]
ρ_{max}	0.2	maximum specific algal nutrient uptake rate [$\text{mg P mg C}^{-1} \text{day}^{-1}$]
v	0.25	algal sinking velocity [m day^{-1}]
z_{max}	1 – 50 ¹⁾	depth of water column [m]
Variable		
A	100 ²⁾	algal carbon density [mg C m^{-3}]
I		light intensity [$\mu\text{mol photons m}^{-2} \text{s}^{-1}$]
p		specific algal production rate [day^{-1}]
R_b	2.2 ²⁾	concentration of particulate nutrients bound in algae [mg P m^{-3}]
R_d	10, 30 ^{1,2)}	concentration of dissolved nutrients [mg P m^{-3}]
R_s	0 ²⁾	pool of sedimented nutrients [mg P m^{-2}]
ρ		specific algal nutrient uptake rate [$\text{mg P mg C}^{-1} \text{day}^{-1}$]
W		depth integrated algal biomass [mg C m^{-2}]
z		depth below water surface [m]

¹⁾ Range of environmental conditions examined

²⁾ Initial values

To assess the extent to which the system's qualitative responses to physical water column characteristics are influenced by flexible algal nutrient to carbon stoichiometry, we repeated all analyses with a model variant in which algal nutrient quota was fixed at the Redfield ratio ($q_{fix} = 0.0244 \text{ mg P mg C}^{-1}$). In this modified model (called the 'fixed stoichiometry' model), specific algal production rate p in eq. 1 depends on the external nutrient concentration R_d as

$$p(I, R) = \mu_{\max} \frac{R_d}{m + R_d} \frac{I}{h + I}, \quad (9)$$

and algal nutrient uptake rate is proportional to algal production rate. Eq. 3 is therefore replaced by

$$\frac{\partial R_d}{\partial t} = q_{fix} l_{bg} A - q_{fix} p(I, R) A + d \frac{\partial^2 R_d}{\partial z^2}. \quad (10)$$

A separate equation for particulate nutrients is not necessary, because $R_b = q_{fix} A$. Boundary conditions, eqs. 4 and 5, and parameter values are identical to the flexible stoichiometry model. The flux of nutrients into the sediment is now calculated by the flux of biomass A multiplied by q_{fix} .

To assess which factors (i.e. sinking losses, light availability, overall nutrient supply, or upward transport of recycled nutrients) limit phytoplankton biomass in the 'standard' model most strongly under different combinations of water column depth and turbulence we repeated all analyses under the assumption of pure light limitation of algal production (called 'light limitation' model) and under the assumption that dissolved nutrients were always mixed with the maximal intensity $d = 1000 \text{ m}^2 \text{ day}^{-1}$, while phytoplankton biomass (and particulate nutrients) experienced a full range of turbulences from 0.01 to $1000 \text{ m}^2 \text{ day}^{-1}$ (called 'mixed nutrient' model). In the 'mixed nutrient' model the influences of turbulence on phytoplankton sinking and entrainment are uncoupled from influences of turbulence on nutrient transport, whereas in the 'light limitation' model phytoplankton is completely released from nutrient limitation. In the 'light limitation' model, specific algal production rate p in eq. 1 is thus only dependent on the light intensity I

$$p(I) = \mu'_{\max} \frac{I}{h + I} \quad (11)$$

To allow a quantitative comparison of the 'standard', 'mixed nutrient' and 'light limitation' models the maximum specific production rate μ'_{\max} in eq. 11 was set to a fraction $(1 - q_{min}/q_{max})$ of μ_{\max} in the 'standard' and 'mixed nutrient' models to account for the fact that the realizable maximum specific production rate in these models is $\mu_{\max} (1 - q_{min}/q_{max})$. Equations for dissolved nutrients, particulate nutrients bound in algae, and the pool of sedimented nutrients are not necessary in the 'light limitation' model.

For all simulation outputs we calculated equilibrium vertical distributions of the following state variables: algal biomass, dissolved nutrients, algal nutrient quota (presented as molar C:P ratio = $1/q \cdot 31/12$), specific algal gross production rate [$= p(I, q)$], and the pool of sedimented nutrients. From these we derived the following quantities: algal standing stock per area, W ($=$ depth-integrated algal biomass), depth-averaged dissolved nutrient concentration, specific sedimentation rate ($=$ flux of biomass to the sediment/ W), and the depth $z(A_{max})$ at which the maximum concentration of algal biomass occurs within the water column. Finally, we derived a quantity called 'optimal mixing intensity' ($=$ mixing intensity yielding the highest depth-integrated biomass for a

given water column depth), and compared its position in z - d space for the ‘standard’, ‘mixed nutrient’ and ‘light limitation’ models as well as its dependency on background turbidity and nutrient enrichment in the ‘standard’ model.

Results

Effects of water column depth and turbulence: basic patterns

At all levels of turbulence a minimum water column depth of c. 0.4 m (not shown in Figs. 1 and 2) is required to sustain an algal population, because sedimentation loss rate exceeds the maximum algal production rate in extremely shallow water columns. Similarly, at all water column depths a minimum turbulence of c. $0.03 \text{ m}^2 \text{ day}^{-1}$ (not shown in Figs. 1 and 2) is required to sustain an algal population, because the downward movement of sinking algae needs to be counteracted by turbulence.

At high turbulence ($d = 100\text{-}1000 \text{ m}^2 \text{ day}^{-1}$) there are nearly no vertical gradients in algal biomass, dissolved nutrients and algal C:P ratio (Fig. 1q-s, v-x). The degree of algal nutrient limitation is therefore the same everywhere in the water column. Consequently, specific algal production is highest at the surface and decreases vertically in parallel with the light gradient (Fig. 1t, y). In water columns $< 5 \text{ m}$ light availability is high, but high sedimentation losses (Fig. 2d)

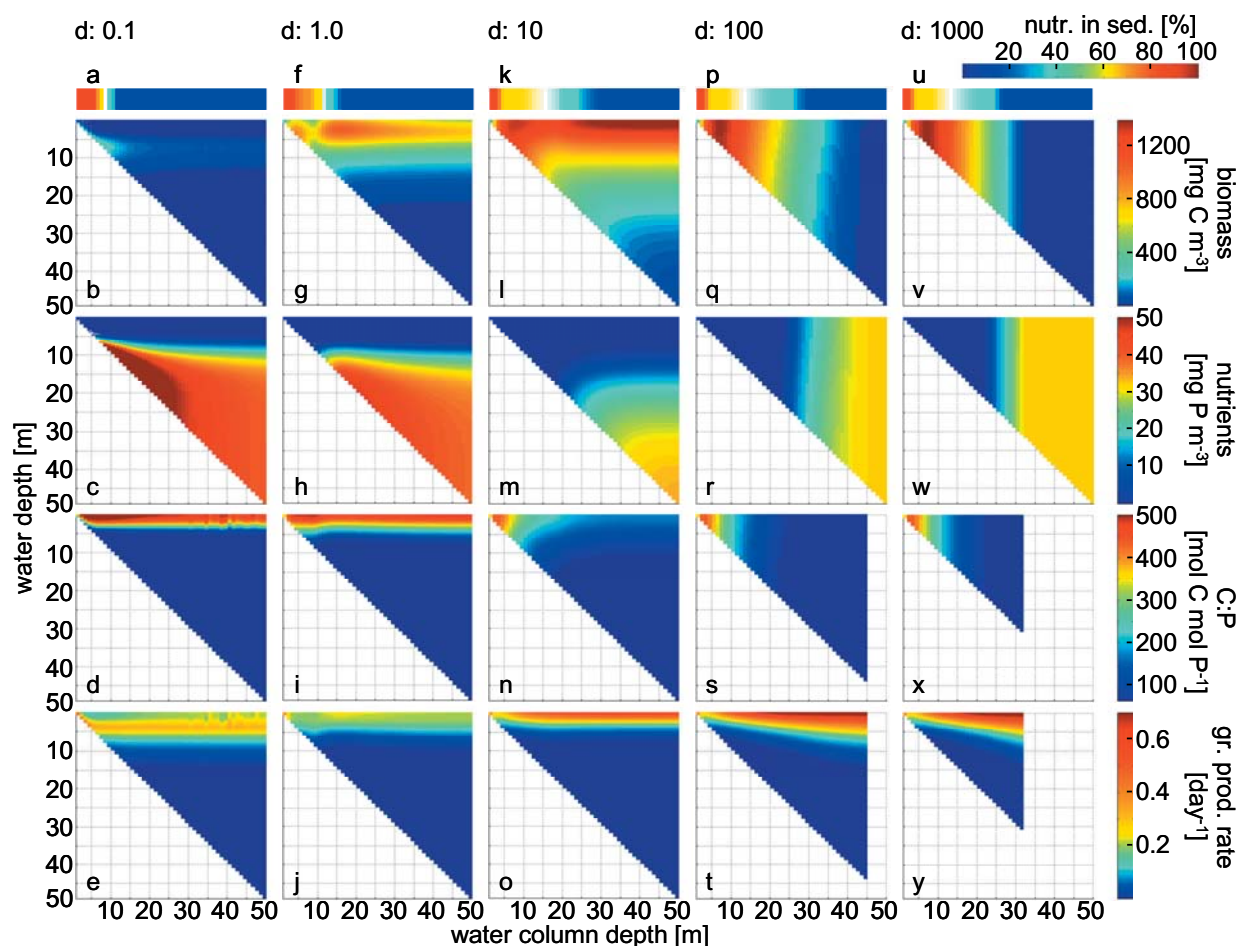
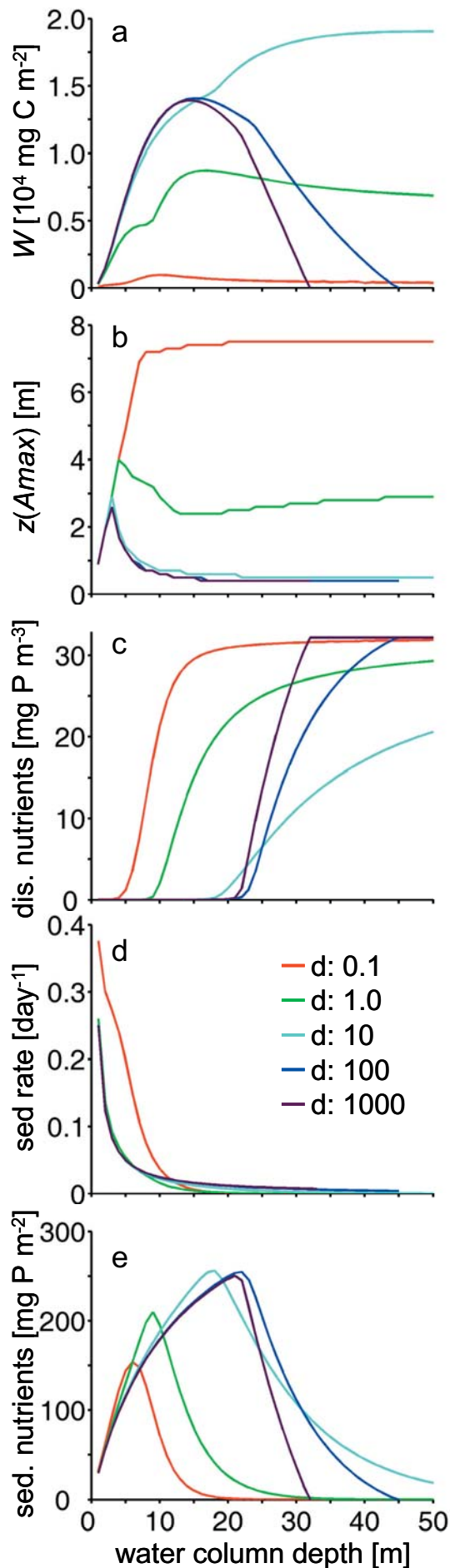


Fig. 1. Equilibrium vertical profiles (y-axes) at different total water column depths (x-axes) of algal biomass concentration (first row of panels), dissolved nutrient concentration (second row), algal C:P ratio (third row), and specific algal gross production rate (fourth row), and the proportion of total nutrients stored in the sediment at different water column depths (horizontal bars at the top). Columns of panels show data for five different levels of turbulence (with a d of 0.1, 1, 10, 100, and 1000 $\text{m}^2 \text{ day}^{-1}$). Color legends are on the right end of each row. Algae die out at total water column depths $> 45 \text{ m}$ and $> 32 \text{ m}$ at $d = 100$ and $d = 1000 \text{ m}^2 \text{ day}^{-1}$, respectively. Algal C:P ratio and gross production rate are therefore not shown for these water column depths. At $d = 0.1 \text{ m}^2 \text{ day}^{-1}$ the system shows persistent, small oscillations in deep water columns, which blur the panels of algal C:P ratio and gross production rate.



cause > 75% of total nutrients to be locked up in the sediment (Fig. 1p, u); consequently, algal C:P ratio is high (Fig. 1s, x) and production is nutrient limited. With increasing water column depth specific sedimentation losses and the proportion of nutrients in the sediment decrease (Fig. 1p, u, 2d). Algal nutrient limitation (C:P ratio) thus decreases and specific algal production at a given depth in the water column increases over the entire gradient of increasing water column depths (Fig. 1s, t, x, y). Initially, algal biomass therefore also increases with water column depth (Fig. 1q, v, 2a). Algae are, however, increasingly entrained into aphotic layers (marked in dark blue in Fig. 1t, y) where respiration exceeds production. Consequently, algal biomass peaks and starts to decline again at intermediate water column depths (Fig. 1q, v, 2a). With further increases in water column depth algal self shading therefore decreases and specific production increases at all depths (Fig. 1t, y). The aphotic part of the water column increases, however, disproportionately (Fig. 1t, y), and the water column eventually exceeds a maximal depth where depth-averaged light supply is too low to sustain an algal population (Huisman et al. 1999). This maximal depth is somewhat smaller at higher turbulence where algal entrainment to aphotic depths is strongest (Fig. 1q, t, v, y, 2a).

At the other extreme, very low turbulence ($d = 0.1 \text{ m}^2 \text{ day}^{-1}$) promotes the establishment of pronounced vertical gradients. Slow transport of dissolved nutrients from depth to the surface and weak algal entrainment produce a steep vertical gradient in the algal C:P ratio (Fig. 1d). Consequently, specific algal

Fig. 2. Effects of water column depth and mixing intensity (indicated by the coefficient of turbulent diffusion d in legend) on equilibrium values of (a) the standing stock of algal biomass, integrated over the water column, (b) the depth at which the vertical algal biomass profile has its maximum, (c) the depth averaged concentration of dissolved nutrients, (d) the algal sedimentation rate, and (e) the pool of nutrients in the sediment layer in the 'standard' model.

production is strongly nutrient limited at the water surface and reaches a (rather low) maximum several meters below, where nutrient limitation is less severe (i.e. algal C:P is lower) and light availability is still moderate (Fig. 1e). Algal sinking is hardly counteracted by turbulent mixing. Algal biomass is therefore extremely low above the depth of maximal specific production (Fig. 1b, e) and is also very low overall (Fig. 2a), as most nutrients are locked up in the sediment (shallow water columns, Fig. 1a) or at aphotic depths (deep water columns, Fig. 1c). In very shallow water columns algal biomass has a maximum closest to the site of nutrient regeneration, i.e. just above the sediment surface (Fig. 1b). When the water column becomes so deep (> 7.5 m) as to be aphotic at the bottom, the biomass maximum ‘detaches’ from the sediment surface (Fig. 1b, e, 2b). Because vertical mixing is negligible, algal downward movement is governed by (relatively slow) sinking. In sufficiently deep water columns biomass and particulate nutrients then never reach the sediment and are instead respired and released into the water column while sinking through the aphotic zone. With increasing water column depth dissolved nutrients therefore accumulate in the aphotic zone (Fig. 1c), whereas algal sedimentation rate and nutrients in the sediment approach zero (Fig. 2d, e). Consequently, depth profiles become independent of water column depth (Fig. 1b-e) and depth-integrated biomass approaches an asymptote at high water column depths (Fig. 2a). At higher water column depths the asymptotic attractor is not an equilibrium but a limit cycle with a very small amplitude (hardly visible in Figs. 1d,e, 2). Environmental conditions leading to unstable attractors will be further treated in the discussion section. Overall, depth-integrated algal biomass is very low because of nutrient limitation. It has a maximum at an intermediate water column depth of 10 m (Fig. 2a), where the vertical nutrient gradient is steepest and the upward transport of nutrients is thus fastest (Fig. 1c).

A turbulence of $d = 1 \text{ m}^2 \text{ day}^{-1}$ is still weak enough to allow the establishment of pronounced vertical gradients that become independent of water column depth in sufficiently deep systems (Fig. 1g-j). Because of faster turbulent transport, nutrient limitation at the water surface is, however, less severe than at $d = 0.1 \text{ m}^2 \text{ day}^{-1}$ (see algal C:P, Fig. 1i). Algal biomass is therefore much higher (Fig. 1g) and specific algal production does not have a subsurface maximum, but is fairly evenly distributed across the upper 3-5 m (Fig. 1j). Higher biomass increases self shading, and the depth of the euphotic zone shrinks to < 4.5 m (Fig. 1j). Consequently, the biomass maximum ‘detaches’ from the sediment surface at a shallower depth than at $d = 0.1 \text{ m}^2 \text{ day}^{-1}$ (Fig. 1g, 2b). In shallow water columns, mineralized nutrients are taken up by algae close to the sediment, a large proportion of which is quickly returned to the sediment through algal sinking (Fig. 1f). This mechanism very effectively reduces the transport of mineralized nutrients to the euphotic zone. However, once water column depth exceeds 9 m, algae are nutrient replete at that depth (nutrient quota is at q_{max}) and remineralized nutrients can accumulate in the lower water column in dissolved form (Fig. 1h, 2c). Consequently, the amount of nutrients stored in the sediment decreases very strongly beyond 9 m water column depth (Fig. 1f, 2e), and a significant fraction of the nutrients recycled in the water column reach the euphotic zone (indicated by decreasing algal C:P, Fig. 1i). This boosts production, resulting in a step-like biomass increase with increasing water column depth (Fig. 2a). For the same reason step-like biomass increases are also observed at $d = 0.1$ and $10 \text{ m}^2 \text{ day}^{-1}$ (Fig. 2a, c, e).

The most complex patterns arise at intermediate turbulence ($d = 10 \text{ m}^2 \text{ day}^{-1}$), where the system is nearly well-mixed in shallow water columns, but exhibits distinct vertical gradients in deep water columns. Until a water column depth of c. 15 m, vertical profiles and depth-integrated/-averaged values of all

variables are therefore very similar to the well-mixed cases ($d \geq 100 \text{ m}^2 \text{ day}^{-1}$, Fig. 1, 2). In deeper water columns, a turbulence of $d = 10 \text{ m}^2 \text{ day}^{-1}$ is not sufficient to mix down a major part of the algal population below the euphotic zone (Fig. 1l), but nutrient transport to the surface is still fast enough to yield low algal C:P ratios and sustain an algal production maximum at the surface (Fig. 1n, o). Consequently, intermediate turbulence yields by far the highest depth-integrated biomass in deep water columns (Fig. 2a), where strongly mixed systems are limited by (depth-averaged) light availability, and more weakly mixed systems are limited by nutrient recycling.

Summarizing the effects of mixing intensity, depth-integrated biomass is highest at high mixing intensities in shallow water columns (where strong mixing prevents nutrient limitation at the surface) and at intermediate mixing intensities in intermediate to deep water columns (where intermediate turbulence best balances the trade off between sufficient nutrient supply to the photic layer and too much downmixing to aphotic depths; Fig. 2a). The depth in the water column where algal biomass concentration has its maximum decreases with increasing mixing intensity (Fig. 2b). Depth-averaged dissolved nutrient concentration uniformly decreases with increasing mixing intensity in relatively shallow water columns, but has a minimum at intermediate mixing intensity in deep water columns (Fig. 2c), because phytoplankton in deep, well-mixed water columns becomes so strongly light limited that only a fraction of the available nutrients can be sequestered. With increasing mixing intensity algal sedimentation rate decreases in shallow water columns (because entrainment counteracts sinking) but increases in deep water columns, because most biomass is respired before it reaches the bottom of a weakly mixed, deep water column (Fig. 2d). Consequently, the peak of sedimented nutrients appears at increasing water column depths with increasing mixing intensity (Fig. 2e).

Robustness of the observed patterns

Extensive numerical runs confirm that the above described patterns are robust against changes in environmental conditions. For example, changes in total nutrient content (initial $R_d = 10$ vs. 30 mg P m^{-3}) and background turbidity ($k_{bg} = 0.2\text{-}0.8 \text{ m}^{-1}$) of the system may have strong quantitative effects on depth-integrated biomass, depth-averaged dissolved nutrient concentration, and the amount of sedimented nutrients; still, at a given total nutrient content or background turbidity, changes in water column depth and turbulence produce the same qualitative patterns as described above (Appendix B, Fig. B1).

Numerical runs also show that the qualitative effects of water column depth and turbulence on the system do not depend on the assumption of flexible algal nutrient stoichiometry. Assuming that algal nutrient stoichiometry is fixed at the Redfield ratio has only relatively minor quantitative effects on most state variables; in contrast, the qualitative patterns produced by changes in water column depth and turbulence are remarkably similar between the fixed and ('standard') flexible stoichiometry models (compare Fig. 2 with Fig. C1 in Appendix C).

Light, nutrients, or sinking losses: what limits algal biomass?

There is a striking symmetry in the effects of water column depth and turbulence on phytoplankton net production, which is most easily seen from a three-dimensional plot of depth-integrated algal biomass in z - d space (Fig. 3a). On the one hand, low mixing intensity has a twofold negative effect on algal net growth, which is independent of water column depth: first, the downward movement of sinking algae out of the photic zone is hardly counteracted; second, the upward transport of recycled nutrients into the photic zone is very slow. On the other hand, low water column depth has also a twofold negative effect on algal net growth, which, in turn, is independent of turbulence: high sinking rates in shallow water columns firstly impose high direct losses on the population and secondly transfer particulate nutrients to the sediment, leading to nutrient depletion in the water column. Finally, the combination of high mixing intensity and a deep water column causes downmixing of phytoplankton to aphotic depths and, consequently, severe light limitation of algal production. Thus, depending on the exact combination of water column depth and mixing intensity, depth-integrated algal biomass may be limited predominantly by sinking losses, nutrient regeneration or light availability. As a result, depth-integrated biomass forms an approximately rectangular ridge in z - d space, with the highest biomasses occurring at intermediate water column depths and/or intermediate levels of turbulence (Fig. 3a; see also Fig. 4).

We explored the dominant mechanisms limiting algal biomass in greater detail using the ‘mixed nutrient’ and ‘light limitation’ models. A comparison of the resulting plots of depth-integrated algal biomass reveals that limitation by light and by sinking losses set the persistence boundaries of the phytoplankton population in z - d space, whereas nutrient regeneration limits algal biomass inside the persistence region (Fig. 3). The factors limiting phytoplankton persistence and biomass in the three model variants are discussed in detail below. In addition, the full set of depth-integrated/averaged state variables for the ‘mixed nutrient’ and ‘light limitation’ models is plotted in Appendix D. The analysis reveals the following patterns.

First, the persistence boundaries in all three model variants are essentially identical (Fig. 3). That this must be the case can be easily seen from an invasion analysis. If an algal population invades an empty system, algal biomass, particulate nutrients, and sedimented nutrients are initially all zero. Consequently, all nutrients are present in dissolved mineral form, allowing fast nutrient uptake by invading algae. Unless the overall nutrient content of the system and/or algal nutrient uptake rate are very low, the nutrient quota of invading algae is therefore maximal and algal growth is purely limited by light also in the ‘standard’ and ‘mixed nutrient’ models. Conditions that are sufficient for successful invasion by a purely light limited population are then also sufficient for successful invasion by a potentially nutrient limited population in the ‘standard’ and ‘mixed nutrient’ models. For reasonable assumptions on the magnitude of the nutrient uptake rate, the persistence boundaries of all three model variants are therefore fully explained by existing theory of light limited systems as follows.

Our ‘light limitation’ model is very similar to the approach of Huisman and Sommeijer (2002), who modeled the dynamics of a purely light limited, sinking phytoplankton population in the mixed surface layer of a stratified water column. Huisman and Sommeijer (2002) characterized four persistence boundaries in z - d space, which also apply to the three variants of our model. At very low turbulence entrainment cannot counteract sinking losses. The resulting persistence boundary (at $d = 0.03 \text{ m}^2 \text{ day}^{-1}$ in Fig. 3) has been

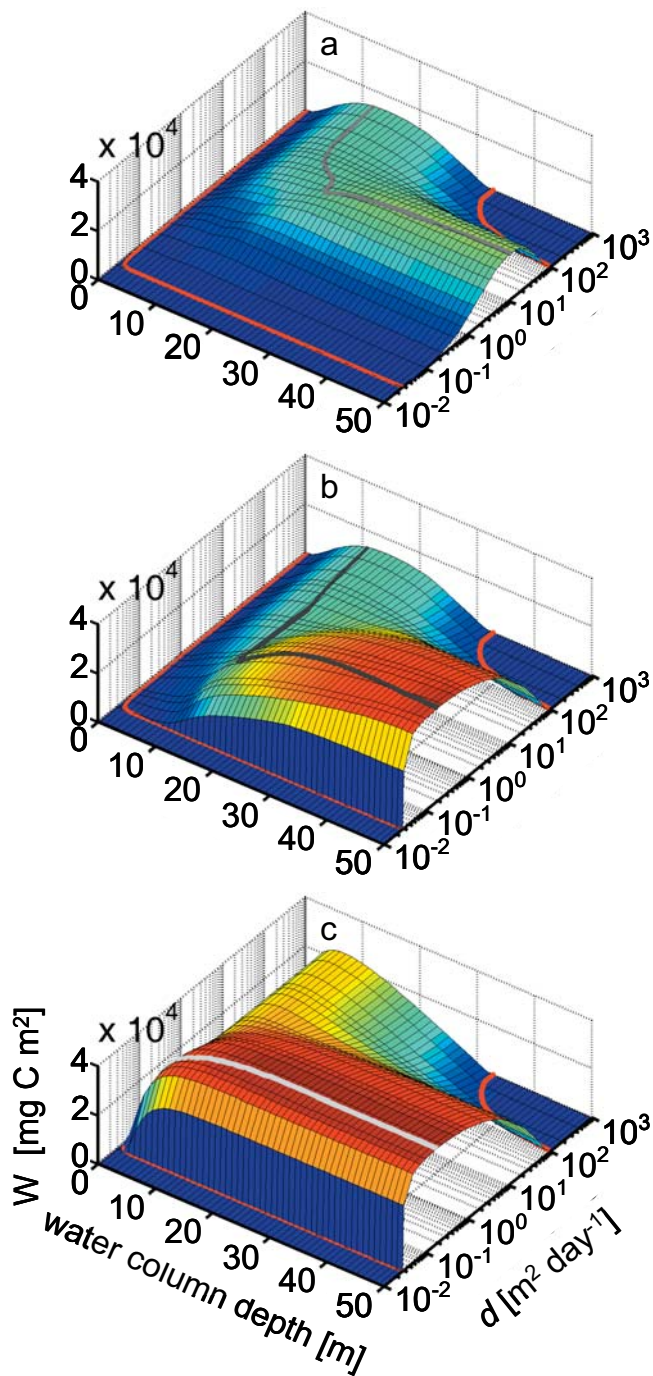


Fig. 3. Effects of water column depth and mixing intensity on the standing stock of algal biomass integrated over the water column in (a) the 'standard' model, (b) the 'mixed nutrient' model (mixing intensity for dissolved nutrients $d = 1000 \text{ m}^2 \text{ day}^{-1}$), and (c) the 'light limitation' model. Gray lines on top of the surfaces indicate the 'optimal mixing intensity' (= mixing intensity yielding the highest depth-integrated biomass for a given water column depth). Red lines at the base of the surfaces indicate persistence boundaries.

termed 'minimal turbulence' by Huisman et al. (2002). In very shallow water columns algal growth cannot compensate sinking losses. The resulting persistence boundary (at $z = 0.4 \text{ m}$ in Fig. 3) has been termed 'minimal depth' by Huisman and Sommeijer (2002). Finally, in deep and highly turbulent water columns algae cannot outgrow downmixing to aphotic depths. The resulting persistence boundaries (at $d = 77 \text{ m}^2 \text{ day}^{-1}$ and $z = 32 \text{ m}$ in Fig. 3) have been termed 'critical turbulence' and 'critical depth', respectively, by Huisman et al. (1999). Similar to earlier work on purely light-limited systems (Huisman and Sommeijer 2002), persistence is largely determined by *either* turbulence *or* depth; i.e., the persistence boundaries in z - d space are almost parallel to the z and d axes and their corners are only slightly rounded (Fig. 3).

Not surprisingly, for a given combination of water column depth and turbulence within the persistence boundaries, the purely light-limited system always attains the highest and the 'standard' system always the lowest algal biomass. The 'mixed nutrient' model takes an intermediate position, showing similar biomass patterns as the 'light limitation' model in deep water columns and as the 'standard' model in highly turbulent and in shallow water columns (Fig. 3, 4a). This supports the following interpretations of the mechanisms limiting biomass in the 'standard' model: (i) In deep water columns of intermediate to low turbulence algal biomass is similar and highest in the 'light limitation' and 'mixed nutrient' models, suggesting that

algal biomass in the ‘standard’ model is limited by the turbulent *transport rate* of mineralized nutrients from aphotic depths. (ii) In shallow water columns algal biomass is highest in the ‘light limitation’ model and similar and lowest in the ‘mixed nutrient’ and ‘standard’ models, suggesting that algal biomass in the latter two models is limited by the *mineralization rate* of nutrients in the sediment. (iii) Close to the upper persistence boundaries in z - d space, all three models attain similar biomasses, suggesting that algal biomass is light limited in deep, turbulent water columns.

The contrasting influences of water column depth and turbulence on nutrient vs. light limitation are also reflected in the position and shape of the ‘optimal turbulence’ isoline, i.e. the turbulence yielding the highest biomass at a given water column depth (Fig. 4b). Increased light limitation (e.g. increasing background turbidity) moves the optimal turbulence towards lower mixing intensities, where downmixing of phytoplankton to light limited layers is reduced; in contrast, increased nutrient limitation (e.g. decreasing total nutrient content of the system or increasing nutrient storage in sediments at lower water column depths) moves the optimal turbulence towards higher mixing intensities, where upward transport of nutrients is increased (Fig. 4b).

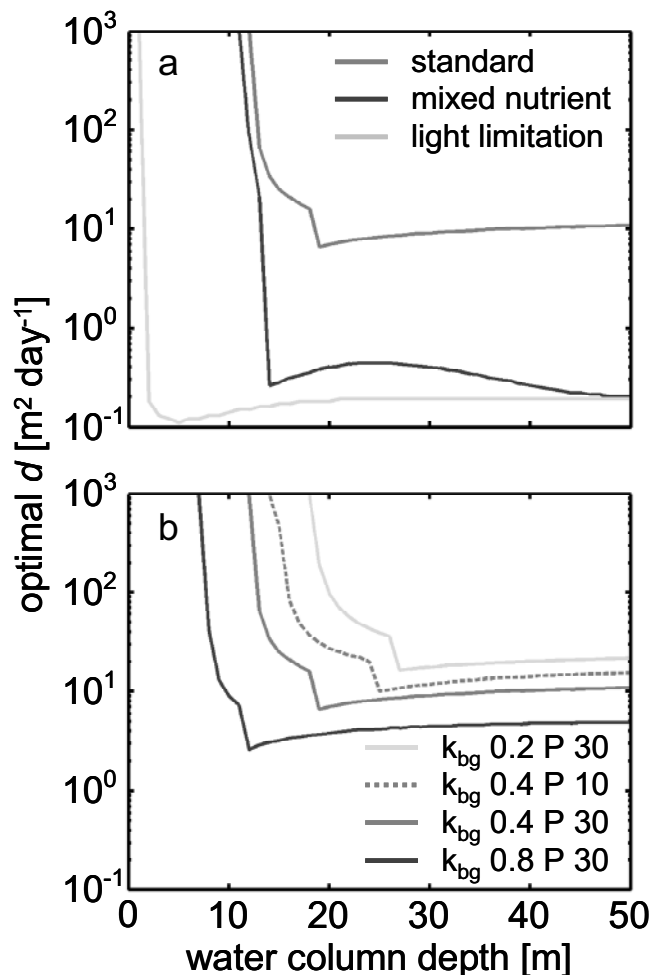


Fig. 4. (a) Effects of water column depth on ‘optimal mixing intensity’ (= mixing intensity yielding the highest depth-integrated biomass for a given water column depth) in the ‘standard’, ‘mixed nutrient’, and ‘light limitation’ models as indicated by legend. (b) Effects of water column depth on ‘optimal mixing intensity’, in the ‘standard’ model at different background turbidities (k_{bg}) and initial nutrient concentrations

Discussion

We have asked in a very general way how water column depth, gravity and turbulence affect the vertical distributions of phytoplankton, dissolved, suspended and sedimented nutrients, and how physical constraints on the vertical fluxes of light, nutrients and algae limit the biomass of pelagic primary producers. Our theoretical analysis reveals that sinking losses and light supply determine the persistence boundaries of a population of negatively buoyant algae in z - d space. This merely confirms earlier results by Huisman and Sommeijer (2002) obtained for light limited phytoplankton. Most natural phytoplankton populations are, however, at least co-limited by nutrients. In the absence of lateral nutrient fluxes and within the persistence boundaries set by sinking losses and light supply, phytoplankton biomass is then expected to be most strongly limited by the rates determining nutrient recycling.

Our analysis suggests that nutrient recycling in shallow water columns is most strongly limited by the mineralization rate in the sediment, whereas in deep water columns turbulent upward transport of mineralized nutrients is most limiting. The highest depth-integrated production is therefore sustained in deep water columns with intermediate turbulence, where convective transport of algae to the sediment is very low (because algal biomass is respired and mineralized before it reaches the bottom) and turbulent upward transport of nutrients mineralized in aphotic strata is relatively fast. In other words, phytoplankton production and biomass are highest the higher the net vertical transport rate of nutrients from the zone of nutrient regeneration (sediment and/or deep water) to the zone of nutrient use by primary producers (well-lit surface strata). This parallels a similar result obtained by Cloern (2007) who analysed the influence of *lateral* connectivity between a shallow, well-lit but nutrient-depleted habitat and a deep, light limited but nutrient replete habitat and found that overall productivity (averaged across both habitats) was highest the higher the water exchange rate and, thus, the nutrient transport rate from the deep to the shallow habitat.

Transient dynamics, persistent oscillations, and competitive interactions

Differences in speed of the two major, opposite vertical nutrient fluxes (sinking of particulate nutrients and upward flux of recycled, dissolved nutrients) are not only responsible for steady state biomass patterns in z - d space but also for the development of transient phytoplankton blooms under most environmental conditions. From initial conditions of high dissolved nutrient concentration, an algal population starting from low initial density goes always through a transient bloom before settling on its asymptotic trajectory, with the exception of strongly light limited conditions close to the persistence boundary at high water column depth and high turbulence (C. Jäger, unpublished results). This happens because the initially high dissolved nutrient concentration stimulates fast algal growth in the upper, well-lit layers, which is followed by algal sinking and rapid nutrient depletion terminating the bloom (see Huppert et al. 2002). Algal sinking leads to a relatively fast downward flux of particulate nutrients. The latter is only slowly counteracted by turbulent upward transport of recycled nutrients from aphotic depths, which subsequently sustains a steady state biomass much smaller than the transient peak biomass.

The interaction of these opposed vertical nutrient fluxes can actually generate persistent oscillations or even chaotic population dynamics of algal biomass. Such unstable attractors occur, if after an algal bloom nutrients are completely depleted in the euphotic zone and when the timescale of algal down

flux is fast compared to the timescale of the nutrient upward flux (Huisman et al. 2006). Usually these requirements are met at low mixing intensities and high algal sinking velocities. The timescale of the nutrient upward flux increases with decreasing mixing intensity and increasing water column depth. Hence, in our model persistent oscillations occur at the lowest mixing intensity ($d = 0.1 \text{ m}^2 \text{ day}^{-1}$) and in deep water columns. The oscillations become more pronounced at a lower overall nutrient content of the system (initial $R_d = 10 \text{ } \mu\text{g P L}^{-1}$), where the nutrient upward flux is reduced, and at a higher light supply ($k_{lg} = 0.2 \text{ m}^{-1}$), where production is possible at greater depths and, consequently, net mineralization in the water column is reduced and more nutrients are mineralized in the sediment layer (Appendix B, Fig. B1, B2).

In real plankton communities consisting of multiple species the dynamic interplay of algal sinking and nutrient recycling at aphotic depths will affect the outcome of competitive interactions among phytoplankton taxa differing in their capabilities of buoyancy regulation. For example, in the absence of nutrient limitation buoyant taxa will often have a competitive advantage under conditions of low turbulence through the formation of surface blooms, thus shading deep water layers where sinking taxa tend to accumulate (Visser et al. 1996; Huisman et al. 2004). Surface blooms can, however, only be sustained when enough nutrients are supplied to the upper water layers to support algal growth. In field enclosures with low turbulent mixing Jäger et al. (submitted) observed that an initial dominance of motile species occupying the upper strata of the water column was subsequently replaced by a dominance of fast sinking diatoms when nutrients became limiting at the surface. A plausible explanation for this observation (consistent with vertical profiles of dissolved nutrients) is that the diatoms, which primarily occupied deeper strata of the water column, intercepted the upward transport of recycled nutrients, causing severe nutrient limitation at the surface.

Spatial structure, flexible algal stoichiometry, and higher trophic levels

In the simple 2-compartment model of Cloern (2007) the beneficial effects on algal production of a high (lateral) exchange rate between a shallow, nutrient limited and a deep, light limited habitat are directly transmitted to the next higher trophic level; i.e., the production of herbivorous zooplankton (averaged across both habitats) is highest the higher the (passive) exchange rate of nutrients and organisms between the two habitats. In contrast, in our model increased primary production may not always translate into increased herbivore production for at least two reasons. First, in contrast to Cloern (2007) we assumed that algal carbon to nutrient stoichiometry is flexible. Second, the distance between nutrient and light limited habitats is short enough to be easily covered by (vertically) migrating herbivores, potentially decoupling the transport rates of nutrients, algae, and herbivores.

Our model analyses suggest that the qualitative influences of water column depth and turbulence on a phytoplankton system lacking herbivores are not crucially dependent on the assumption of flexible vs. fixed algal carbon to nutrient stoichiometry. In a system with herbivores flexible producer stoichiometry may, however, lead to a mismatch of producer elemental composition and herbivore nutrient requirements. In particular, depending on the light to nutrient supply ratio there is often a trade-off between food quantity (algal carbon density) and food quality (carbon to nutrient ratio of algal biomass) (Urabe and Sterner 1996). In water columns of differing depth and turbulence, herbivore production may therefore not always follow the same pattern as primary production. For well-mixed water columns an extension

of our model including herbivores suggests indeed that low algal quality (high algal C:P ratio) can limit herbivore biomass at relatively shallow depths (more generally speaking: at relatively high light supply) where algal biomass in the absence of grazers would be close to maximal (Diehl 2007; Jäger et al. 2008), a phenomenon called the ‘paradox of energy enrichment’ that has been observed in several experiments (Andersen et al. 2004).

In incompletely mixed water columns the situation is more complex. Mobile grazers such as *Daphnia* can sense vertical gradients in foraging profitability (determined by algal density and quality) and move along them towards the depth offering optimal food conditions (Schatz and McCauley 2007). Additionally, grazers performing diel vertical migrations could benefit from carbon rich algal food close to the surface during night and nutrient rich food in deeper layers during day (Sterner and Schwalbach 2001). Because grazers rarely incorporate all ingested nutrients into new biomass, vertically migrating herbivores may furthermore act as a vector moving particulate nutrients from the depth of ingestion to the depth of waste excretion. Thus, many more processes may contribute to the vertical transport of grazers, algae and nutrients in stratified vs. well-mixed water columns. Preliminary modelling suggests indeed that grazer biomass responds differently to water column depth in stratified vs. well-mixed water columns (S. Diehl, unpublished results).

Physical water column structure and community dynamics

Ecologists increasingly appreciate the roles of spatial structure and biological and physical transport processes as mechanisms of population, community and ecosystem dynamics (Polis et al. 1997; Reiners and Driese 2001). Driven by weather and climate, the physical environment of aquatic systems can be highly variable. In the actual debate on global climate change the physical environment has therefore been set into new focus (Behrenfeld et al. 2006; Falkowski and Oliver 2007). For example, there is evidence that global warming will lead to earlier and more shallow stratification and increased water column stability (Sarmiento et al. 1998; Lehman 2000; George and Hewitt 2006; Coats et al. 2006). In temperate lakes the timing and depth of stratification sets, in turn, the stage for events such as the phytoplankton spring bloom, a clearwater phase caused by intense grazing, and the subsequent establishment of a summer community (Sommer et al. 1986; Straile 2002; Berger et al. 2006; 2007; Peeters et al. 2007b). Clearly, the physical structure of the water column has potentially far reaching implications not only for the ecosystem processes (primary production, sinking export, nutrient recycling etc.) explored in our study, but also for community processes such as food web dynamics and seasonal succession. Although we have so far restricted our analyses to a system with a single algal species, we believe our approach provides a useful framework for the investigation of these more complex community interactions in pelagic environments.

Acknowledgments

We thank O. Richter for the introduction into COMSOL. This study was supported by funding from Deutsche Forschungsgemeinschaft (DI 745/2-4).

Appendix A: Technical details of the numerical approach and boundary conditions

The model was implemented in COMSOL with two 1-dimensional compartments: a water column and a sediment layer. The water column runs from the surface (0) to the bottom (z_{\max}). Within the water column we calculated algal carbon biomass (A), particulate nutrients bound in algae (R_b) and dissolved mineral nutrients (R_d) and light intensity (I). A , R_b , and R_d were calculated with eqs. 1-3. COMSOL is a software package designed for the solution of multiphysical problems in time and in space by means of a finite element method. The special requirements of our computation are most easily implemented within this software package if they are formulated as differential equations. Therefore, the light intensity within the water column was implemented as:

$$0 = -(k \cdot A + k_{bg})I + \frac{\partial I}{\partial z} \quad (\text{A1})$$

This alternative, but equivalent formulation to eq. 4 has two major advantages within the given framework of the finite-element software: first, the evaluation of the integral is not necessary each time the value of I is needed somewhere in the calculation. Second, the computation of I is implicit in time similar to the computation of the other variables. Consequently, time steps are not limited by any explicit computation and the correlation enters properly the coefficient matrix of the implicit solver. The boundary conditions are assumed to be a fixed concentration at the surface (I_0) and ‘convective flux’ at the bottom (Table A1). Within the sediment layer only the pool of sedimented nutrients was calculated. Therefore the ordinary differential equation (eq. 5), which is the amount of nutrients per area, was transformed into a partial differential equation, which calculates the concentration of nutrients (i.e. per volume):

$$\frac{\partial R_s}{\partial t} = d_s \frac{\partial^2 R_s}{\partial z^2} \quad (\text{A2})$$

To simplify the calculations we assumed a fixed thickness of the sediment layer of 1 m, where the concentration of nutrients [mg P m^{-3}] is equal to the pool of nutrients [mg P m^{-2}]. The mixing intensity within the sediment layer of $d_s = 1000 \text{ m}^2 \text{ day}^{-1}$ prevented any vertical gradients of R_s . Changes of R_s were implemented by boundary fluxes over the sediment-water interface, with an influx of sedimented particulate nutrients and an outflux of remineralized nutrients (i.e. $v \cdot R_b(z_{\max}) - r \cdot R_s$) (Table A1).

The calculations were performed using standard Lagrange elements of 2nd order with a vertical grid of 0.02 m. Time discretization is done implicitly, where the time step was chosen automatically by the solver. The resulting system of linearized algebraic equations was solved by a direct solver. No convergence problems were encountered.

Table A1. Boundary conditions for algal biomass (A), particulate nutrients (R_b), dissolved nutrients (R_d), light (I), and sedimented nutrients (R_s) at the surface ($z = 0$), at the sediment-water interface ($z = z_{\max}$) and at the bottom of the sediment layer ($z = z_{\max} + 1$ m)

	$z = 0$	$z = z_{\max}$	$z = z_{\max} + 1$ m
A	$vA - d \frac{\partial A}{\partial z} = 0$	$\frac{\partial A}{\partial z} = 0$	
R_b	$vR_b - d \frac{\partial R_b}{\partial z} = 0$	$\frac{\partial R_b}{\partial z} = 0$	
R_d	$\frac{\partial R_d}{\partial z} = 0$	$-rR_s - d \frac{\partial R_d}{\partial z} = 0$	
I	$I = I_0$	$\frac{\partial I}{\partial z} = 0$	
R_s		$-vR_b + rR_s - d_s \frac{\partial R_s}{\partial z} = 0$	$\frac{\partial R_s}{\partial z} = 0$

Appendix B.

Effects of water column depth and turbulence under different environmental conditions.

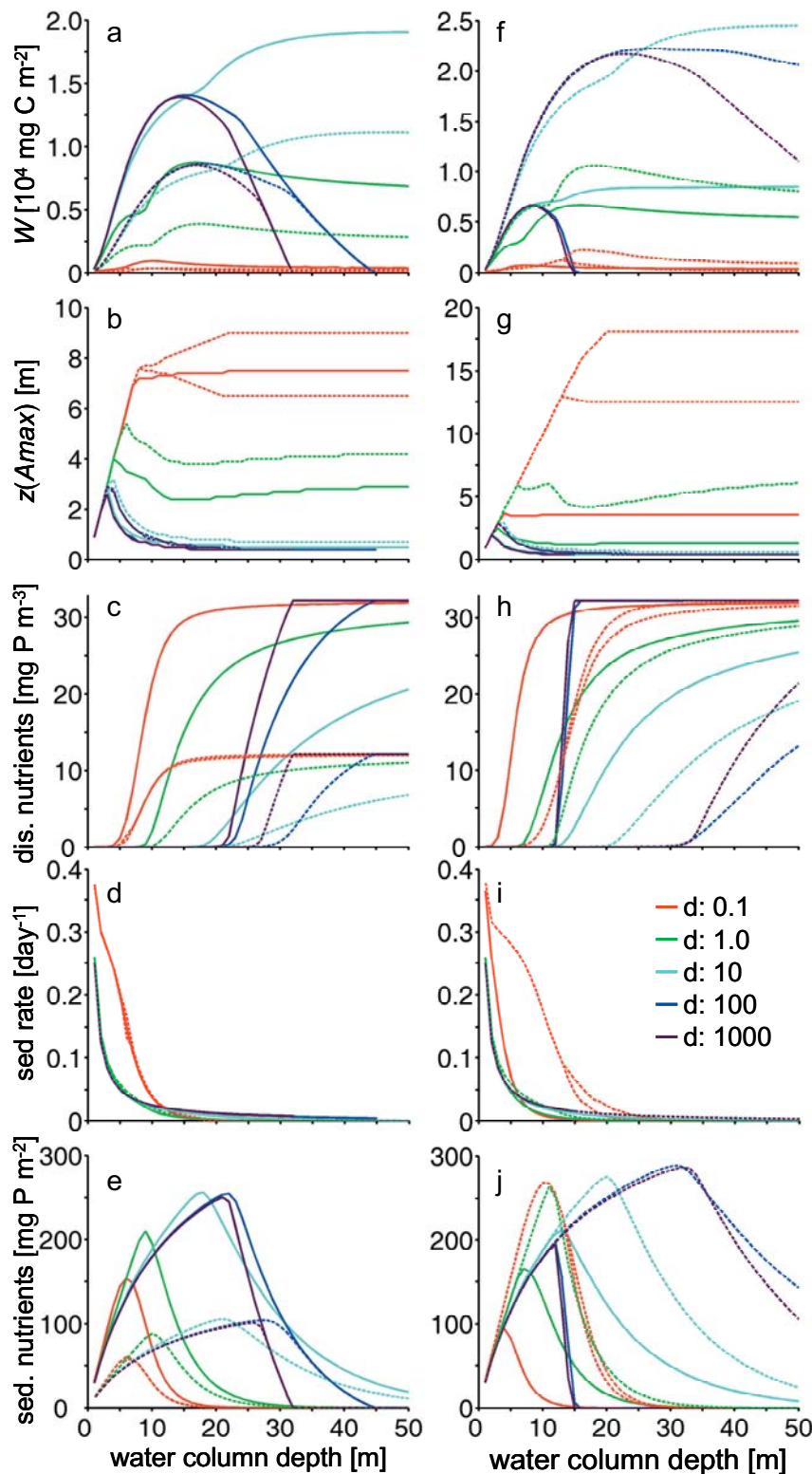


Fig.B1. Effects of water column depth and mixing intensity (indicated by the coefficient of turbulent diffusion d in legend) on equilibrium values of (a, f) the standing stock of algal biomass, integrated over the water column, (b, g) the depth at which the vertical algal biomass profile has its maximum, (c, h) the depth averaged concentration of dissolved nutrients, (d, i) the algal sedimentation rate, and (e, j) the pool of nutrients in the sediment layer. Left column of panels (a-e): comparison of different initial dissolved nutrient concentrations (full lines: initial concentration = 30 mg P L^{-1} , dashed lines: initial concentration = 10 mg P L^{-1} ; background turbidity $k_{bg} = 0.4\text{ m}^{-1}$ in both cases). Right column of panels (f-j): comparison of different background turbidities (full lines: $k_{bg} = 0.8\text{ m}^{-1}$, dashed lines: $k_{bg} = 0.2\text{ m}^{-1}$; initial dissolved nutrient concentration $R_d = 30\text{ mg P L}^{-1}$ in both cases). At an initial dissolved nutrient concentration of 10 mg P L^{-1} and at a background turbidity of $k_{bg} = 0.2\text{ m}^{-1}$ the system oscillates at a coefficient of turbulent diffusion d of $0.1\text{ m}^2\text{ day}^{-1}$; in these cases upper and lower bounds are shown in the panels by branching lines.

Appendix C.

Effects of water column depth and turbulence in the fixed stoichiometry model.

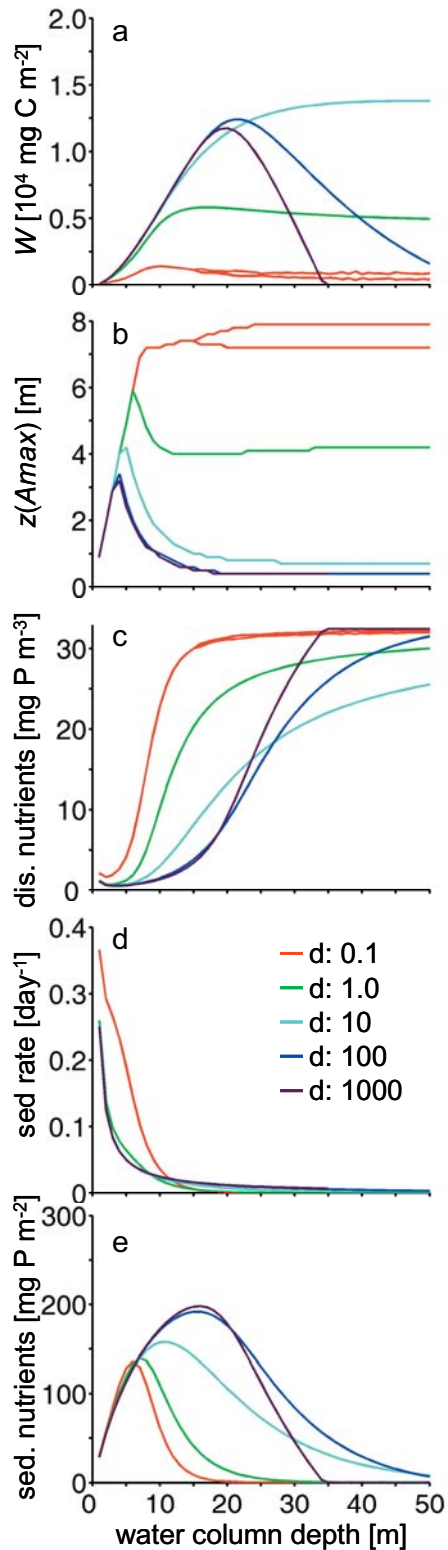


Fig. C1. Effects of water column depth and mixing intensity (indicated by the coefficient of turbulent diffusion d in legend) on equilibrium values of (a) the standing stock of algal biomass, integrated over the water column, (b) the depth at which the vertical algal biomass profile has its maximum, (c) the depth averaged concentration of dissolved nutrients, (d) the algal sedimentation rate, and (e) the pool of nutrients in the sediment layer in the 'fixed stoichiometry' model with ($q_{fix} = 0.0244$). The system oscillates at a coefficient of turbulent diffusion d of $0.1 \text{ m}^2 \text{ day}^{-1}$; in these cases upper and lower bounds are shown in the panels by branching lines.

Appendix D.

Effects of water column depth and turbulence in the 'mixed nutrient' and 'light limitation' models.

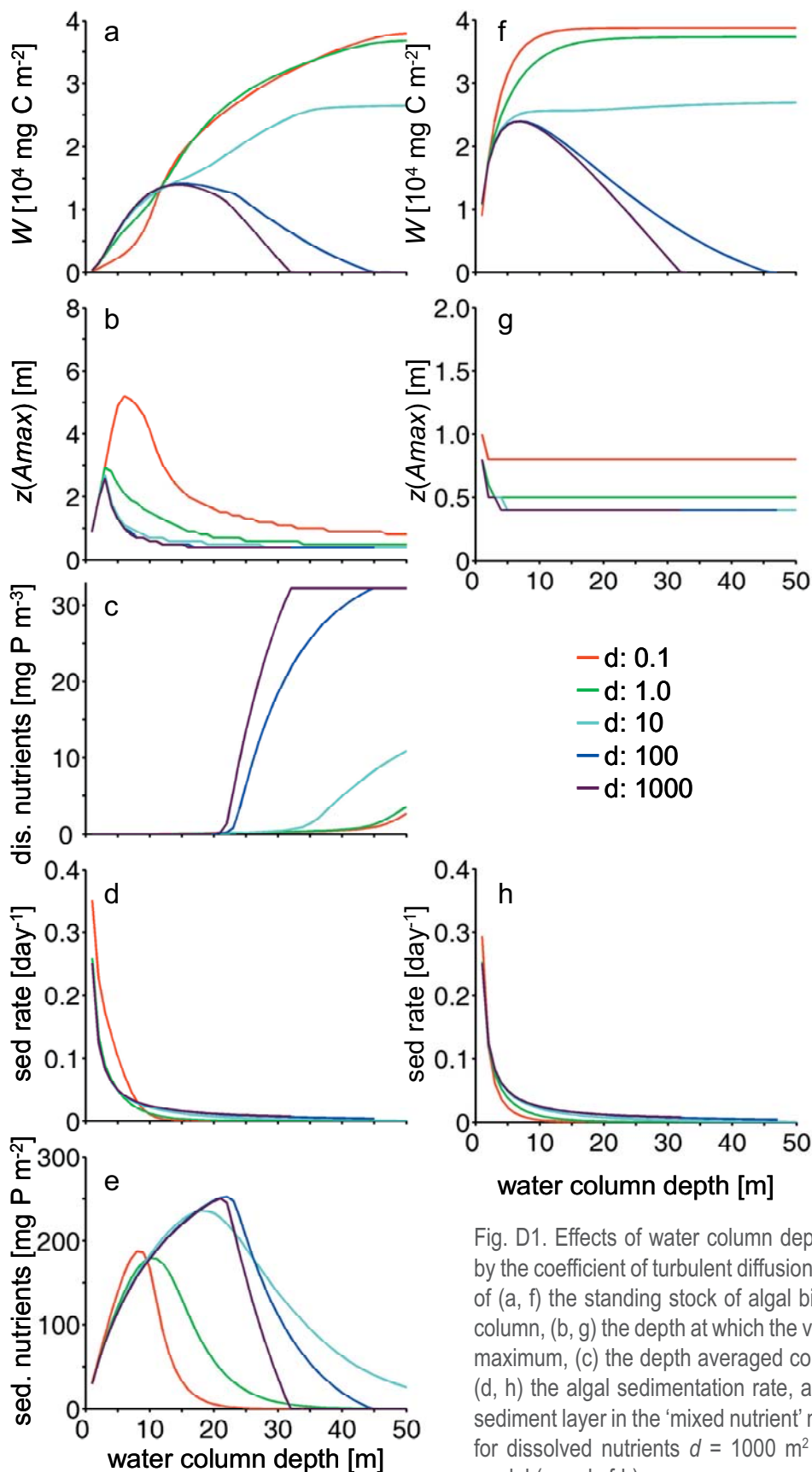


Fig. D1. Effects of water column depth and mixing intensity (indicated by the coefficient of turbulent diffusion d in legend) on equilibrium values of (a, f) the standing stock of algal biomass, integrated over the water column, (b, g) the depth at which the vertical algal biomass profile has its maximum, (c) the depth averaged concentration of dissolved nutrients, (d, h) the algal sedimentation rate, and (e) the pool of nutrients in the sediment layer in the 'mixed nutrient' model (panels a-e; mixing intensity for dissolved nutrients $d = 1000 \text{ m}^2 \text{ day}^{-1}$) and in the 'light limitation' model (panels f-h).

Chapter 2

Influence of water column depth and mixing on phytoplankton biomass, community composition, and nutrients

Christoph G. Jäger,
Sebastian Diehl,
and Gertraud M. Schmidt

in revision: Limnology and Oceanography

Abstract

We independently manipulated mixing intensity (strong artificial mixing vs. background turbulence) and water column depth (2, 4, 8, and 12 m) to explore their separate and combined effects in a field enclosure experiment. To accentuate the vertical light gradient, enclosures had black walls resulting in a euphotic depth of only 3.7 m. All enclosures were placed in a well-mixed water bath to equalize temperature across treatments. Phytoplankton responded to an initial phosphorus pulse with a transient increase in biomass, which was highest in the shallowest, least light limited water columns where dissolved mineral phosphorus subsequently became strongly limiting. As a consequence, the depth-averaged mineral phosphorus concentration increased and the seston C:P ratio decreased with increasing water column depth. Low turbulence enclosures became quickly dominated by motile taxa (flagellates) in the upper water column, whereas mixed enclosures became gradually dominated by pennate diatoms, which resulted in higher average sedimentation rates in the mixed enclosures over the 35 day experimental period. Low turbulence enclosures showed pronounced vertical structure in water columns > 4 m, where diversity was higher than in mixed enclosures, suggesting vertical niche partitioning. This interpretation is supported by a primary production assay, where phytoplankton originating from different water depths in low turbulence treatments had the relatively highest primary productivity when incubated at their respective depths of origin.

Introduction

Physical conditions, notably the depth of the water column and the intensity of mixing, influence population dynamics of pelagic primary producers by affecting the average light climate, sedimentation losses, and the availability of nutrients (Huisman et al. 1999, 2006; O'Brien et al. 2003). For example, under well-mixed conditions phytoplankton are passively entrained in the entire water column and, over time, each algal cell experiences the depth-averaged light intensity, which is a decreasing function of water column depth. Consequently, depth-averaged specific primary production decreases with increasing water column depth (Huisman 1999; Diehl et al. 2002, 2005) and will become insufficient for the maintenance of a viable population when the mixed water column exceeds a 'critical depth' (Sverdrup 1953). In contrast, in a weakly mixed water column the velocity of entrainment will often be slower than the rate of algal reproduction. Consequently, algal cells can remain in the well-lit upper part of the water column for long enough to maintain a population even if the water column exceeds the 'critical depth' (Huisman et al. 1999).

Water column depth and mixing intensity also affect algal sedimentation losses. The probability of an individual algal cell or colony to sink out of the water column increases with increasing sinking velocity and decreasing water column depth, but decreases with increasing mixing intensity (Visser et al. 1996; Condie and Bormans 1997; Ptacnik et al. 2003). The latter occurs because turbulent mixing disperses phytoplankton in the water column and therefore partly counteracts sedimentation; overall, sinking losses should thus be most severe for fast sinking algae in shallow and weakly mixed water columns (Diehl 2002; Huisman et al. 2002).

Algal sedimentation constantly removes particular nutrients from the water column, which are subsequently mineralized and recycled back into the water column from below. In sufficiently deep and weakly mixed water columns nutrients may therefore become strongly limiting close to the surface but be available in excess in deeper layers, creating a vertical gradient in mineral nutrient concentration (Klausmeier and Litchman 2001; Huisman et al. 2006). In well-mixed water columns vertical gradients are absent and nutrient availability is expected to depend exclusively on total water column depth. Nutrient concentrations should be low in shallow water columns, where algal sinking removes particulate nutrients at high rates, and high in deep water columns, where algal production and nutrient use is strongly light limited (Huisman and Weissing 1995; Diehl 2002). Flexible algal stoichiometry may, however, weaken or even mask this relationship (Diehl et al. 2005). It is well known that the elemental composition (e.g., the carbon to phosphorus ratio, C:P) of algal biomass varies in response to the relative supplies with light and nutrients (Sterner et al. 1997). 'Excess' nutrients in deep water columns may therefore be taken up (and stored) by phytoplankton even if production is light limited, leading to pronounced differences in algal C:P - and less pronounced differences in mineral nutrient concentration - among well-mixed water columns of different depths (Diehl et al. 2005; Berger et al. 2006). Similarly, within weakly mixed water columns gradients of vertically decreasing seston C:P ratios are to be expected (Rothhaupt 1991; Elser and George 1993; Park et al. 2004).

By mediating light and nutrient availability, water column depth and mixing intensity may also profoundly affect the outcome of competition among planktonic algae. In well-mixed systems, nutrients and algae are homogeneously distributed in the water column. Strong mixing therefore minimizes the

possibilities for spatial niche differentiation. Under constant environmental conditions, those taxa that reduce the light intensity at the bottom of the water column to the lowest level and the limiting nutrients to the lowest concentrations will then displace all other competitors, allowing at best a few species to persist in the long run (Sommer 1985; Huisman and Weissing 1995; Passarge et al. 2006). In contrast, coexistence by means of vertical niche separation is possible in weakly mixed systems (Reynolds 1992). For example, a superior competitor for light may coexist with a superior competitor for nutrients, with the former dominating at deeper and the latter at shallower water depths (Huisman et al. 2006).

The outcome of algal competition in response to mixing intensity and water column depth depends, however, not only on algal traits related to resource use but also on buoyancy. Several studies have reported that systems could be moved back and forth from dominance of buoyant taxa in weakly or shallowly mixed water columns to dominance of fast sinking taxa in deeply mixed water columns by turning off and on artificial mixing (Reynolds et al. 1983; Visser et al. 1996; Huisman et al. 2004). Thus, buoyant taxa benefit from stratified conditions (Sherman et al. 1998). Buoyancy may also enable coexistence of a weaker competitor (for light) with a superior one (Litchman 2003). In particular, motile taxa may benefit from weak mixing intensity, because low turbulence enables them to move to depths with optimal growth conditions (Klausmeier and Litchman 2001). Such habitat choice could accentuate vertical niche separation of different taxa (Elliott et al. 2002; Clegg et al. 2007). Thus, if weak mixing leads to the development of multiple gradients of growth enhancing and inhibiting environmental parameters, this could enable substantial vertical niche partitioning and enhance diversity compared to a well-mixed system of the same overall depth.

In conclusion, water column depth and mixing intensity influence phytoplankton biomass, community composition, and vertical distribution through a multitude of interacting processes. Clearly, our understanding of the interplay among these processes would benefit from appropriately designed field experiments. So far, however, experiments on the role of mixing intensity have been limited to cases where periods of intermittent stratification and mixing were alternated (Reynolds et al. 1983, 1984; Flöder and Sommer 1999) and experiments on the role of water column depth have been limited to well-mixed systems (Diehl et al. 2002, 2005; Ptacnik et al. 2003). We therefore conducted a field experiment in which we manipulated mixing intensity and water column depth independently from each other in a full factorial design. To our knowledge this is the first experiment of its kind.

Methods

Study site and experimental design

The experiment was carried out in Lake Brunnsee near the University of Munich's Limnological Research Station at Seeon (90 km east of Munich, Germany). At the beginning of our experiment chlorophyll *a* (Chl *a*) concentration in this 5.8 ha, low productivity hardwater lake was $2.5 \mu\text{g L}^{-1}$, and total phosphorus concentration was $10 \mu\text{g L}^{-1}$. The concentrations of other potentially growth limiting nutrients were far in excess of algal needs (nitrogen: 2.3 mg L^{-1} , silicate: 2.6 mg L^{-1}). The euphotic depth in the lake was about 16 m during the experiment.

We independently manipulated four enclosure depths (2, 4, 8, and 12 m) and two contrasting mixing intensities [no artificial mixing (subsequently called 'unmixed') and strong, artificial mixing (subsequently called 'mixed')] in two replicates per treatment (Plate 1). The enclosures (cylindrical, transparent plastic bags of 0.95 m diameter, heat sealed at the bottom and open to the atmosphere) were suspended from a raft and filled with $30 \mu\text{m}$ filtered epilimnetic lake water containing the ambient phytoplankton community on 27-28 July 2005. To stimulate algal production we fertilized the enclosures with $30 \mu\text{g P L}^{-1}$, added as KH_2PO_4 , on 02 August (= day 0 of the experiment). We maintained the artificial mixing of the 'mixed' enclosures for 56 days (until 27 September). However, convective nightly mixing occurred frequently in the 'unmixed' treatments from day 35 on (*see below*), diminishing the differences between the two turbulence treatments. We therefore analyzed in detail only the samples covering the first 35 days of the experiment and restrict the presentation of results to this period.

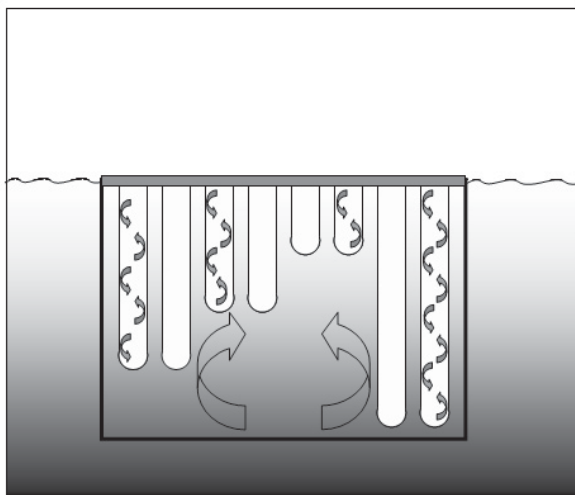


Plate 1. Schematic diagram of the experimental raft with enclosures of four different depths (2, 4, 8, and 12m) and two contrasting mixing treatments (no artificial mixing and strong, artificial mixing [indicated by arrows]). The entire raft was surrounded by a well-mixed outside bag.

The transparent enclosure walls were surrounded by black silage film to mimic higher background turbidity and to isolate them optically from the surrounding water. This resulted in a depth averaged light attenuation coefficient of 1.2 m^{-1} and a euphotic depth (where photosynthetic active radiation (PAR) was reduced to 1% of incident PAR) of 3.7 m during the experiment. The depth-averaged light availabilities in the mixed 2, 4, 8, and 12 m enclosures corresponded to the ambient light levels at water depths of 0.8, 1.3, 1.9, and 2.2 m, respectively, in a non-mixed column. The mixed enclosures were intermittently mixed (for 5 min every 30 min) to maintain homogeneous conditions by pumping air to the bottom of each enclosure.

To accomplish true independence of the turbulence and water column depth treatments, turbulence had to be the same everywhere in the different water columns, which required the absence of vertical temperature gradients. To this end we surrounded the entire raft with a 14 m deep bag of clear plastic. The water inside this bag was intermittently mixed (for 5 min every 30 min), creating a water bath of homogeneous temperature. The mixing was highly effective. Water temperatures in any two enclosures differed by less than 0.5°C at 1 m depth, and vertical temperature differences between the surface and 11 m in the outside bag were, averaged over the experimental duration, less than 1°C. A further average decline of 1.3°C occurred at the bottom of the unmixed 12 m enclosures. Despite the heat exchange with the well-mixed outside bag, slight warming (mean 0.6°C, maximum 1.6°C) could not be entirely prevented near the surface of the unmixed enclosures during daytime. To prevent unmixed enclosures from being convectively mixed by nightly cooling, we covered all enclosures with isolating styrofoam boards (specific heat conductivity: 0.040 W m⁻¹ K⁻¹) approximately 10 cm above the water surface during nighttime. We monitored the isolating effect of this procedure by recording once every 30 minutes the water temperature at the surface and the air temperature between the water surface and the isolating boards (K204 Datalogger; Voltcraft Plus, Conrad Elektronik, Germany) in one deep and one shallow, unmixed enclosure. Simultaneously, the air temperature on the raft and the water temperature at the surface of the outside bag were recorded. During the reported experimental period (days 0-35) surface temperatures in the outside bag ranged from 13.3 to 16.4°C.

We roughly estimated the intensity of turbulence in the two mixing treatments by measuring the vertical spread of a fluorescein-sodium tracer released in the middle of the water columns (Peeters et al. 1996). The coefficient of vertical turbulent diffusion was approximately 330 m² d⁻¹ (= 3.8 10⁻³ m² s⁻¹) in the mixed enclosures, measured once at the end of the experiment. In the unmixed enclosures we expected mixing intensity to vary over time (depending on water and air temperatures) and therefore performed several tracer measurements during the course of the experiment. To avoid interference with the experiment we performed these measurements in separate, non-mixed enclosures (one per enclosure depth). Mixing intensities in these additional unmixed enclosures ranged from 0.02 m² d⁻¹ (= 2.3 10⁻⁷ m² s⁻¹, at daytime on a sunny day) to 3.2 m² d⁻¹ (= 3.7 10⁻⁵ m² s⁻¹, in the morning hours of a cold night) during the first 35 days. Because measurements of mixing intensities were only taken sporadically, we used the continuous temperature recordings to estimate the occurrence of nightly convective mixing events. When early morning water temperatures at the surface of the unmixed enclosures were lower than the water temperature in the surrounding, well-mixed outside bag, we took this as evidence of nightly convective mixing events. Two such (very short) events were recorded in the mornings of days 25 and 34, but became increasingly common after day 35. This was corroborated by our turbulence measurements, which showed a complete convective mixing up to 4 m water depth with a corresponding diffusivity constant higher than 17.5 m² d⁻¹ (= 2.0 10⁻⁴ m² s⁻¹) on day 56. The measured constants of diffusivity cover the full range observed in natural systems from about 0.01 m² d⁻¹ (~ 10⁻⁷ m² s⁻¹) in stratified systems up to 1000 m² d⁻¹ (~10⁻² m² s⁻¹) in highly mixed systems (MacIntyre et al. 1999; Peeters et al. 2007b).

Sampling program and laboratory analyses

Three times during the experiment we measured vertical profiles of photosynthetic active radiation (PAR) in 1 m steps with a spherical quantum sensor (LI-193SA, Licor, Lincoln, Nebraska.). Once per week all enclosures were sampled for physical, chemical, and biological parameters. In vertical steps of 1 m, we measured water temperature and electrical conductivity (Lf 191 with probe LT1/T, WTW, Weilheim, Germany). In the mixed enclosures we sampled water at a depth of 0.5 m just after a mixing event. In the unmixed enclosures we sampled water from the depths of 0.5, 2.0, 3.5, 5.0, 7.5, and 11.5 m (where available) with a hand pump that did not disrupt the vertical structure of the water column. Water samples were analyzed within a few hours after sampling. The concentration of dissolved inorganic phosphorus (SRP) was measured using standard methods (Wetzel and Likens 1991). Seston was filtered on pre-combusted acid-washed glass fiber filters (Whatman GF/F) to determine particulate organic carbon (POC) with an elemental analyzer (EA 1110 CHNS, CE Instruments, UK) and particulate phosphorus (PP) by sulphuric acid digestion followed by molybdate reaction. Chlorophyll *a* (Chl *a*) concentrations were determined in vivo with a fluorometer (TD 700; Turner Design, USA).

Phytoplankton samples were immediately preserved with acid Lugol's iodine and later counted in an inverted microscope. In each sample we counted at least 100 individual cells from every abundant taxon and measured 20 to 50 individual cells using a digital image analysis system. Length measurements were converted to biovolume using appropriate geometrical forms.

To estimate sedimentation loss rates of phytoplankton, we suspended sedimentation traps just above the bottom of each enclosure. Each trap was a screw-lock glass jar (depth, 90 mm; opening diameter, 34 mm) with its locks removed. We replaced the traps weekly and filtered the contents on pre-combusted glass fiber filters (GF6, Schleicher & Schüll, Germany). Sedimented POC was determined by infrared-spectrophotometry (C-Mat 500, Stöhlein, Korschbroich, Germany).

Depth-specific primary production assay

To examine possible adaptations of the phytoplankton communities to the vertical light gradient, we performed a primary production assay in the two unmixed 12 m enclosures on 01 September (day 30). To this end we took water from 0.5, 2.0, and 5.0 m water depth (= depth of origin) and incubated in a reciprocal transplant design water from each depth of origin in culture flasks at 0.5, 2.0, and 5.0 m water depth (= depth of incubation) with ^{14}C marked $\text{NaH}^{14}\text{CO}_3$. SRP concentrations were similar at all depths (around $2.5 \mu\text{g P L}^{-1}$), but Chl *a* concentrations differed slightly (4.5 , 5.7 , and $3.4 \mu\text{g Chl } a \text{ L}^{-1}$ in the water originating from 0.5, 2.0, and 5.0 m, respectively). The incubation took place on a sunny day around noon and lasted for 2.5 hours, with PAR intensities of approximately 1600 , 40 , and $3.5 \mu\text{E m}^{-2} \text{ s}^{-1}$ at incubation depths of 0.5, 2.0, and 5.0 m, respectively. Since we were only interested in relative differences in specific production, we incubated light bottles from each depth of origin in duplicate at each depth of incubation and used no dark bottles. We present data as decays per minutes (DPM) per Chl *a* as a relative measure of the specific production of the algal community during the incubation.

Data processing and statistics

For all comparisons of unmixed with mixed enclosures, we calculated depth averaged values for the unmixed enclosures by linearly interpolating between samples at different water depths.

As a measurement of algal diversity we calculated a biomass-based version of the Shannon-Wiener-Index (H) as

$$H = -\sum_i^n \frac{B_i}{B_{sum}} \log_2 \left(\frac{B_i}{B_{sum}} \right), \quad (1)$$

where B_i is the biovolume of algal taxon i , B_{sum} is the biovolume of the entire algal community, and n is the number of algal taxa. For unmixed enclosures we calculated H based on the depth-integrated total algal biovolume per enclosure.

From our weekly measurements of sedimented POC and the concurrent changes in water column POC we calculated the specific sedimentation loss rate, l_s , of seston POC in each enclosure over weekly intervals as described in Visser et al. (1996). These calculations assume that specific primary production and l_s were constant over the weekly intervals and that sedimentation was the only significant loss process besides respiration. We calculated mean l_s during the first 35 days as the average of the weekly sedimentation rates of weeks 1 to 5.

We analyzed effects of enclosure depth (z_{max}) and mixing intensity (mixis) on depth-averaged values on days 7, 14, 21, 28, and 35 with repeated measures ANOVA, where sampling dates are the repeated measures. To detect vertical gradients within the unmixed enclosures of a given water column depth we performed repeated measures ANOVA on the two replicates, using sampling depth within each enclosure as the repeated measure. Percentages were arcsine transformed (Sokal and Rohlf 1981) and we log-transformed all biovolume data to improve homogeneity of variances. The effects of enclosure depth and mixing intensity on the heights of transient algal biomass peaks and on seston sedimentation rates were examined by two-way ANOVA. Two-way ANOVA was also used to analyze effects of incubation depth and depth of origin in the primary production assay.

Mesozooplankton

To monitor the occurrence of (unwanted) crustacean zooplankton, we sampled the mixed enclosures by means of vertical hauls with a 250 μm mesh net on days 36, 49, and 56. To minimize disturbance of the vertical water column structure, we sampled the unmixed enclosures only at the end of the experiment (day 56). On days 36 and 49 crustacean zooplankton densities were below 0.1 ind. L^{-1} in all mixed enclosures. At the end of the experiment crustacean zooplankton densities were still far below 0.1 ind. L^{-1} in all enclosures, except for one unmixed 12 m enclosure (0.37 ind L^{-1}) and one mixed 4 m enclosure (0.12 ind L^{-1}). Hence grazing pressure of crustacean zooplankton on phytoplankton was negligible during the experiment.

Results

Effects of water column depth and mixing on phytoplankton and nutrients

In spite of the initial fertilization, depth-averaged algal biovolume (Fig 1, Table 1a) showed only minor changes during the first 14 days. Subsequently algal biovolume increased to a peak followed by a decrease in all enclosures except for one 12 m mixed enclosure where algal biomass increased until day 35 (Fig. 1; Table 1a: time). In the mixed enclosures the time needed to reach the peak increased with increasing enclosure depth, whereas in the unmixed enclosures the timing of the peak seemed to be less dependent on mixing depth (Fig. 1; Table 1a: time x z_{\max} x mixis). Averaged over the entire 35-day period, algal biovolume decreased with increasing mixing depth, but showed no clear difference between the mixing treatments (Fig. 1; Table 1a: z_{\max}). The latter was also true for peak biovolume, which was negatively affected by water column depth but unaffected by the mixing treatment (ANOVA: z_{\max} : $p = 0.006$; mixis: $p = 0.14$; z_{\max} x mixis: $p = 0.54$).

Mixing intensity in the unmixed enclosures was sufficiently low to allow the establishment of vertical gradients in phytoplankton biomass (Figs. 1, 2). Not surprisingly, these gradients were most distinct in the 8 and 12 m enclosures, weakly expressed in the 4 m enclosures, and almost absent from the 2 m enclosures. This pattern was likely related to the steep vertical light gradient yielding an estimated compensation depth of only 3.7 m. Algal production should thus have been very low at depths > 4 m, promoting the establishment of vertical biomass gradients in the 8 and 12 m enclosures.

A statistically significant vertical heterogeneity of algal biovolume had already developed on day 7 in several of the deeper unmixed enclosures (Fig. 1). Vertical profiles were, however, only weakly expressed on days 7-14, when algal biomass had not yet increased. Vertical profiles of algal biomass were much steeper in the 4-12 m enclosures on days 21-28, when most enclosures had reached their depth-averaged algal biovolume peaks. When vertical profiles were present the concentration of algal biovolume was in most cases highest near the surface (most cases) and in a few cases at 2 m water depth (Fig. 1). On day 35 no clear vertical profile could be seen anymore, which may be related to the nightly convective mixing event on day 34.

Table 1. Summary of results of repeated measures ANOVA of the effects of water column depth (z_{\max}) and mixing intensity (mixis) on the depth averaged response variables phytoplankton biovolume, proportion by biovolume of motile taxa, Shannon diversity (H), SRP concentration and seston C:P

factor	df	(a)	(b)	(c)	(d)	(e)
		bio- volume p	prop. motile p	H p	SRP p	C:P ratio p
z_{\max}	3, 8	0.002	0.060	0.279	0.000	0.000
mixis	1, 8	0.339	0.001	0.001	0.001	0.121
z_{\max} x mixis	3, 8	0.769	0.135	0.040	0.044	0.024
time	4, 5	0.000	0.004	0.000	0.000	0.000
time x z_{\max}	12, 21	0.014	0.024	0.137	0.160	0.197
time x mixis	4, 5	0.896	0.015	0.181	0.002	0.173
time x z_{\max} x mixis	12, 21	0.030	0.008	0.129	0.095	0.160

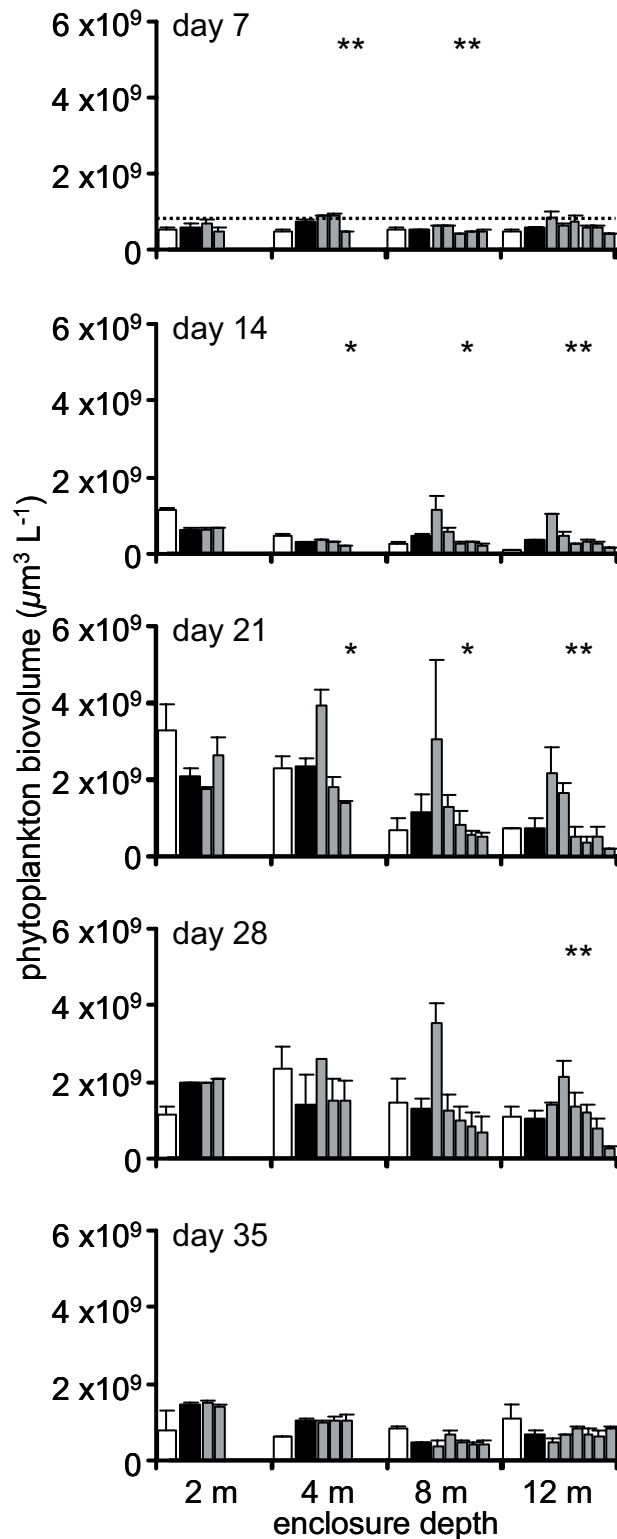


Fig. 1. Effects of enclosure depth and mixing intensity on algal biovolume on days 7-35. White and black bars show depth-averaged values (white = mixed; black = unmixed). The vertical profiles in unmixed enclosures are shown as thin gray bars at 0.5, 2.0, 3.5, 5.0, 7.5, and 11.5 m where present. Shown are means + 1 SE. Asterisks indicate that vertical profiles were non-uniform as determined by repeated measures ANOVAs of the homogeneity of the vertical profile: *** $p < 0.001$; ** $p < 0.01$; * $p < 0.05$. The dashed line in the upper panel indicates the starting concentration. One replicate of the unmixed 4 m enclosures at 0.5 m is missing on day 28.

We categorized phytoplankton into motile taxa (= flagellates) and non-motile taxa (= all other taxa). Motile taxa consisted mostly of *Carteria* sp., *Chlamydomonas* sp., *Cryptomonas* spp., *Rhodomonas* sp., *Dinobryon* spp., *Mallomonas* sp., and *Gymnodinium* sp.. Averaged over the entire 35-day period there was a clear, positive effect of reduced mixing intensity on the proportion of motile taxa (Fig. 2; Table 1b: mixis). In contrast, the effect of enclosure depth on the proportion of motile taxa was time and mixis dependent. Seven days after the start the proportional contribution of motile taxa to total (depth-integrated) algal biovolume had already increased in the unmixed enclosures, while no such increase was observed in the mixed enclosures throughout the entire experiment (Fig. 2; Table 1b: time x mixis). In the 2 m unmixed enclosures the proportion of motile taxa peaked on day 7 and was higher than in the mixed treatment until day 14; in contrast, in most of the deeper, unmixed enclosures the proportion of motile taxa peaked on day 14 and remained higher than in mixed treatments until day 28 (Fig. 2; Table 1b: time x z_{\max} x mixis). On day 35, after the first convective mixing events, only one unmixed 8 m enclosure still showed an elevated proportion of motile algae. Within the water column the proportion of motile taxa tended to decrease with increasing water depth in all unmixed enclosures throughout the entire experiment; this pattern was statistically significant in the 8 and 12 m enclosures, where the proportion of motile taxa in the upper strata was usually at least two times as high as in the deepest ones. Also, motile taxa dominated algal biomass in the uppermost layer (0.5 m) of all unmixed treatments ≥ 4 m water column depth throughout the entire experiment (Fig. 2).

We classified non-motile taxa further into centric diatoms (mostly *Cyclotella* spp.), pennate diatoms (mostly single-celled *Fragillaria* sp. and *Synedra* sp.), non-flagellated chlorophytes (mostly *Ankistrodesmus* sp., *Coenochloris* sp., *Elakatothrix* sp., *Oocystis* sp., *Scenedesmus* sp.), and cyanobacteria (mostly *Anabaena* sp., *Chroococcus* sp. and *Stigonema* sp.). At the beginning of the experiment, non-motile chlorophytes, centric diatoms and motile taxa contributed with approximately 30, 40, and 30%, respectively, to total phytoplankton biovolume, whereas pennate diatoms were almost absent. In addition to the increase of motile taxa in unmixed enclosures, the main successional pattern was an almost complete disappearance of centric diatoms and an increasing dominance of pennate diatoms in all enclosures (Fig. 3). In mixed enclosures and in the unmixed 2 m enclosures pennate diatoms became the dominant group from day 21 onward; in the deeper, unmixed enclosures pennate diatoms replaced flagellates as the dominant group on day 35. Cyanobacteria contributed less than 1% to total biomass throughout the experiment (Fig. 3).

Algal diversity as measured by the Shannon-Wiener-Index was positively related to the occurrence of motile taxa. With the exception of the 2 m enclosures (where motile taxa had already declined on day 21), diversity was therefore higher in the unmixed than in the mixed enclosures on days 7-28 (Fig. 4; Table 1c: mixis, z_{\max} x mixis). On day 35, when the proportion of motile taxa had declined in almost all unmixed enclosures, there were no longer any clear differences in diversity between the unmixed and mixed treatments.

Although algal biomass did not immediately respond to the initial fertilization, much of the added phosphorus was taken up by the algal community already in the first week, especially in shallow enclosures. Consequently, the depth-averaged SRP concentration was positively related to enclosure depth on day 7 (Fig. 5). This pattern was subsequently weakened in the mixed enclosures but accentuated in the unmixed enclosures (Fig. 5; Table 1d: z_{\max} , z_{\max} x mixis). In the deeper, unmixed enclosures increasing concentrations of SRP remained unused at water depths > 5 m (where light was presumably insufficient to support net

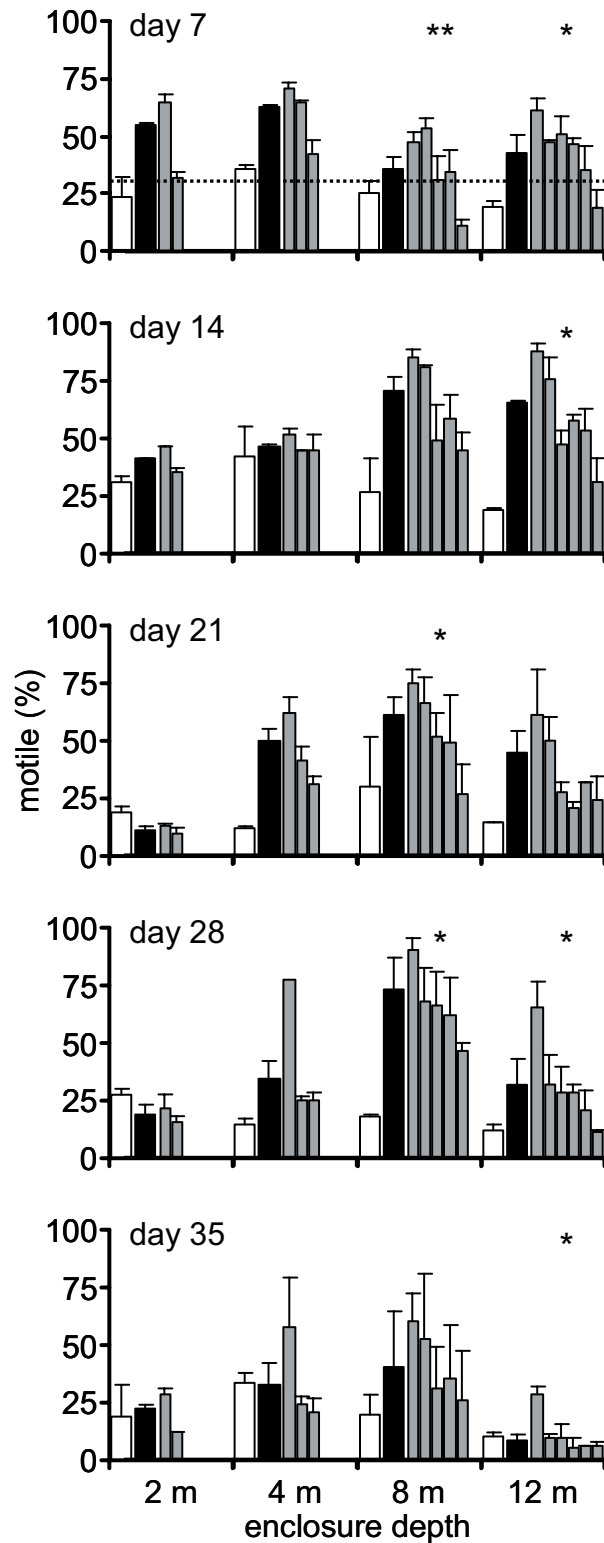


Fig. 2. Effects of enclosure depth and mixing intensity on the proportional contribution of motile taxa (= flagellates) to total algal biovolume on days 7-35. White and black bars show depth-averaged values (white = mixed; black = unmixed). The vertical profiles in unmixed enclosures are shown as thin gray bars at 0.5, 2.0, 3.5, 5.0, 7.5, and 11.5 m where present. Shown are means + 1 SE. Asterisks indicate that vertical profiles were non-uniform as determined by repeated measures ANOVAs of the homogeneity of the vertical profile: *** $p < 0.001$; ** $p < 0.01$; * $p < 0.05$. The dashed line in the upper panel indicates the starting proportional contribution. One replicate of the unmixed 4 m enclosures at 0.5 m is missing on day 28.

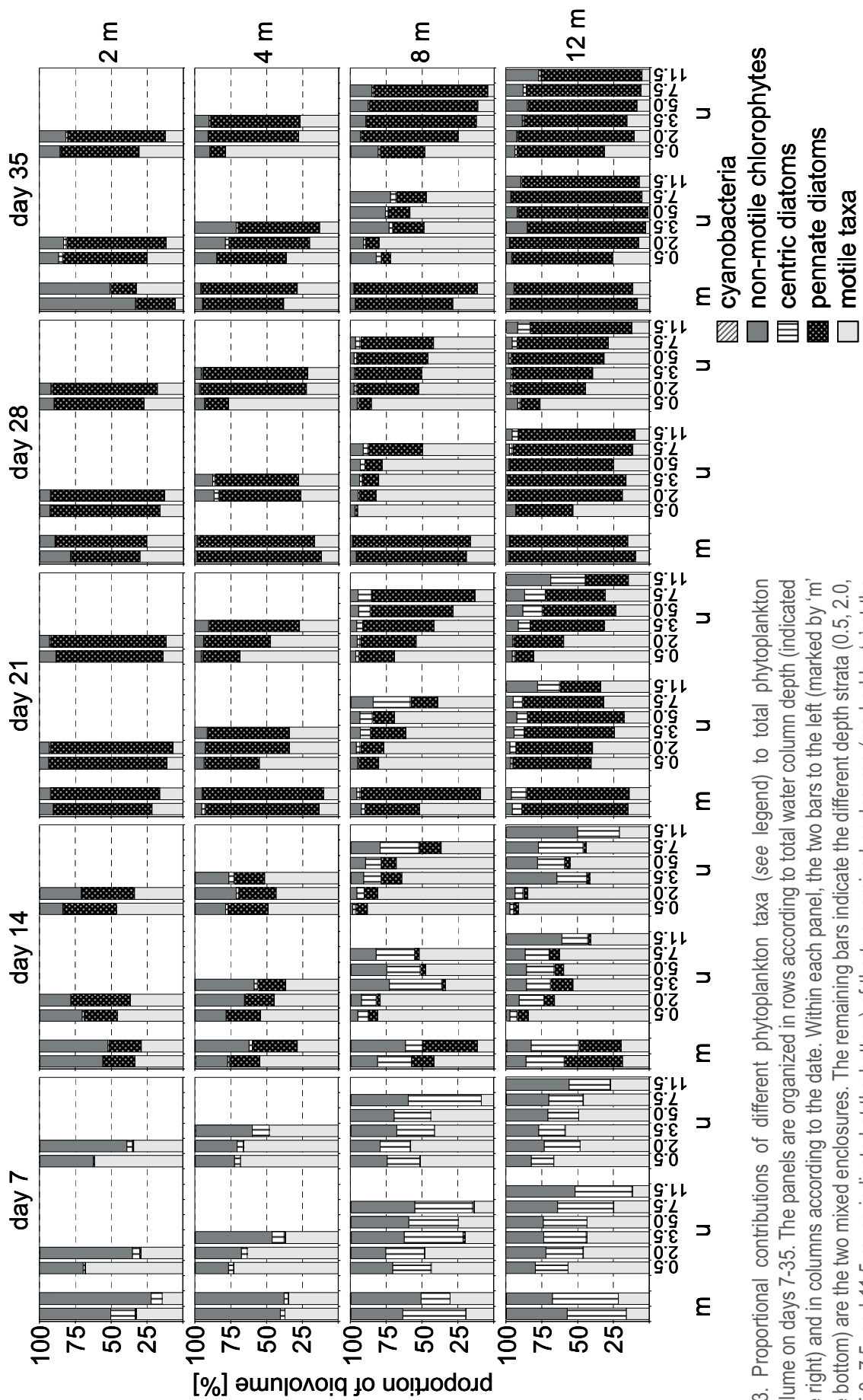


Fig. 3. Proportional contributions of different phytoplankton taxa (see legend) to total phytoplankton biovolume on days 7-35. The panels are organized in rows according to total water column depth (indicated to the right) and in columns according to the date. Within each panel, the two bars to the left (marked by 'm' at the bottom) are the two mixed enclosures. The remaining bars indicate the different depth strata (0.5, 2.0, 3.5, 5.0, 7.5, and 11.5 m, as indicated at the bottom) of the two unmixed enclosures (marked by 'u' at the bottom). One replicate of the unmixed 4 m enclosures at 0.5 m is missing on day 28.

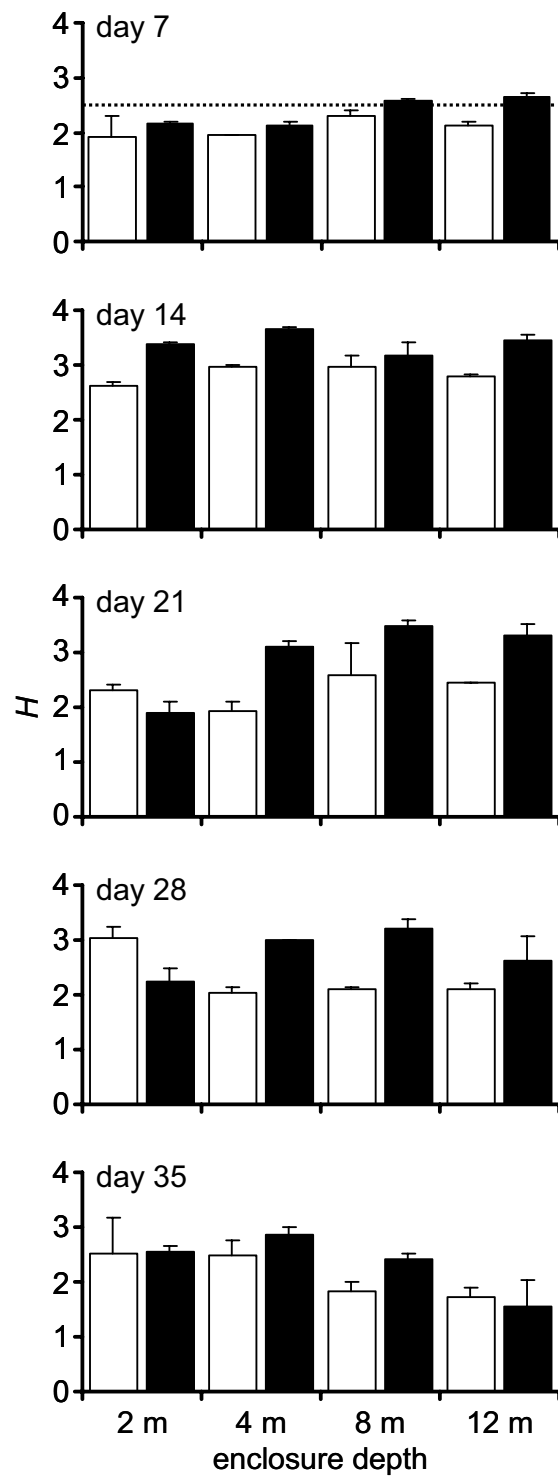


Fig. 4. Effects of enclosure depth and mixing intensity on taxonomic diversity of depth-averaged algal communities as calculated by the Shannon-Wiener-Index (H) on days 7-35 (white = mixed; black = unmixed). Shown are means + 1 SE. The dashed line in the upper panel indicates the starting taxonomic diversity.

algal growth), resulting in a distinct, vertically increasing SRP gradient in the 8 m enclosures (days 14-21) and in the 12 m enclosures (days 21-35; Fig. 5; the reversed vertical gradient in the 12 m enclosures on days 7-14 was an artifact of insufficient vertical mixing after the initial addition of the fertilizer). In the 12 m enclosures, deep water SRP concentrations eventually exceeded initial concentrations, suggesting that remineralized phosphorus (originating from sedimented algae) was accumulating. In contrast, in the mixed enclosures remineralized phosphorus was constantly mixed to the surface where it could be utilized by the phytoplankton community. Consequently, SRP concentrations were generally lower in mixed than in unmixed enclosures throughout the latter half of the experiment (Fig. 5; Table 1d: time x mixis).

Corresponding to the high phosphorus uptake following fertilization, depth-averaged seston C:P ratios were low on day 7 and subsequently increased over time, particularly in the shallowest enclosures (Fig. 6; Table 1e: time). In parallel with the light gradient, the seston C:P ratio decreased with increasing enclosure depth on days 7-35, indicating a higher algal production at shallower enclosure depth (Fig. 6; Table 1e: z_{\max}). Compared to the mixed enclosures, depth-averaged C:P ratios in the unmixed enclosures were lower at shallower enclosure depths and slightly higher at deeper enclosure depths (Fig. 6; Table 1e: z_{\max} x mixis). The seston C:P ratio did not show any strong or consistent vertical gradients in the unmixed enclosures on any of the sampling dates.

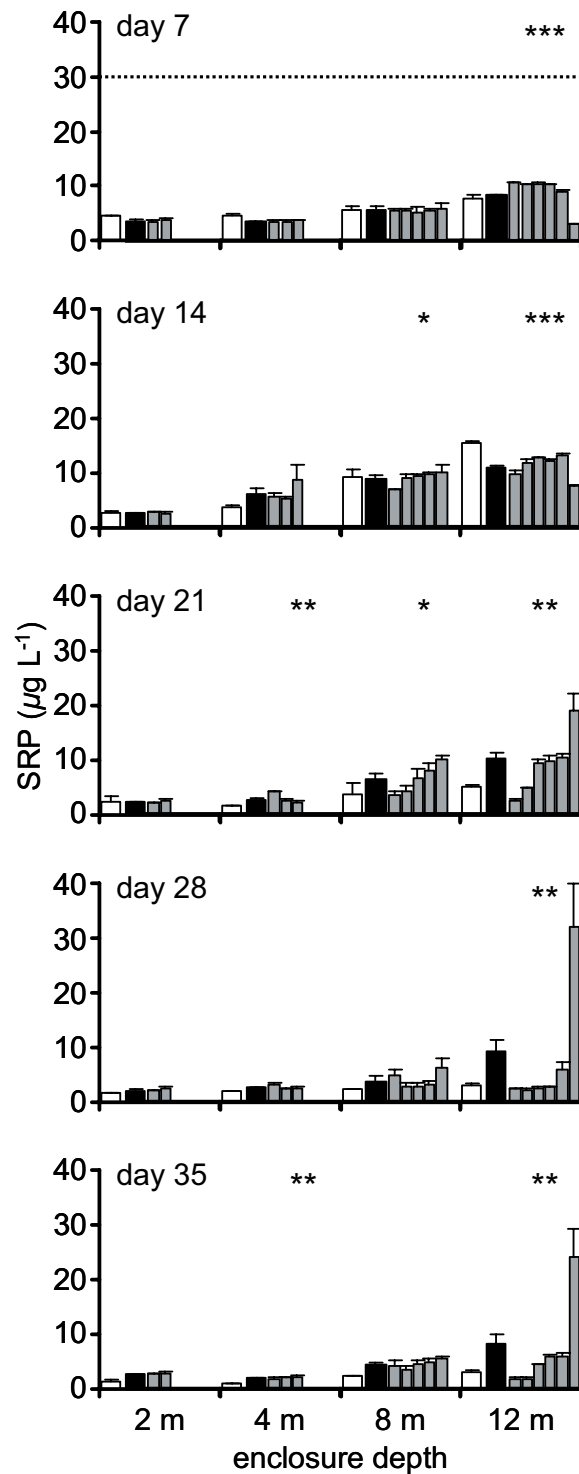


Fig. 5. Effects of enclosure depth and mixing intensity on SRP concentrations on days 7-35. White and black bars show depth-averaged values (white = mixed; black = unmixed). The vertical profiles in unmixed enclosures are shown as thin gray bars at 0.5, 2.0, 3.5, 5.0, 7.5, and 11.5 m where present. Shown are means + 1 SE. Asterisks indicate that vertical profiles were non-uniform as determined by repeated measures ANOVAs of the homogeneity of the vertical profile: *** $p < 0.001$; ** $p < 0.01$; * $p < 0.05$. The dashed line in the upper panel indicates the starting concentration.

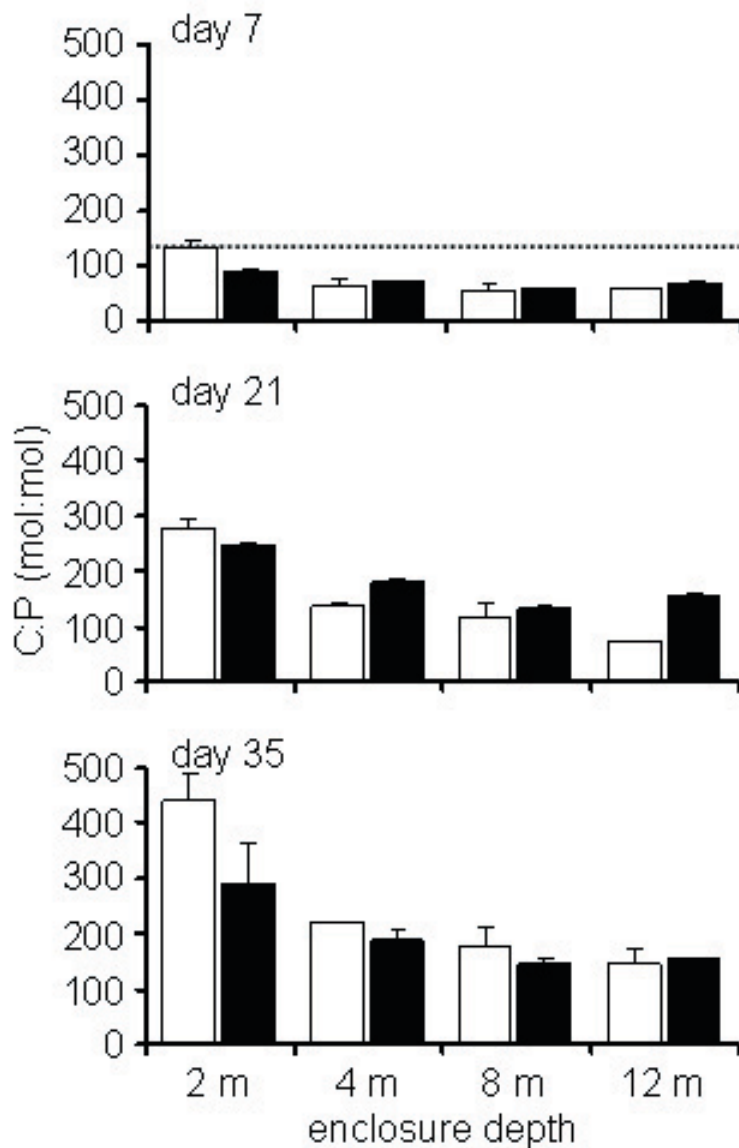


Fig. 6. Effects of enclosure depth and mixing intensity on depth averaged seston C:P ratios on days 7, 21, and 35 (white = mixed; black = unmixed). Shown are means + 1 SE. The dashed line in the upper panel indicates the starting seston C:P ratio. Vertical profiles in the unmixed enclosures were very weak and not statistically significant. Because the effects of z_{\max} and mixis were similar on all days the data of days 14 and 28 are not shown.

Sedimentation losses

As expected, the specific sedimentation loss rate of seston POC (averaged over days 0-35) decreased with increasing enclosure depth in both mixed and unmixed enclosures (Fig. 7; ANOVA: effects of z_{\max} : $p < 0.001$). Congruent with the higher proportion of motile, non-sinking taxa in the unmixed enclosures, sedimentation rates were lower in unmixed than in mixed water columns, except for the deepest enclosures (ANOVA: effects of mixis: $p < 0.001$, z_{\max} x mixis: $p < 0.001$). Fitting the mechanistic equation for specific sedimentation rate in well-mixed systems, $l_s = v/z_{\max}$ (where v is sinking velocity and z_{\max} is enclosure depth; Reynolds 1984), to the data of the mixed enclosures yielded estimated average seston sinking velocities of 0.32 m d^{-1} ($R^2 = 0.99$, $p = 0.000$).

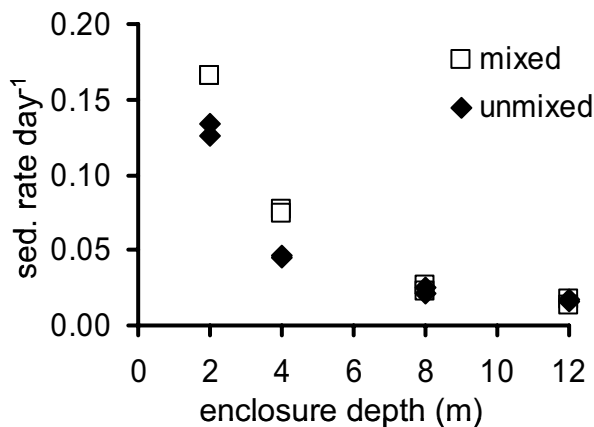
Depth-specific primary production assay

Fig. 7. Effects of enclosure depth and mixing intensity on the specific sedimentation rate averaged over days 0-35.

incubation depth, whereas the 'low light' community (from 5.0 m depth of origin) showed the relatively highest carbon incorporation at 5.0 m incubation depth, suggesting that the communities were adapted to the respective light climate at their depth of origin. The observed differences in light-dependent performance of 'high light' and 'low light' communities may have been related to differences in taxonomic composition: the phytoplankton biomass of 'high light' communities was dominated by 65% motile taxa, whereas the biomass of 'low light' communities was dominated by 70% pennate diatoms.

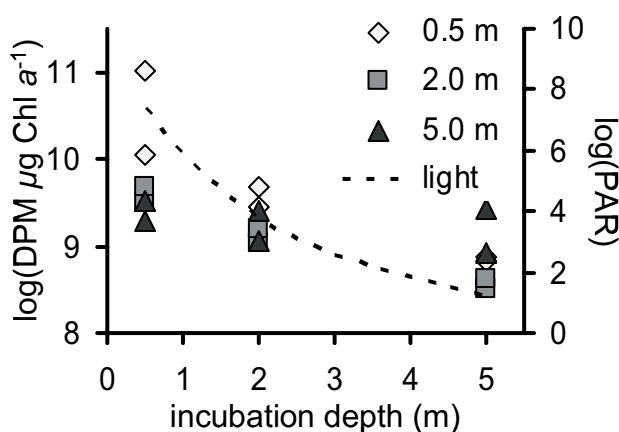


Fig. 8. Effects of incubation depth and depth of origin (shown in legend) on specific carbon incorporation in the primary production assay. Left axis shows the natural logarithm of decays per minute per $\mu\text{g Chl } a$. Right axis shows the natural logarithm of photosynthetic active radiation ($\mu\text{mol photons m}^{-2} \text{s}^{-1}$) during the incubation.

Discussion

Algal biomass responses in mixed vs. unmixed enclosures

After an initial lag phase of 7-14 days, which coincided with a major change in taxonomic composition, phytoplankton in both mixed and unmixed water columns responded to the initial nutrient pulse with a transient increase in (depth-averaged) biomass, the initial increase being highest in either the 2 m or 4 m enclosures. In the mixed enclosures the resulting transient phytoplankton peak was reached the earlier the shallower the water column. Both results conform to theoretical expectations: first, the time until a transient biomass peak is reached is expected to follow the inverse of algal growth rate and, consequently, should increase with increasing light limitation and, thus, with increasing water column depth (Jäger et al. 2008); second, the height of a transient biomass peak should be limited by high sinking losses in very shallow (< 2 m) water columns and by low light availability in deeper water columns, and therefore be highest at intermediate water column depths, which under the prevailing conditions of high background turbidity and high initial nutrient availability should span the approximate range of 2-5 m (Diehl et al. 2005; Jäger et al. 2008). While the transient nature of the phytoplankton peak in this experiment was likely a consequence of nutrient depletion caused by sedimentation losses (Huppert et al. 2002), similar observations have been made in well-mixed water columns in the presence of grazers, where the phytoplankton decline was a consequence of grazing from an increasing herbivore population (Berger et al. 2007; Jäger et al. 2008).

In contrast to the mixed enclosures, the timing of the transient phytoplankton peak was only weakly related to water column depth in unmixed enclosures. The latter developed steep vertical biomass gradients early on. Most algae contributing to the biomass peak in unmixed water columns had therefore been growing in the well-lit surface layer where initial growth rates were probably largely independent of total water column depth.

Patterns of succession and vertical segregation of functional algal groups

High initial phytoplankton production in shallow water columns was accompanied by a subsequent reduction in SRP and a concomitant increase in algal P limitation, as indicated by a decrease in depth-averaged SRP concentration and an increase in seston C:P with decreasing water column depth in both mixed and unmixed water columns. These trends were more strongly expressed in mixed than in unmixed water columns, probably because phytoplankton in mixed enclosures experienced higher sinking losses, removing limiting nutrients from the water column at a faster rate. The latter was likely a consequence of contrasting successional patterns in mixed vs. unmixed enclosures. While mixed water columns became quickly dominated by fast sinking, pennate diatoms, algal biomass in unmixed water columns ≥ 4 m total depth was dominated by $\geq 50\%$ motile, non-sinking algae throughout most of the experiment.

The early dominance of pennate diatoms in mixed enclosures was likely related to their competitive abilities. Strong vertical mixing prevents spatial niche differentiation, and, under constant environmental conditions, those taxa that reduce light in the water column to the lowest level and the limiting nutrient to the lowest concentration will displace all other competitors (Sommer 1985; Huisman and Weissing 1995; Passarge et al. 2006). Pennate diatoms are superior competitors for phosphorus, if silicon is available in excess (Smith and Kalff 1983; Sommer 1985; Grover 1997), and they can become a dominant group under

low light intensities (Litchman 1998; Flöder et al. 2002; Reynolds 2006). Both environmental conditions were met in our experiment, at least until day 28 (*see below*). Thus the dominance of pennate diatoms in the mixed enclosures from day 21 onward (when phosphorus had become limiting) is not unexpected and is in good accordance with previous enclosure experiments in Lake Brunnsee (Ptacnik et al. 2003).

In spite of their high sinking velocities, pennate diatoms became dominant even in the shallowest (= 2 m) mixed water columns. This contrasts with the experimental results of Reynolds et al. (1983, 1984), who found that fast sinking diatoms were replaced by buoyant and motile taxa when the depth of (artificial) mixing fell below 2 m. Reynolds et al. (1983, 1984) used stratified enclosures with a deep water layer, where sinking removed algae permanently from the mixed surface layer. In contrast, sedimented algae in our mixed 2 m enclosures accumulated at the enclosure bottom, where light levels were still sufficient to support algal growth and where artificial mixing may have produced some resuspension. Still, on the final day of the experiment (day 35), the proportional contribution of pennate diatoms to total algal biovolume increased with increasing water column depth in the mixed enclosures (linear regression of the arcsine square root transformed proportion of pennate diatoms vs. enclosure depth: $p = 0.005$, $R^2 = 0.77$, $n = 8$), suggesting a measurable competitive disadvantage of these fast sinking algae at the most shallow depths (*see* Ptacnik et al. 2003 for a similar result). This competitive disadvantage of diatoms was probably not only a consequence of high sinking losses. Silicon was available in excess (2.6 mg L^{-1}) at the beginning of the experiment, but decreased with increasing dominance of diatoms. With the exception of one mixed 2 m enclosure on day 21, molar dissolved, mineral Si:P ratios were always > 50 before day 28. Consequently, relative to phosphorus, silicon supply has been sufficient to not limit diatom growth (Sommer 1985). On day 28, the mineral Si:P ratio dropped below 30 in the mixed 2 and 4 m enclosures and in the unmixed 2 m enclosures. Thus pennate diatoms are likely to have suffered from increasing silicon limitation in the shallow enclosures towards the end of the experiment.

Reduced turbulence has been suggested to give buoyant plankton taxa a competitive advantage over sinking taxa (Visser et al. 1996; Huisman et al. 2004), and several authors have proposed that reduced turbulence may favor vertical niche separation (Elliott et al. 2002; Clegg et al. 2007). Our data support both hypotheses. Motile taxa became quickly dominant in all unmixed water columns and remained so in water columns ≥ 4 m total depth until day 28. The dominance of motile taxa in unmixed treatments was accompanied by a pronounced vertical structure in water columns ≥ 4 m, with higher phytoplankton biomass and higher proportions of motile taxa in the well-lit, uppermost strata, and higher proportions of pennate diatoms and higher concentrations of SRP in the deeper, darker strata. As a result of this vertical separation of taxa phytoplankton diversity was higher in unmixed than in mixed water columns ≥ 4 m total depth, suggesting that reduced turbulence provided opportunities for vertical niche separation. The 'primary production assay' suggested indeed local depth adaptation of the algal community in unmixed enclosures. Water samples originating from 0.5 and 5 m, respectively, performed best when incubated at their depths of origin.

The dominance of pennate diatoms in the deeper layers of unmixed water columns was probably related to their high sinking velocities (Ptacnik et al. 2003) and their tolerance against low light conditions (Litchman 1998; Flöder et al. 2002). In contrast, under the prevailing conditions of low turbulence motile species should have been able to actively move along opposing vertical gradients of light and nutrient availability to a depth where their growth was maximized (Klausmeier and Litchman 2001). Given the

high background turbidity and the relatively weak vertical SRP gradients in the euphotic zone (0-4 m), the depth of maximal production should have been close to the surface throughout the experiment, which conforms with the observation that the biomass of motile taxa was always highest in the uppermost layer of unmixed enclosures (Figs. 1 and 2).

In spite of their long-lasting dominance, motile taxa were eventually replaced by pennate diatoms also in unmixed enclosures. There are at least two non-exclusive explanations for this shift. First, pennate diatoms already dominant in deeper layers may have intercepted recycled nutrients on their way from the sediment to shallow strata. As nutrients from the initial fertilization pulse became increasingly depleted near the surface, motile species may therefore have been outcompeted by pennate diatoms. Second, turbulence gradually increased in the unmixed enclosures, and weak nightly mixing events such as the ones recorded on days 25 and 34 may have eroded the competitive advantage of motile species.

Both of the above mechanisms may also explain the relatively early shift towards pennate diatoms in the unmixed 2 m enclosures, which experienced phosphorus depletion fairly early and should have been most strongly affected by nightly mixing events. The latter can be estimated from the Peclet number $Pe = v z_{\max} D^{-1}$, which describes the relative importance of the transports by sedimentation vs. turbulent mixing based on algal sinking velocity v , water column depth z_{\max} , and the coefficient of vertical diffusion D . Specifically, $Pe \ll 1$ implies that transport by turbulent mixing dominates over sedimentation losses (Peeters et al. 2007b). In a similar experiment we observed sinking velocities of pennate diatoms ranging from 0.5 - 0.9 m d⁻¹ (Ptacnik et al. 2003) and our sporadic turbulence measurements indicated that nighttime mixing intensities were $> 3 \text{ m}^2 \text{ d}^{-1}$ in cold nights. Based on these numbers, Pe should have been at least occasionally < 1 in the unmixed 2 m enclosures but always > 1 in all other unmixed enclosures during the 35 days of our experiment, suggesting that nightly convective mixing events should have been sufficiently strong to favor pennate diatoms only in the shallowest 'unmixed' water columns.

Seston C:P ratios

In agreement with theoretical expectations and with earlier experiments (Diehl et al. 2002, 2005) we observed a strong negative influence of water column depth on the depth-averaged seston C:P ratio. In accordance with field observations (Sterner et al. 1997) this result paralleled a similar trend in the supply ratio of depth-averaged light intensity vs. depth-averaged SRP concentration. Interestingly, the negative effect of water column depth on depth-averaged seston C:P was much more strongly expressed in mixed than in unmixed enclosures. Moreover, and in spite of the strong and opposing vertical light and nutrient gradients, there were no consistent indications of a vertical gradient in seston C:P ratio within unmixed enclosures.

The latter two results are largely a consequence of the relatively low seston C:P ratios in unmixed high light environments (i.e., in 2 m enclosures and in the upper layers of deeper enclosures) and we propose that they may have been related to the high proportion of motile taxa in the unmixed enclosures. Occasional sampling of the diurnal vertical distribution of phytoplankton in several of the unmixed enclosures indicated that motile taxa stayed close to the well-lit surface during day but moved towards deeper strata with higher SRP concentrations at night (Schmidt 2006). The latter suggests that motile taxa residing in shallow strata during the day could have balanced increased carbon fixation by increased phosphorus uptake at night. Most of the flagellates included in our category of motile taxa are furthermore

known to be mixotrophic. A recent study (Katechakis et al. 2005) has shown that mixotrophic flagellates maintained relatively low and almost invariant cellular C:P ratios when exposed to a large gradient of light:phosphorus supply regimes, possibly because they could balance increased carbon fixation at high light levels by uptake of particulate phosphorus in the form of bacteria, which are known to be rich in phosphorus (Vadstein 2000). Our hypothesis that limited variability in seston C:P in unmixed enclosures was related to high proportions of flagellates is supported by the fact that only the 2 m enclosures showed elevated C:P ratios and only after the proportion motile taxa there had dropped to similar levels as in the mixed enclosures.

General effects of turbulence

In our experiment water column depth had strong effects on phytoplankton biomass, seston C:P ratio and dissolved nutrients. In contrast, mixing intensity had no clear effects on any of these (depth-integrated) variables, but strongly affected functional community composition (motile vs. sinking taxa) and taxonomic diversity. The latter suggests that different algal communities in different mixing treatments were equally well adapted to their respective mixing environments and were therefore equally successful in transforming the available resources into biomass. Although the initial phosphorus fertilization created meso- to eutrophic conditions, algal community development was constrained by the taxonomic composition of the starting community, which is typical for an oligotrophic lake. In naturally eutrophic or nitrogen limited systems buoyant cyanobacteria rather than flagellates would be expected to become dominant in stratified water columns (Visser et al. 1996; Scheffer et al. 1997; Huisman et al. 2004). Under such conditions cyanobacteria are expected to form surface blooms, which strongly shade lower strata and therefore greatly diminish the possibility of coexistence for negatively buoyant species (Visser et al. 1996; Scheffer et al. 1997; Huisman et al. 2004). Similar to our experiment, increased vertical mixing can affect phytoplankton taxonomic composition also in eutrophic systems and move them from a dominance of surface-dwelling cyanobacteria to a dominance of green algae, with relatively minor effects on depth-integrated phytoplankton biomass (Huisman et al. 2004). The available empirical evidence thus suggests that mixing intensity primarily affects functional composition of the phytoplankton but not its biomass. This pattern is consistent with theoretical expectations for water columns of shallow to intermediate depth (Huisman et al. 2002). In very deep water columns phytoplankton biomass is, however, always expected to decrease at high mixing intensities, because algal motility and buoyancy regulation then cannot counteract downmixing to aphotic depths.

Acknowledgments

We thank Angelika Wild and Achim Weigert for laboratory analyses, and Florian Haupt and the students of the 2005 Aquatic Ecology class for help during the field experiment. We also thank Jef Huisman, Elena Litchman, Silvia Bartholomé, Alex Elliott, and an anonymous reviewer for their comments. This study was supported by funding from Deutsche Forschungsgemeinschaft (DI 745/2-4).

Chapter 3

Transient dynamics of pelagic producergrazer systems in a gradient of nutrients and mixing depths

Christoph G. Jäger,
Sebastian Diehl,
Christian Matuschek,
Christopher A. Klausmeier*,
and Herwig Stibor

*Kellogg Biological Station, Michigan State University, Hickory Corners MI 49060, U.S.A

Ecology in press.

Abstract.

Phytoplankton-grazer dynamics are often characterized by long transients relative to the length of the growing season. Using a phytoplankton-grazer model parameterized for *Daphnia pulex* with either flexible or fixed algal carbon:nutrient stoichiometry, we explored how nutrient and light supply (the latter by varying depth of the mixed water column) affect the transient dynamics of the system starting from low densities. The system goes through an initial oscillation across nearly the entire light-nutrient supply space. With flexible (but not with fixed) algal stoichiometry, duration of the initial algal peak, timing and duration of the subsequent grazer peak, and timing of the algal minimum are consistently accelerated by nutrient enrichment but decelerated by light enrichment (decreasing mixing depth) over the range of intermediate to shallow mixing depths. These contrasting effects of nutrient vs. light enrichment are consequences of their opposing influences on food quality (algal nutrient content): algal productivity and food quality are positively related along a nutrient gradient but inversely related along a light gradient. Light enrichment therefore slows down grazer growth relative to algal growth, decelerating oscillatory dynamics; nutrient enrichment has opposite effects. We manipulated nutrient supply and mixing depth in a field enclosure experiment. The experimental results were qualitatively much more consistent with the flexible than with the fixed stoichiometry model. Nutrient enrichment increased *Daphnia* peak biomass, decreased algal minimum biomass, decreased the seston C:P ratio and accelerated transient oscillatory dynamics. Light enrichment (decreasing mixing depth) produced the opposite patterns, except that *Daphnia* peak biomass increased monotonously with light enrichment, too. Thus, while the model predicts the possibility of the ‘paradox of energy enrichment’ (a decrease in grazer biomass with light enrichment) at high light and low nutrient supply, this phenomenon did not occur in our experiment.

Introduction

When studying ecological models, theoreticians typically focus on their limit sets, such as locally stable or unstable equilibria, limit cycles, and chaotic trajectories (May 1975; Gurney and Nisbet 1998). However, environmental conditions often vary over time scales that are significantly shorter than the time needed to reach an attractor (Hutchinson 1961; DeAngelis and Waterhouse 1987). It is increasingly recognized that times to reach an attractor can be very long and that a better understanding of transient dynamics is sorely needed (Huisman and Weissing 2001; Hastings 2004; Neubert et al. 2004). Both stable and unstable limit sets can influence the transient dynamics (Cushing et al. 1998), so knowledge about them is still useful, but they do not paint the entire picture.

The predominance of transient dynamics is particularly evident in planktonic systems in seasonal environments such as temperate lakes. These systems are usually driven by fluctuations in water temperature, solar irradiation and terrestrial runoff and associated variation in thermal stratification and nutrient supply (Sommer 1986; Sommer et al. 1986; Reynolds 1988). In addition, the tight coupling of many planktonic resource-consumer interactions tends to promote oscillations under a large range of environmental conditions (McCauley et al. 1999; Fussmann et al. 2000; Huisman and Weissing 2001; Scheffer et al. 2003). Sommer (1985) concluded for phytoplankton communities that “steady state is the exception rather than the rule”. This conjecture probably applies to many ecosystems, making studies of transient dynamics an important field of ecological research (DeAngelis and Waterhouse 1987; Hastings 2004).

In deep, temperate lakes, seasonal succession of the plankton is usually initiated by spring circulation bringing nutrients to the water surface and subsequent thermal stratification creating a well-lit mixed surface layer, both of which stimulate planktonic primary production (Sommer et al. 1986). The resulting phytoplankton spring bloom is frequently terminated by the grazing activity of a growing crustacean zooplankton population producing the ‘clearwater phase’, a period of low phytoplankton biomass; the latter, in turn, is often followed by a crash of the crustacean population that has temporally overexploited its resource base (Lampert et al. 1986; Sarnelle 1993; Talling 2003). Empirical evidence suggests that the magnitude and timing of such transient producer-grazer oscillations depend on the nutrient and light regime, with more nutrient rich and more shallow systems experiencing earlier and more pronounced phytoplankton and zooplankton peaks and troughs (Sommer et al. 1986; Berger et al. 2007).

The above patterns are probably a consequence of higher algal and grazer growth rates (stimulated by higher nutrient and/or light supply) speeding up and intensifying successional events. Because phytoplankton is passively entrained in well mixed water bodies, a shallower mixed water column implies higher average light availability and increased specific primary production (Huisman 1999; Diehl et al. 2002; 2005). In a shallower water column a smaller fraction of the external light supply is ‘consumed’ by abiotic absorbents (water molecules, suspended solids and solutes derived from the catchment) and, consequently, more light is available for photosynthesis. Decreasing mixing depth is therefore a form of light enrichment and has similar consequences for primary production as has nutrient enrichment (Diehl 2002).

Nutrient and light supply do, however, not only affect the growth rate of phytoplankton, but also its carbon to nutrient stoichiometry. For example, when light supply is high relative to phosphorus availability,

phytoplankton biomass tends to be carbon rich and phosphorus poor (Sterner et al. 1997; Berger et al. 2006). This may create a mismatch with the nutritional needs of grazers such as *Daphnia* spp., whose body composition is characterized by a relatively low carbon to phosphorus (C:P) ratio (Andersen and Hessen 1991; Sterner et al. 1993). An increase in light supply may therefore decrease grazer production if the benefits of increased food quantity (increased algal carbon fixation) are outweighed by decreased food quality (increased algal C:P ratio) and, thus, decreased conversion efficiency of algal into *Daphnia* biomass [reviewed in Andersen et al. (2004)]. Flexible algal C:P stoichiometry is therefore likely to affect the timing and magnitude of transient producer-grazer oscillations, because phytoplankton peaks should often be associated with high C:P ratios (i.e., low quality) of algal biomass. Long delays in the build-up of *Daphnia* population peaks have indeed been observed in the presence of high biomasses of low quality (high C:P) algal food (Sommer 1992; Urabe et al. 2002).

In summary, empirical evidence and conceptual considerations suggest that transient phytoplankton-grazer dynamics should be greatly influenced by nutrient supply and mixing depth. Both factors may vary substantially among lakes within a limited geographic region and are thus highly relevant to study. Here we explore how nutrient supply and mixing depth affect the dynamics of a phytoplankton-grazer system starting from low population densities until the end of the first grazer peak, when natural phytoplankton communities often shift towards less edible taxa (Sommer et al. 1986; Sarnelle 1993). Using a producer-grazer model parameterized for *Daphnia* feeding on edible algae, we first explore how the timing and magnitudes of population peaks and troughs are affected by nutrient supply and mixing depth. While it is well documented that the carbon to nutrient stoichiometry of primary producers changes depending on environmental conditions, it is unclear how such a flexible stoichiometry affects transient producer-grazer dynamics. To examine the potential importance of variable algal stoichiometry, we therefore investigated two variants of the model, one with fixed and one with flexible algal C:P ratio. We then compare the two model outputs with the results of a field enclosure experiment in which we manipulated nutrient supply and mixing depth in a factorial design.

Model Structure

The models describe the growth of a grazer population with fixed carbon:nutrient stoichiometry feeding on a phytoplankton population with either flexible or fixed carbon:nutrient stoichiometry in a well-mixed water column of depth z . Both models assume that phytoplankton and grazer production are limited by energy (in the form of light and food carbon, respectively) and a single mineral nutrient (assumed to be phosphorus) and describe the dynamics of five state variables: the concentrations of algal (A) and grazer (G) carbon biomasses and of dissolved mineral nutrients (R), a pool of sedimented (detrital) nutrients (R_s), and the light intensity ($I(s)$) at depth s of the water column. The nutrient content (quota) per algal carbon biomass (Q), is a sixth state variable in the flexible stoichiometry model but a constant parameter in the fixed stoichiometry model. The system is mixed to the sediment surface and closed for nutrients. Thus, nutrient supply to the perfectly well-mixed water column originates exclusively from excretion and from remineralization of sedimented biomass. The total amount of nutrients in the system (expressed as the concentration $R_{tot} = R + R_s/z + QA + qG$) is then a measure of nutrient enrichment.

The dynamic equations of the two model variants are listed in Table 1 and all state variables and parameters are defined in Table 2. The underlying assumptions are motivated in detail in Diehl et al. (2005) and Diehl (2007) and are only briefly described here. We assume grazers to have constant respiration and death rates, a saturating functional response and to use ‘synthesizing units’ (Kooijman 1998; 2000) to produce new biomass with a fixed carbon to nutrient stoichiometry. The synthesizing unit formulation describes grazer growth as a smooth, continuous function of carbon and nutrient intake. Algal growth is co-limited by light and nutrients as described by a multiplicative, saturating function of light intensity and either the algal nutrient quota (flexible stoichiometry model) or the external nutrient concentration (fixed stoichiometry model). Vertical light attenuation follows Lambert-Beer’s law. Algae respire carbon at a constant rate and settle out of the water column at a rate proportional to their sinking velocity and inversely proportional to mixing depth. Nutrients stored in dead grazers and sedimented algae enter the sedimented nutrient pool, where they are mineralized and returned to the water column at a constant rate. Nutrients excreted by grazers go directly into the pool of dissolved mineral nutrients. Algal nutrient uptake is an increasing function of the external nutrient concentration and, in the flexible stoichiometry model, also a decreasing function of internal algal nutrient stores. Finally, algal nutrient quota is by definition constant in the fixed stoichiometry model, while it increases through nutrient uptake and carbon respiration and decreases through growth in the flexible stoichiometry model.

Table 1. Dynamic equations and rate functions. Symbols are defined in Table 2.

	Flexible stoichiometry model	Fixed stoichiometry model
Dynamic equations		
Algal carbon density [mg C m ⁻³]	$\frac{dA}{dt} = \frac{A}{z} \int_0^z p(I(s), Q) ds - I_A A - \frac{v}{z} A - J_A G$	$\frac{dA}{dt} = \frac{A}{z} \int_0^z p(I(s), R) ds - I_A A - \frac{v}{z} A - J_A G$
Grazer carbon density [mg C m ⁻³]	$\frac{dG}{dt} = gG - (l_G + d)G$	$\frac{dG}{dt} = gG - (l_G + d)G$
Dissolved mineral nutrient concentration [mg P m ⁻³]	$\frac{dR}{dt} = \frac{r}{z} R_S + q I_G G + (Q J_A - q g) G - \rho(Q, R) A$	$\frac{dR}{dt} = \frac{r}{z} R_S + Q I_A A + q I_G G + (Q J_A - q g) G - Q \frac{A}{z} \int_0^z p(I(s), R) ds$
Pool of sedimented nutrients [mg P m ⁻²]	$\frac{dR_S}{dt} = v Q A + q d G z - r R_S$	$\frac{dR_S}{dt} = v Q A + q d G z - r R_S$
Algal nutrient quota [mg P mg C ⁻¹]	$\frac{dQ}{dt} = \rho(Q, R) + I_A Q - \frac{Q}{z} \int_0^z p(I(s), Q) ds$	$Q = \text{constant}$
Light intensity at depth s of the water column [$\mu\text{E m}^{-2} \text{s}^{-1}$]	$I(s) = I_{in} e^{-(k_{A_s} + k_{R_g} s)}$	$I(s) = I_{in} e^{-(k_{A_s} + k_{R_g} s)}$
Rate functions		
Specific grazer growth rate [day ⁻¹]	$g = \frac{c J_A}{c q + \frac{Q}{Q}} \frac{Q}{c q + Q}$	$g = \frac{c J_A}{c q + \frac{Q}{Q}} \frac{Q}{c q + Q}$
Ingestion rate of algae per grazer [day ⁻¹]	$J_A = \frac{A}{K_S + A} f_{\max}$	$J_A = \frac{A}{K_S + A} f_{\max}$
Specific algal production rate [day ⁻¹]	$p(I, Q) = P_{\max} \left(1 - \frac{Q_{\min}}{Q} \right) \frac{I}{h + I}$	$p(I, R) = P_{\max} \frac{R}{m + R} \frac{I}{h + I}$
Specific algal nutrient uptake rate [mg P mg C ⁻¹ day ⁻¹]	$\rho(Q, R) = P_{\max} \left(1 - \frac{Q - Q_{\min}}{Q_{\max} - Q_{\min}} \right) \frac{R}{m + R}$	$Q p(I, R) = Q P_{\max} \frac{R}{m + R} \frac{I}{h + I}$

Table 2. Definitions and units of parameters and variables and basic set of parameter values and initial conditions.

Parameter	Value	Definition and Units
c	0.5	fraction of ingested carbon assimilated by grazers [mg C mg C ⁻¹]
d	0.03	specific grazer death rate [day ⁻¹]
f_{max}	1.0	maximum ingestion rate of algae by grazers [day ⁻¹]
h	120	half saturation constant for light-dependent algal production [$\mu\text{mol photons m}^{-2} \text{s}^{-1}$]
I_{in}	300	light intensity at the surface [$\mu\text{mol photons m}^{-2} \text{s}^{-1}$]
k	$3.6 \cdot 10^{-4}$	specific light attenuation coefficient of algal biomass [$\text{m}^2 \text{mg C}^{-1}$]
k_{bg}	0.45	background light attenuation coefficient [m^{-1}]
K_s	156	half saturation constant for ingestion of algae by grazers [mg C m ⁻³]
l_A	0.1	specific algal maintenance respiration losses [day ⁻¹]
l_g	0.09	specific grazer maintenance rate [day ⁻¹]
m	1.5	half saturation constant for nutrient uptake of algae [mg P m ⁻³]
p_{max}	1.2	maximum specific algal production rate [day ⁻¹]
q	1/31	grazer nutrient quota [mg P mg C ⁻¹]
Q^a	1/41	constant algal nutrient quota, fixed to Redfield ratio [mg P mg C ⁻¹]
Q_{max}	1/25	algal maximum nutrient quota [mg P mg C ⁻¹]
Q_{min}	1/250	algal minimum nutrient quota [mg P mg C ⁻¹]
r	0.05	specific mineralization rate of sedimented nutrients [day ⁻¹]
R_{in}	5-50 ^{b)}	dissolved mineral nutrient concentration at the start [mg P m ⁻³]
R_{tot}		total nutrients in the system, expressed by volume ($=R+R_s/z+QA+qG$)
ρ_{max}	0.2	maximum specific algal nutrient uptake rate [mg P mg C ⁻¹ day ⁻¹]
v	0.25	algal sinking velocity [m day ⁻¹]
z	1-20 ^{b)}	depth of mixed layer [m]
Variable		
A	50 ^{c)}	algal carbon density [mg C m ⁻³]
g		specific grazer growth rate [day ⁻¹]
G	1 ^{c)}	grazer carbon density [mg C m ⁻³]
$I(s)$		light intensity at depth s [$\mu\text{mol photons m}^{-2} \text{s}^{-1}$]
J_A		ingestion rate of algae per grazer [day ⁻¹]
p		specific algal production rate [day ⁻¹]
Q^a	0.01 ^{c)}	algal nutrient quota [mg P mg C ⁻¹]
R		dissolved mineral nutrient concentration [mg P m ⁻³]
R_s	0 ^{c)}	pool of sedimented nutrients [mg P m ⁻²]
s		depth below water surface [m]

^{a)} Q is a constant parameter in the fixed stoichiometry model but a variable in the flexible stoichiometry model.

^{b)} Range of environmental conditions examined

^{c)} Initial values

Model analyses: General approach

We performed numerical simulations to explore how mixing depth and nutrient supply influence the transient dynamics of the two algae-grazer models when started from low population densities. We investigated combinations of 39 mixing depths (evenly spaced between 1 and 20 m) with four levels of nutrient enrichment (initial concentration of mineral phosphorus 5, 10, 20 or 50 mg P m⁻³) spanning most of the range of conditions encountered in temperate lakes. The remaining environmental and algal parameter values and initial conditions (listed in Table 2) are representative of a generic temperate clearwater lake inhabited by phytoplankton with average traits. We took parameter values for *Daphnia pulex* from McCauley et al. (1996) and Nisbet et al. (1997). All parameter values are close to identical to the ones used in Diehl (2007), with the exception of background turbidity and algal sinking velocity, which were adapted to the experimental conditions.

The temporal dynamics of the system depend on mixing depth and nutrient enrichment, which we illustrate with a few examples of the dynamics of algae, algal cell quota and grazers in the flexible stoichiometry model (Fig. 1). Further examples and the concomitant

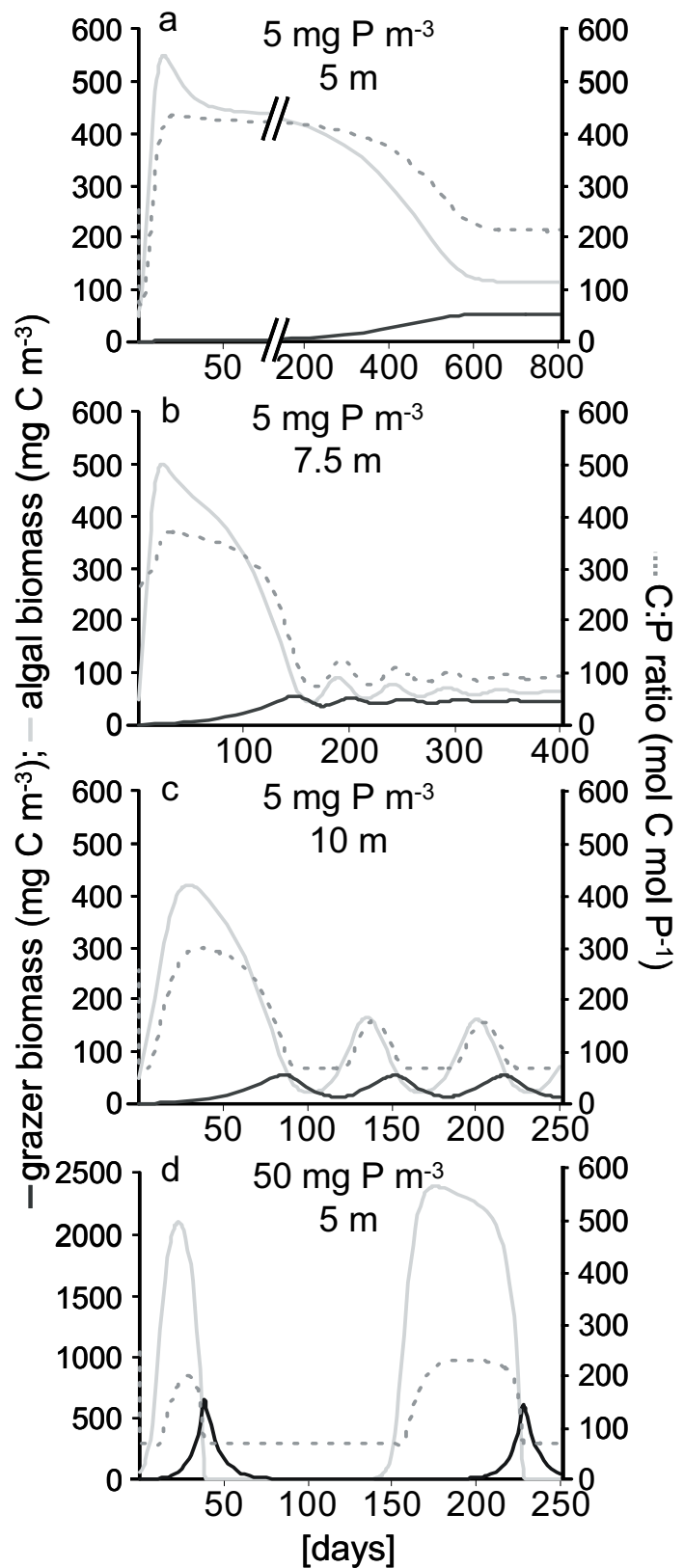


Fig. 1. Numerical examples of time courses of *Daphnia* biomass (dark gray line), algal biomass (light gray line), and algal C:P ratio (dashed line) for different combinations of initial dissolved phosphorus concentration and mixing depth, as written above each panel. Note the differences in scale on both axes.

nutrient dynamics are shown in Appendix A. Independent of whether algal stoichiometry is flexible or fixed, algae and grazers go through at least one oscillation for most combinations of nutrient enrichment and mixing depth: phytoplankton initially increases followed by a build-up of grazers which overgraze their algal food base; the resulting reduction of algal biomass is followed by a crash of the grazer population. These transient algae-grazer oscillations subsequently decay to an equilibrium (e.g., Fig. 1b) or settle to a limit cycle (e.g., Fig. 1c).

We characterized the initial algae-grazer dynamics by the following metrics: (1) algal biomass at the first algal peak; (2) time to the first algal peak; (3) algal food quality (C:P ratio) at the time of the first algal peak (only flexible stoichiometry model); (4) duration of the first algal peak (arbitrarily defined as the no. of days with $> 50\%$ of peak biomass); (5) grazer biomass at the first grazer peak; (6) time to the first grazer peak; (7) algal food quality (C:P ratio) at the time of the first grazer peak (only flexible stoichiometry model); (8) duration of the first grazer peak (= no. of days with $> 50\%$ of peak biomass); (9) algal biomass at the first minimum following the algal peak; (10) time to the first algal minimum.

Several of the above behaviors do not always occur. When grazers approach a stable equilibrium without overshooting (Fig. 1a), we counted the equilibrium grazer biomass as equivalent to the maximum biomass and defined the day of the maximum as the day when grazer biomass reaches equilibrium. A peak duration is, however, not meaningful to define in this case as well as in the case when an initial grazer peak does not decline to less than 50% of its maximum. Similarly, when algal biomass declines from an initial peak towards a stable equilibrium without producing a minimum (Fig. 1a), we counted equilibrium biomass as equivalent to minimum biomass and defined the day of minimum as the day when algal biomass reaches equilibrium. When grazers cannot persist and the population dies out soon after the start, none of the above metrics was calculated. This case occurred under very restricted conditions of low nutrient levels ($R_{tot} = 5 \text{ mg P m}^{-3}$) combined with shallow mixing depths ($\bar{z} < 4.5 \text{ m}$ and $\bar{z} < 2 \text{ m}$ in the flexible and fixed stoichiometry models, respectively).

Below, we report the results of numerical simulations starting from low initial densities ($A = 50 \text{ mg C m}^{-3}$, $G = 1 \text{ mg C m}^{-3}$). In Appendices C and D we show that these results are qualitatively closely approximated by properties of the asymptotic model behavior and by properties of boundary equilibria (see also Table 3). As long as initial population densities are reasonably low the results, summarized in Figs. 2 and 3, are thus independent of initial conditions (this was confirmed by numerical simulations with initial algal and grazer biomasses up to 250 mg C m^{-3} and 5 mg C m^{-3} , respectively) and are therefore representative for the full range of initial conditions typical for the beginning of the season in a temperate lake.

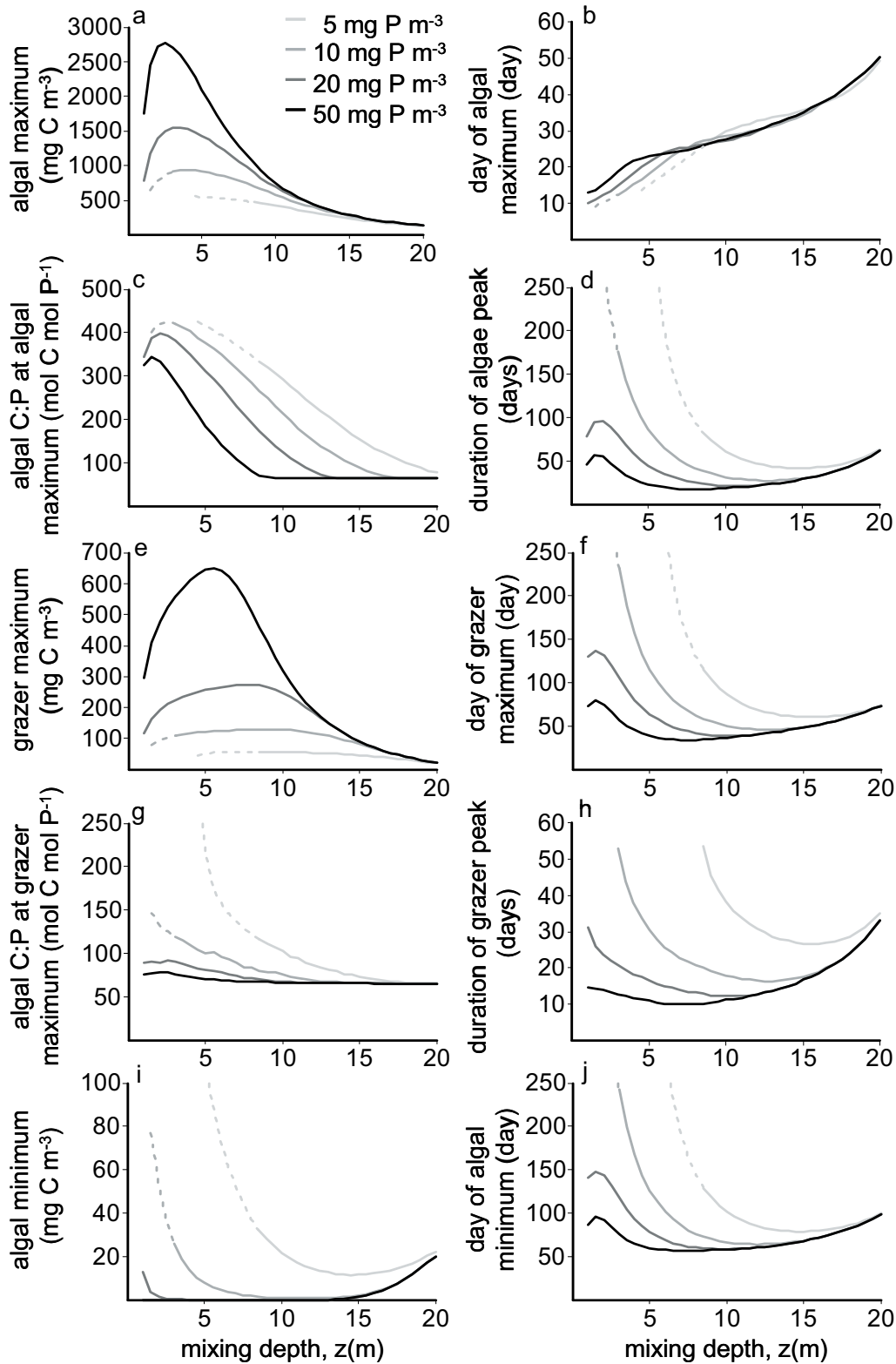


Fig. 2. Flexible stoichiometry model predictions. Effects of mixing depth (z) and initial dissolved phosphorus concentration (as indicated by legend) on (a) algal biomass at the first algal peak; (b) time to the first algal peak; (c) algal carbon to phosphorus ratio at the first algal peak; (d) duration of the first algal peak (= number of days with more than 50% of peak biomass); (e) grazer biomass at the first grazer peak; (f) time to the first grazer peak; (g) algal carbon to phosphorus ratio at the first grazer peak; (h) duration of the first grazer peak (= number of days with more than 50% of peak biomass); (i) algal biomass at the first minimum following the algal peak; (j) time to the first algal minimum. Dashed lines indicate that the initial grazer peak does not decline to less than 50% of its maximum (which implies that a grazer peak duration cannot be defined). Parameter values are as in Table 2.

Model analyses: Results

Flexible stoichiometry model: effects of nutrient enrichment

With increasing mixing depth algal production becomes increasingly limited by light. At the deepest mixing depths algae-grazer dynamics are therefore largely independent of nutrient supply (see Appendix A Fig. A1e vs. f). Consequently, all metrics characterizing transient dynamics converge towards deeper mixing depths and most nutrient effects are the stronger the shallower the system (Fig. 2). At shallow and intermediate mixing depths nutrient enrichment enhances algal growth and increases algal nutrient content (reduces algal C:P; see Fig. 1a vs. d and Fig. 2c, g). Improved food production and quality, in turn, accentuate and speed up grazing-driven dynamics: with increasing nutrient enrichment the initial grazer peak becomes higher (Fig. 2e), is reached earlier (Fig. 2f), and lasts for a shorter period (Fig. 2h). The latter occurs, because more grazers drive algae to a lower minimum (Fig. 2i) that is reached earlier (Fig. 2j). Thus, with increasing nutrient enrichment grazers overexploit their food resource faster and more strongly, resulting in a shorter duration of the grazer peak.

Highly productive algae may temporarily escape from grazer control (see Fig. 1a, b, d). At shallow to intermediate mixing depths (where light supply is sufficient) nutrient enrichment therefore prolongs the initial algal growth phase: the algal peak is reached slightly later and attains higher levels than at low nutrient enrichment (Fig. 2a, b). Nutrient enrichment nevertheless shortens the duration of the algal peak in shallow systems (Fig. 2d), because the grazer population catches up more quickly and grazes down the algal peak faster.

Flexible stoichiometry model: effects of mixing depth

Transient responses to mixing depth can be broadly categorized into two patterns along the mixing depth gradient: (i) unimodal (e.g., algae and grazer maxima) or (ii) monotonously declining to U-shaped (e.g., timing and duration of most transient events) (Fig. 2). These patterns are explained as follows. Going from intermediate to deep mixing depths, increasing light limitation slows down algal growth and overall dynamics. Consequently, timing and duration of all transient events are increasingly delayed and peak biomasses are reduced towards the deepest mixing depths (Fig. 2). Going from intermediate to shallow mixing depths, algal nutrient content at the algal peak may become so low (algal C:P may become so high; Fig. 2c) that grazers increase very slowly in spite of high food abundance. Grazers therefore reach their first peak later and peak biomass is lower at shallow than at intermediate mixing depths (Fig. 2e, f). Consequently, grazers in shallow systems do not overexploit algal resources as much (the algal minimum is higher and occurs later; Fig. 2i, j) allowing the grazer peak to last longer compared to intermediate mixing depths (Fig. 2h).

The described mechanisms operate most strongly at low to intermediate nutrient levels. At higher nutrient levels algal quality is high even in shallow water and all decreasing and U-shaped responses to mixing depth flatten out (Fig. 2). The unimodal responses of peak biomasses are, instead, more accentuated at higher nutrient levels, because production responds most strongly to nutrients at shallow mixing depths where light is abundant. At the shallowest mixing depths algal biomass decreases, however, again due to high sinking losses (this would not happen with neutrally buoyant algae). The decline of grazer peak biomass at the shallowest mixing depths depends, instead, largely on the declining food quality at the algal biomass peak and would therefore be observed also with neutrally buoyant algae.

Fixed stoichiometry model

We illustrate the results for the fixed stoichiometry model with an example where the algal C:P ratio was fixed at the Redfield ratio. Using a different fixed algal C:P ratio yields the same qualitative patterns. The flexible stoichiometry model's biomass responses to nutrient supply and mixing depth are also observed in the fixed stoichiometry model. Algal and grazer peaks increase and the algal minimum decreases with nutrient enrichment. Similarly, algal and grazer peaks are unimodally related to mixing depth, and the algal minimum in a U-shaped manner, because algal net production is limited by sinking losses at shallow and by light at deep mixing depths (see Appendix B Fig. B1a, d, g).

In contrast, most metrics describing the timing of events differ between the two models. Ignoring cases where grazers approach an equilibrium without a transient oscillation (dashed lines in Fig. 3), the duration of the algae and grazer peaks, the day of the grazer peak, and the day of the algal minimum all increase more or less monotonically with mixing depth in the fixed stoichiometry model (Fig. 3a, b, c, d), which contrasts with the mostly decreasing or U-shaped responses in the flexible stoichiometry model (Fig. 2d, f, h, j). This difference arises because, with flexible stoichiometry, grazer growth is slowed down by decreasing food quality at shallow mixing depths, a phenomenon that cannot arise with fixed stoichiometry. Finally, while at shallow mixing depths nutrient enrichment speeds up the timing of most events in the flexible stoichiometry model (Fig. 2d, f, h, j), such a remarkable effect of nutrient enrichment is not seen in the fixed stoichiometry model (Fig. 3a, b, d). The explanation for this difference is that nutrient enrichment may considerably improve algal quality (especially at shallow mixing depths) which, in turn, speeds up

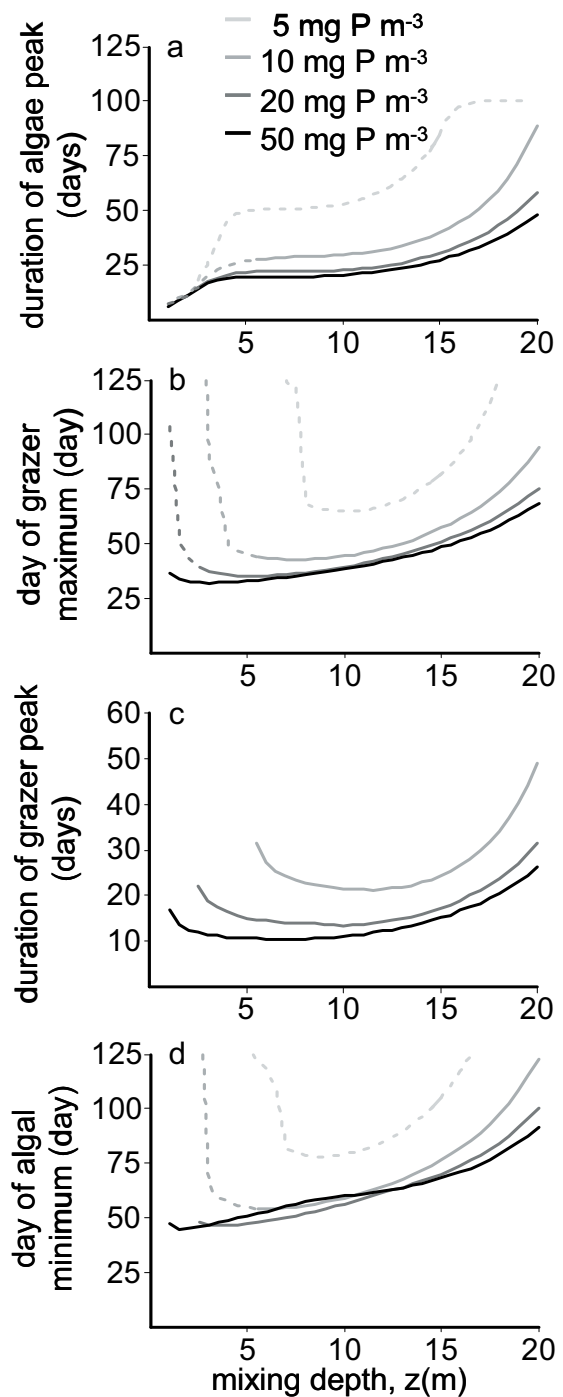


Fig. 3. Fixed stoichiometry model predictions. Effects of mixing depth (z) and initial dissolved phosphorus concentration (as indicated by legend) on (a) duration of the first algal peak (= number of days with more than 50% of peak biomass); (b) time to the first grazer peak; (c) duration of the first grazer peak (= number of days with more than 50% of peak biomass); (d) time to the first algal minimum. Dashed lines indicate that the initial grazer peak does not decline to less than 50% of its maximum (which implies that a grazer peak duration cannot be defined). Parameter values are as in Table 2 with Q fixed at the Redfield ratio ($1/41 \text{ mg P mg C}^{-1}$).

algal and grazer growth rates. Such an effect is only possible in the flexible stoichiometry model. Thus, algal and grazer responses to nutrient enrichment differ qualitatively and quantitatively between the two models, especially at shallow mixing depths.

Analytical approximations to transient dynamics

How robust are the above described results against changes in initial conditions? While our numerical simulations produced similar results over a broad range of initial conditions, it is actually possible to obtain the qualitative response pattern of the first transient oscillation to nutrient and light enrichment without numerical simulations. In Appendix C, we illustrate that transient responses of the flexible stoichiometry model to light and nutrient supply are qualitatively well approximated by properties of the asymptotic attractor and of boundary equilibria with one or both species missing, which we call ‘analytical correlates’. Specifically, the following intuitive relationships emerge (Table 3): (i) algal biomass and C:P ratio at the first algal peak correlate with equilibrium algal biomass and C:P ratio in a system without grazers; (ii) time to the first algal peak correlates inversely with the specific growth rate of an algal population invading an empty system; (iii) duration of the first algal peak, time to the first grazer peak, and time to the first algal minimum all correlate inversely with the specific growth rate of a grazer invading an algal monoculture at equilibrium; (iv) grazer biomass and algal C:P ratio at the first grazer peak, duration of the grazer peak, and algal biomass at the first algal minimum correlate with the corresponding quantities evaluated on the system’s limit cycle or at its stable equilibrium, whichever applies.

To quantify the match between properties of the first oscillation and their analytical correlates, we calculated rank correlations between them across the grid of environmental parameters used in the numerical simulations (39 mixing depths times 4 nutrient levels); since not all simulation runs yielded transient oscillations (see dashed parts of the lines in Fig. 2) sample size was 136 rather than 156. For the flexible stoichiometry model all ten possible correlations are good to excellent (Table 3). With the exception of (iii), this is also true for the fixed stoichiometry model [Table 3; Appendix D, which includes an explanation for the deviation from pattern (iii)].

Table 3. Analytical Correlates of properties of the first transient algae-grazer oscillation derived from properties of asymptotic attractors and of boundary equilibria with one or both species missing. The tightness of the correlations between transient population dynamics and their analytical correlates is shown separately for the flexible and fixed stoichiometry models as the rank correlation coefficient Spearman's rho.

Property of first oscillation	Analytical Correlate		Spearman's rho	
	Flexible (N = 136)	Fixed (N = 100)	Flexible (N = 136)	Fixed (N = 100)
Algal biomass at the first algal peak	Equilibrium algal biomass in system without grazers		0.85 ^{***}	0.56 ^{***}
Time to the first algal peak	Inverse of specific growth rate of algal population invading an empty system		1.00 ^{***}	0.97 ^{***}
Algal C:P ratio at the first algal peak	Algal C:P ratio in system without grazers		0.99 ^{***}	-
Duration ^{a)} of the first algal peak	Inverse of specific growth rate of grazer population invading an algal monoculture at equilibrium		0.63 ^{***}	0.48 ^{***}
Grazer biomass at the first grazer peak	Grazer biomass at grazer maximum on limit cycle <i>or</i> : Equilibrium Grazer biomass		0.92 ^{***}	0.94 ^{***}
Time to the first grazer peak	Inverse of specific growth rate of grazer population invading an algal monoculture at equilibrium		0.65 ^{***}	0.35 ^{***}
Algal C:P ratio at the first grazer peak	Algal C:P ratio at grazer maximum on limit cycle <i>or</i> : Algal C:P ratio at grazer equilibrium		1.00 ^{***}	-
Duration ^{a)} of the first grazer peak	Duration ^{a)} of grazer maximum of limit cycle (no correlate exists for this property in a locally stable system)		0.92 ^{***}	0.93 ^{***}
Algal biomass at the first algal minimum	Algal biomass at algal minimum on limit cycle <i>or</i> : Equilibrium algal biomass		0.92 ^{***}	0.94 ^{***}
Time to the first algal minimum	Inverse of specific growth rate of grazer population invading an algal monoculture at equilibrium		0.57 ^{***}	0.08 ^{NS}

^{a)} number of days with more than 50% of peak biomass

*** p < 0.001

NS p > 0.05

Field Experiment - Material and Methods

Study site and experimental design

The enclosure experiment was carried out in Lake Brunnsee near the University of Munich's Limnological Research Station at Seeon (90 km east of Munich, Germany). Chlorophyll *a* concentrations in this low productive hardwater lake are usually $< 3 \text{ mg m}^{-3}$, Secchi depth is 7-15 m, and total phosphorus concentrations are 4-10 mg m^{-3} . Other nutrients are available far in excess of algal needs (Diehl et al. 2002).



Plate 1. The experimental raft with the 24 enclosures at Lake Brunnsee with (from left to right) C. Matauschek, A. Wild, and C. Jäger.

We crossed four enclosure depths (1, 3, 6, and 12 m) with three nutrient levels (ambient and addition of 20 or 50 mg P m^{-3}) in two replicates per treatment. The enclosures (cylindrical, transparent plastic bags of 0.95 m diameter, heat sealed at the bottom and open to the atmosphere) were suspended from a raft (Plate 1). Well-mixed conditions were maintained by intermittently blowing air

into to the bottom of each enclosure (for 3 min every 40 min). To prevent differences in temperature between the different depth treatments, we surrounded the raft with a 13 m deep bag of clear plastic. The water inside this bag was intermittently mixed (for 6 min every 20 min), creating a water bath of homogeneous temperature for 20 enclosures. The remaining enclosures (four 12 m deep replicates) had to be suspended outside the water bath and were mixed at the same interval as the latter. Average enclosure temperature decreased over the course of the experiment from an initial 19.2°C to 13.2°C at the end. The mixing was highly effective. Vertical temperature gradients were negligible and any two enclosures inside the water bath differed by less than 0.9°C. The four outside enclosures were on average 1.5°C warmer than the corresponding 12 m enclosures inside the water bath.

For logistical reasons we had to perform the experiment in late summer rather than in spring. Because Lake Brunnsee receives a constant input of silicon rich spring water, spring and summer phytoplankton communities do, however, not differ greatly. In both seasons, the edible central diatom *Cyclotella* spp. usually makes up $\geq 50\%$ of total phytoplankton biovolume. We therefore expected the starting community to not deviate substantially from a typical spring community in Lake Brunnsee. This is supported by a detailed comparison of the starting community in this experiment and an experiment conducted in the

following spring (Berger et al. 2007), which gave 55% compositional overlap at the genus level and > 80% overlap at the level of algal classes (C. Matauschek and G. Trommer, unpublished data).

On 16-19 August 2004 we filled the enclosures with 30 μm filtered epilimnetic lake water to remove larger zooplankton and any larger inedible algae from the initial community. On 23 August we stocked *Daphnia hyalina* (the naturally occurring *Daphnia* species in the lake) at a density of about 0.5 ind. L^{-1} . Because previous experiments suggested that *D. hyalina* need one to two weeks of acclimation to enclosure conditions before the population starts to grow, we added phosphorus to fertilization treatments in two doses (50% each time, loaded as KH_2PO_4) on 30 August and 6 September. Subsequently, we label 30 August as day 0 (and 23 August as day -7). Counting from day 0, the experiment lasted for 49 days until 19 October.

Sampling program and laboratory analyses

All enclosures were sampled once per week. We measured water temperature and electrical conductivity in vertical steps of 1m. Water column samples were 250 μm filtered to remove mesozooplankton. Concentrations of dissolved inorganic phosphorus (SRP), particulate phosphorus (PP) and total phosphorus (TP) were measured with standard methods (Wetzel and Likens 1991). Seston particulate organic carbon (POC) was filtered on pre-combusted glass fiber filters (GF6, Schleicher & Schüll, Germany) and determined by infrared-spectrophotometry (C-Mat 500, Ströhlein, Korschebroich, Germany).

Phytoplankton samples were immediately preserved with acid Lugol's iodine and later counted in an inverted microscope (Utermöhl 1958). In each sample we counted at least 100 cells from every abundant taxon and measured 20 to 50 cells. Length measurements were first converted to biovolume using appropriate geometrical forms (Hillebrand et al. 1999) and then to carbon biomass using a conversion factor for cells fixed in Lugol's iodine of $1 \mu\text{m}^3 \text{ cell volume} = 0.145 \text{ pg carbon}$ (Montagnes et al. 1994).

Because our model considers phytoplankton to be edible, we exclude grazing resistant taxa from the analyses presented here. Thus, the subsequently presented data on algal biomass refer to the summed carbon biomass of all 'edible' taxa. Phytoplankton taxa were considered edible for *D. hyalina* when their longest axial dimension did not exceed 30 μm (Burns 1968). Cyanobacteria, which never exceeded 7% of total algal biomass, were generally considered as grazing resistant regardless of cell size (Briand and McCauley 1978; Sommer et al. 2001).

Zooplankton samples were taken by vertical hauls with a 250 μm mesh net from the enclosure bottom to the water surface. Samples were immediately frozen and subsequently counted under a dissecting microscope. In each sample we measured the lengths of 30 haphazardly chosen *D. hyalina* and counted the eggs in their brood pouches. We calculated the dry masses of *D. hyalina* as $W = 5.59 \cdot L^{2.2}$, where W is dry mass in μg and L is length in mm (Stibor and Lüning 1994). The dry mass of eggs was estimated as 1.415 $\mu\text{g}/\text{egg}$ (Lynch et al. 1986). Total dry mass (including eggs) was converted to carbon biomass using a conversion factor of 0.46 g C per g dry mass (Andersen and Hessen 1991).

Data processing and statistics

In accordance with model expectations, *Daphnia* time series showed one fairly distinct, transient peak in all but one replicate (Appendix E). The latter was subsequently excluded from all analyses. In order to estimate the magnitude, timing and duration of the *Daphnia* peak with a finer resolution than our weekly sampling interval, we fitted a smooth, continuous function to each *Daphnia* time series. The following Weibull function gave an excellent fit to most time series [Appendix E; see also Berger et al. (2007)]:

$$G(t) = m \left[\frac{b}{a} \left(\frac{t}{a} \right)^{(b-1)} \exp \left(- \left(\frac{t}{a} \right)^b \right) \right] \quad (1)$$

where $G(t)$ is *Daphnia* biomass [mg C m^{-3}] m , a , and b are fitted parameters, and t is time in days since day 0 of the experiment. Magnitude, timing and duration of each *Daphnia* peak were subsequently estimated from the fitted functions. With very few exceptions, these estimates were very close to the directly measured values (Appendix E). We used the fitted values because of their continuous time resolution and because they use information from all sampling dates and therefore should be less influenced by single measurement errors.

Most replicates deviated from model expectations in that they did not show a transient phytoplankton peak; phytoplankton biomass did, however, always reach a minimum during or after the *Daphnia* peak (Appendix F1). No single function could be fitted to the diverse patterns of phytoplankton time series. We therefore estimated the timing of the phytoplankton minimum and the corresponding minimum biomass directly from the data.

To statistically analyze the effects of mixing depth and nutrients on response variables we performed two-way ANOVAs with enclosure depth and fertilization level as fixed factors. To improve homogeneity of variances we log-transformed all biomass and nutrient data.

Table 4. Summary of ANOVA results

dependent variable	factor	df	p
ln <i>Daphnia</i> maximum biomass	fertilization	2, 11	0.00
	mixing depth	3, 11	0.00
	interaction	6, 11	0.09
day of <i>Daphnia</i> maximum	fertilization	2, 11	0.02
	mixing depth	3, 11	0.00
	interaction	6, 11	0.02
ln C:P ratio at <i>Daphnia</i> maximum	fertilization	2, 11	0.00
	mixing depth	3, 11	0.01
	interaction	6, 11	0.06
duration of <i>Daphnia</i> maximum	fertilization	2, 11	0.00
	mixing depth	3, 11	0.00
	interaction	6, 11	0.03
ln algal minimum biomass	fertilization	2, 11	0.00
	mixing depth	3, 11	0.26
	interaction	6, 11	0.28
day of algal minimum	fertilization	2, 11	0.00
	mixing depth	3, 11	0.10
	interaction	6, 11	0.55

Results

At the start of the experiment, TP concentration in the unfertilized treatments was about 7 mg P m^{-3} with no measurable SRP and approximately 4 mg P m^{-3} of dissolved organic P [determined as the difference $\text{TP} - (\text{SRP} + \text{particulate P})$]. The TP concentration decreased over time because of sedimentation losses. In most treatments edible phytoplankton biomass decreased over time without reaching a peak, but showed a minimum after 21-49 days. In contrast, *Daphnia* biomass increased in all but one replicate and reached a peak after 13-35 days. In most fertilized (but not in the unfertilized) treatments inedible algae became abundant about one week after the *Daphnia* peak. Inedible algae were dominated by the filamentous chlorophyte *Mougeotia*, which became noticeable as detached wall growth in the fertilized enclosures from day 21 on. The measured seston C:P ratios are therefore based on a mix of edible and inedible algae. The time trajectories of the biomasses of edible phytoplankton and *Daphnia* are shown for all replicates in Appendix F1, and the time trajectories of seston C:P ratio and TP concentration are shown in Appendix F2. Rather than describing these results in detail, we focus on a comparison of the observed transient dynamics with model expectations using the metrics defined in the section *Model analyses: General approach*. Because we do not have access to parameter values characterizing *D. hyalina* and because algal parameter values are not specific to our system, we compare data with model expectations in a qualitative rather than a quantitative manner. Since there was no phytoplankton peak in most enclosures, we focus on the grazer peak, the seston C:P ratio, and the phytoplankton minimum.

Transient Daphnia peak (Fig. 4a, b, d). - As expected from both models, peak biomass of *Daphnia* decreased towards deeper mixing depths and was higher at higher levels of nutrient enrichment (Table 4). Also as expected, the positive effect of nutrient enrichment was highest at the shallowest mixing depth (marginally significant depth by fertilization interaction, Table 4). In contrast to expectations, peak biomass was not unimodally related to mixing depth.

Nutrient enrichment speeded up *Daphnia* dynamics: the *Daphnia* peak occurred earlier (predicted by both models) and lasted shorter (predicted by the flexible stoichiometry model) at higher nutrient levels. *Daphnia* dynamics were slower (the peak occurred later and lasted longer) at shallow compared to intermediate mixing depths (predicted by the flexible stoichiometry model). Compatible with both models, this trend was reversed towards the deepest mixing depths in some nutrient treatments (depth by fertilization interaction, Table 4).

Seston C:P ratio (Fig. 4c). - The seston C:P ratio at the time of the *Daphnia* peak decreased with nutrient enrichment and with increasing mixing depth (predicted by the flexible stoichiometry model). In contrast to expectations, this mixing depth trend was, however, only observed in the fertilized enclosures (depth by fertilization interaction, Table 4). In the unfertilized enclosures, seston C:P ratios at the *Daphnia* peak were generally fairly high and unrelated to mixing depth.

Phytoplankton minimum (Fig. 4e, f). - The phytoplankton biomass minimum occurred earlier (predicted by the flexible stoichiometry model) and reached lower levels (predicted by both models) at higher nutrient enrichment. Both the timing and magnitude of minimum biomass showed a weak tendency (predicted by both models) to decline from shallow to intermediate mixing depth, but these trends were not statistically significant (Table 4).

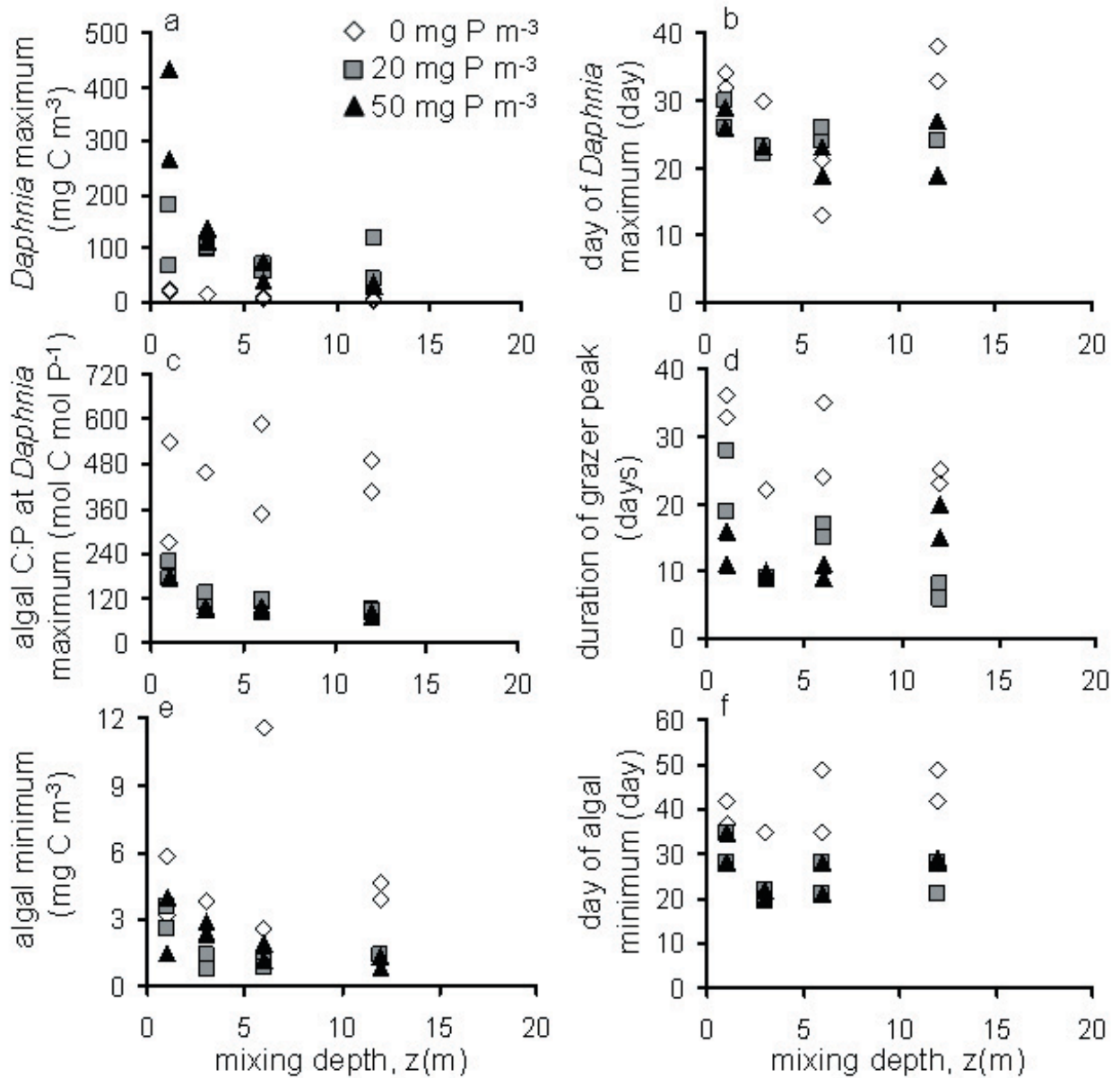


Fig. 4. Results of the field experiment. Effects of mixing depth (z) and initial dissolved phosphorus addition (as indicated by legend) on (a) *Daphnia* biomass at the transient *Daphnia* peak; (b) time to the transient *Daphnia* peak; (c) seston carbon to phosphorus ratio at the transient *Daphnia* peak; (d) duration of the transient *Daphnia* peak (= number of days with more than 50% of peak biomass); (e) algal biomass at the algal minimum; (f) time to the algal minimum.

Discussion

Analyses of transient dynamics

Transient population dynamics have long received very little attention in theoretical ecology. While new methods have recently been developed to characterize transient dynamics of systems with stable equilibria (Neubert and Caswell 1997; Neubert et al. 2004), the producer-grazer systems we investigated lack stable equilibria over large parts of the light-nutrient supply space (Diehl 2007). The exploration of transient dynamics through numerical simulation is daunting, because a system's transients depend both on its asymptotic attractor(s) and on an unlimited set of initial conditions. However, many initial conditions are unlikely to occur in nature. The exploration of transient dynamics can therefore be restricted to the most relevant initial conditions. Planktonic producer-grazer systems in temperate lakes are regularly set back to low population densities during winter (Sommer et al. 1986). We have therefore focused our exploration of transient dynamics to an initial condition where both population densities are low. It is nevertheless important to note that, although the long-term dynamics of the algae-grazer system may not be reached on an ecologically meaningful time scale, long-term attractors play an important role in shaping transient dynamics. This is illustrated by the analyses using the 'analytical correlates'. These analyses suggest that the qualitative response patterns of the two models depicted in Figs. 2 and 3 (and Appendix B) are robust against changes in initial conditions (as long as initial population densities are sufficiently low that a sequence of an algae and grazer peak is observed) and therefore provide a solid basis for comparison with empirical data.

Similar to our phytoplankton-*Daphnia* models, most consumer-resource models with biotic resources go through transient oscillations when started from low densities (Murdoch et al. 2003). Our description of transient dynamics in terms of the magnitude, timing and duration of population peaks and troughs should therefore be of general applicability. It is possible to characterize small oscillations rigorously in terms of the characteristic equation of the equilibrium (Gurney and Nisbet 1998), but the period of a large amplitude limit cycle is usually much larger than that of the corresponding oscillations closer to equilibrium. Furthermore, the first oscillation frequently deviates substantially from subsequent ones (e.g., Fig. 1b, c, d). We have therefore explored the initial, oscillatory dynamics of our model primarily through numerical simulation.

Opposing effects of light vs. nutrient enrichment on population coupling and interaction strength

Inside a parameter region ($\leq 20 \text{ mg P m}^{-3}$ and $\leq 10 \text{ m}$ mixing depth) where the algal C:P ratio is highly sensitive to changes in nutrient and light supply, transient dynamics are accelerated by nutrient enrichment but slowed down by light enrichment in the flexible stoichiometry model. These opposing effects of nutrient vs. light enrichment are explained by the negative influence of increased algal C:P ratio on the tightness of phytoplankton grazer coupling. At a given nutrient level, moving from intermediate to shallow mixing depths yields faster growing phytoplankton with a higher C:P ratio during the initial algal peak, i.e., algal productivity and quality as food are inversely correlated. This loosens the coupling of phytoplankton-grazer dynamics and thus extends the duration of the algal peak and delays the grazer peak. In contrast, at a given mixing depth, increasing the nutrient supply yields faster growing phytoplankton with a lower C:P ratio during the initial algal peak, i.e., algal productivity and

quality are positively correlated. This tightens the coupling of phytoplankton and grazers and speeds up transient dynamics, except at the deepest mixing depths where low light supply causes predominant energy limitation of algal and grazer growth rates.

Generally, the phytoplankton-grazer coupling is tightest at the highest nutrient levels, where algal quality changes the least in response to light enrichment. Consequently, the timing of transient events shows the flattest response to changes in mixing depth when nutrient supply is very high ($\geq 50 \text{ mg P m}^{-3}$, Fig. 2). At the same time, the amplitudes of transient oscillations are highest (have higher maxima and lower minima) when the phytoplankton grazer coupling is tightest. In contrast lower algal quality constrains the energy flow to the grazer and reduces the amplitude of the transient oscillations and thus stabilizes the phytoplankton-grazer interaction (see also Loladze et al. 2000; Diehl 2007). This is in line with McCann's (2000) suggestion that weak interactions stabilize food web dynamics.

Comparison of experimental data with model expectations

The experimental system differed from the model in that the former included a diverse phytoplankton community containing both edible and inedible taxa. While we were able to separate out the dynamics of the edible phytoplankton, the C:P ratio could only be determined for bulk seston. With these caveats in mind, there was nevertheless rather good qualitative agreement between experimental results and expectations from the flexible stoichiometry model, whereas several expectations from the fixed stoichiometry model were not corroborated. In particular, the fixed stoichiometry model could not explain the decrease in algal C:P ratio and the acceleration of transient dynamics with nutrient enrichment, as well as the increase in algal C:P ratio and the deceleration of transient dynamics with light enrichment (decreasing mixing depth). Clearly, the observed qualitative influences of nutrient and light enrichment on transient dynamics of edible phytoplankton and *Daphnia*, are in much better agreement with the predictions from the flexible than the fixed stoichiometry model.

The flexible stoichiometry model prediction that nutrient effects should be stronger in shallower systems was, however, only born out by *Daphnia* peak biomass. The remaining metrics did not converge towards deeper mixing depths, largely because unfertilized treatments showed in most cases only weak trends along the mixing depth gradient. Unfertilized treatments deviated from model assumptions in that there was no measurable SRP at the beginning of the experiment, but a fairly large fraction of dissolved organic P, which is largely unavailable to phytoplankton. Severe nutrient deficiency of the initial phytoplankton community probably explains the persistently high seston C:P ratios in all unfertilized enclosures. Because of low seston quality phytoplankton-grazer dynamics should have been only loosely coupled, which may explain the delayed timing of the *Daphnia* peak and the algal minimum even at deep mixing depths.

The absence of an initial algal peak in most fertilized enclosures was unexpected and contrasts with observations from a similar experiment conducted in spring (Berger et al. 2007). The initial decline of algal biomass cannot be explained by grazing pressure, which ranged from < 0.01 to max. 0.04 per day on days -7 to 7 [as estimated from empirical body length-filtration rate relationships (Knoechel and Holtby 1986)]. Possibly, the lack of an algal peak was related to a concomitant shift in the taxonomic composition of the algal community from an initial dominance of central diatoms, dinoflagellates and the chlorophyte *Oocystis* towards pennate diatoms and the chlorophytes *Scenedesmus* and *Coenochloris* (C.G. Jäger, unpublished data).

Finally, in contrast to expectations from both models, we did not observe a unimodal response of *Daphnia* peak biomass to mixing depth in the fertilized treatments. Lower *Daphnia* peak biomasses at the shallowest depths are predicted because high sinking losses are assumed to turn a large fraction of algal biomass into sedimented detritus. In contrast sedimented algae probably continued to photosynthesize at the relatively well lit bottom of the shallow enclosures (>35 % of incident radiation reached down to 1 m depth), where they remained accessible to grazing by *Daphnia*.

Transient dynamics and the paradox of energy enrichment

For some parameter sets the flexible stoichiometry model may have an equilibrium consisting of a high density of low quality (high C:P) algae with *Daphnia* being extinct. Along a gradient of light enrichment, this equilibrium may either appear suddenly as an alternative attractor to a pre-existing phytoplankton-*Daphnia* state or it may emerge from a phytoplankton-*Daphnia* equilibrium, where *Daphnia* biomass decreases with light enrichment (Diehl 2007). The latter phenomenon has been termed the ‘paradox of energy enrichment’ (Loladze et al. 2000). In our model the paradox of energy enrichment occurs in a rather limited parameter space of very high light supply combined with very low nutrient supply (Diehl 2007). A ‘ghost’ of the phytoplankton-only attractor can, however, be seen as a transient phenomenon in adjacent parameter space, where it produces a long lasting initial algal peak with a high algal C:P ratio (Fig. 1a). Because of low food quality, the grazer population grows very slowly in spite of high food abundance and only slowly grazes down the algal peak.

The duration of this transient algal peak may exceed the length of the growing season in a temperate lake. The parameter space producing the paradox of energy enrichment as a transient phenomenon should therefore be larger than predicted solely based on asymptotic model behavior. Transient peaks of high C:P algal biomass persisting for up to 90 days have indeed been reported from experiments with *Daphnia* feeding on chlorophytes (Sommer 1992; Nelson et al. 2001; Urabe et al. 2002). Given the absence of transient phytoplankton peaks in most of our enclosures we found no evidence of such system behavior. On the contrary, *Daphnia* peak biomass increased with light enrichment (decreasing mixing depth) along the entire mixing depth gradient even in the unfertilized enclosures where the paradox of energy enrichment would be most likely. This discrepancy between observations and theory suggests that there may be a factor or mechanism masking or mitigating the paradox of energy enrichment in natural communities. For example *Daphnia* can feed on diverse organisms including bacteria, microzooplankton and mixotrophs in addition to autotrophic algae. Since C:P ratio of these heterotrophs and mixotrophs is generally low (Katechakis et al. 2005), feeding on these organisms would act as a buffer against negative effects of enrichment.

Outlook

We have studied transient phytoplankton-*Daphnia* dynamics under constant environmental conditions. However, in temperate lakes, the observed intrinsic oscillations interact with climate driven environmental forcing to produce a diverse pattern of seasonal dynamics (Scheffer et al. 1997). Spring successional patterns in temperate lakes appear to be in good agreement with our model predictions. They often show relatively fast and pronounced transient oscillations in nutrient rich lakes and slower dynamics with less pronounced peaks and troughs in nutrient poor lakes (Sommer et al. 1986). More research on the interaction of these intrinsic and extrinsic forces is required to gain a better understanding of how climate influences seasonal plankton dynamics (Scheffer et al. 2001; De Senerpont Domis et al. 2007). Global climate change has already been described to affect the timing of events in seasonal plankton succession (e.g., Straile 2002; Winder and Schindler 2004a). Our modeling approach, which explicitly recognizes flexible algal nutrient to carbon stoichiometry, may prove a particularly useful tool in future research, because global climate change will influence temporal patterns of thermal stratification and terrestrial runoff and, thus, the light and nutrient supply to lakes.

Acknowledgments

We thank Angelika Wild and Achim Weigert for laboratory analyses, Pia Gabriel, Peter Herrmann, and the students of the 2004 Aquatic Ecology class for help during the field experiment and Andreas Buckenmaier for help with the model coding. We also thank Elena Litchman, Chris Steiner and all other members of a KBS discussion group, and Silvia Bartholmé, Andreas Buckenmaier, Florian Haupt, Maren Striebel, and two anonymous reviewers for valuable input on an earlier draft of the manuscript. This study was supported by funding from Deutsche Forschungsgemeinschaft (DI 745/3-2) and the US National Science Foundation (DEB-0610531 and DEB-0610532). This is KBS contribution number 1430.

Appendix A.

Examples of population and nutrient dynamics in the flexible stoichiometry model

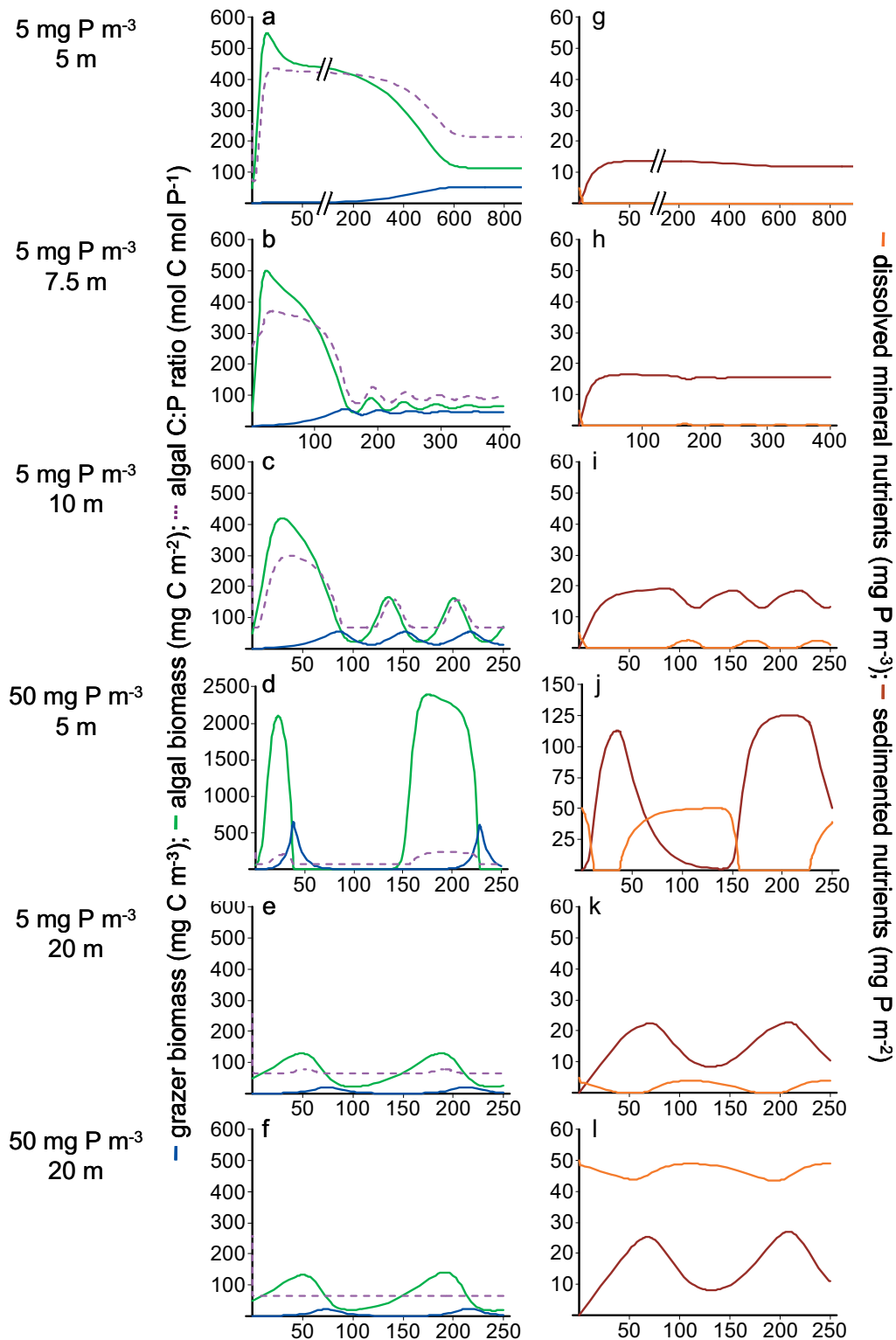


Fig. A1. Numerical examples of time courses of state variables in the flexible stoichiometry model for different combinations of initial dissolved phosphorus concentration and mixing depth, as indicated left of the panel rows. The left column of panels shows *Daphnia* biomass (blue lines), algal biomass (green lines) and algal C:P ratio (dashed violet lines). The right column of panels shows the corresponding dissolved mineral phosphorus concentration (orange line) and the pool of sedimented nutrients (brown line). Panels a-d are identical to a-d in Fig. 1.

Appendix B.

Complete set of predictions for the fixed stoichiometry model

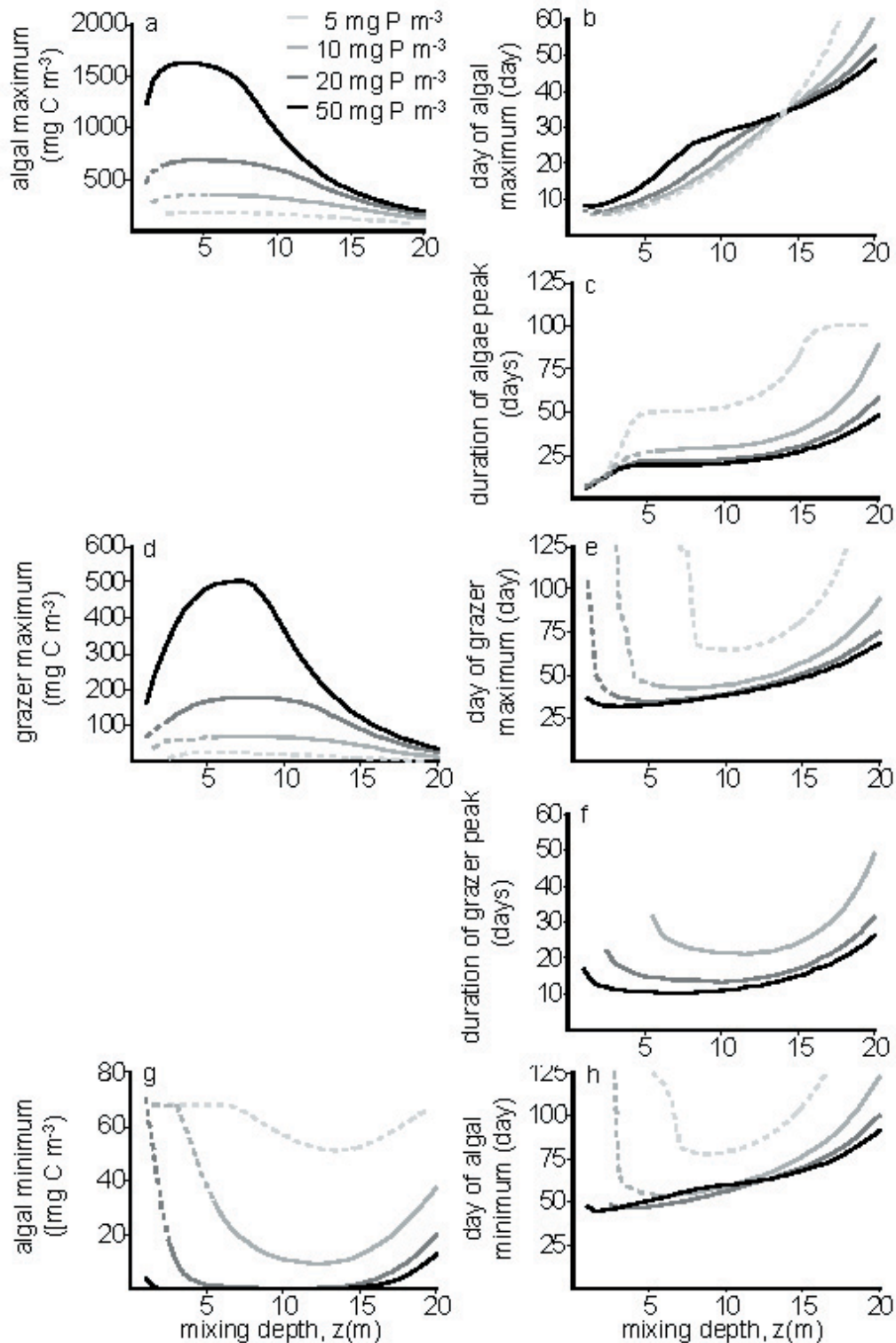


Fig. B1. Effects of mixing depth (z) and initial dissolved phosphorus concentration (as indicated by legend) on (a) algal biomass at the first algal peak; (b) time to the first algal peak; (c) duration of the first algal peak (= number of days with more than 50% of peak biomass); (d) grazer biomass at the first grazer peak; (e) time to the first grazer peak; (f) duration of the first grazer peak (= number of days with more than 50% of peak biomass) (g) algal biomass at the first minimum following the algal peak; (h) time to the first algal minimum. Dashed lines indicate that the initial grazer peak does not decline to less than 50% of its maximum (which implies that a grazer peak duration cannot be defined). Parameter values are as in Table 2 with Q fixed at the Redfield ratio ($1/41 \text{ mg P mg C}^{-1}$).

Appendix C.

Analytical correlates of transient oscillation properties of the flexible stoichiometry model

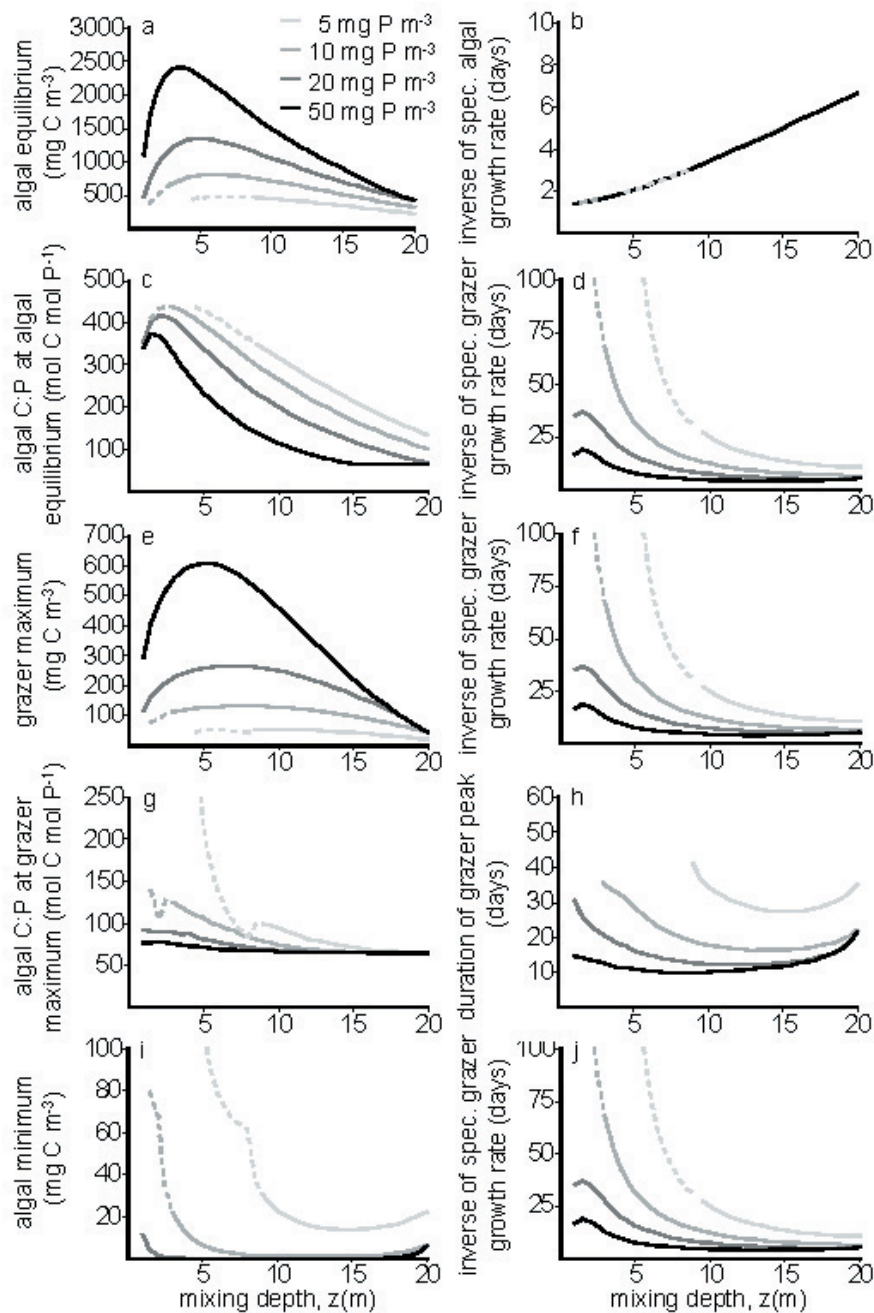


Fig. C1. Flexible stoichiometry model predictions. Effects of mixing depth (z) and initial dissolved phosphorus concentration (as indicated by legend) on properties of the asymptotic attractor and of boundary equilibria with one or both species missing, which represent analytical correlates of the transient oscillation properties shown in Fig. 2. Panels are arranged exactly as in Fig. 2 to facilitate comparison: (a) equilibrium algal biomass in absence of grazers; (b) inverse of specific growth rate of an algal population invading an empty system; (c) equilibrium algal carbon to phosphorus ratio in absence of grazers; (d, f, j) inverse of specific growth rate of a grazer invading an algal monoculture at equilibrium; (e) grazer biomass at its maximum on limit cycle or at its stable equilibrium, whichever applies; (g) algal carbon to phosphorus ratio at grazer maximum on a limit cycle or at stable grazer equilibrium, whichever applies; (h) duration of grazer peak on limit cycle (when applicable); (i) algal biomass at its minimum on limit cycle or at its stable equilibrium, whichever applies. Dashed lines indicate that the algae-grazer system has a stable equilibrium. Parameter values are as in Table 2. Note the good qualitative congruence with the patterns in Fig. 2, as summarized in Table 3.

Appendix D.

Analytical correlates of transient oscillation properties of the fixed stoichiometry model

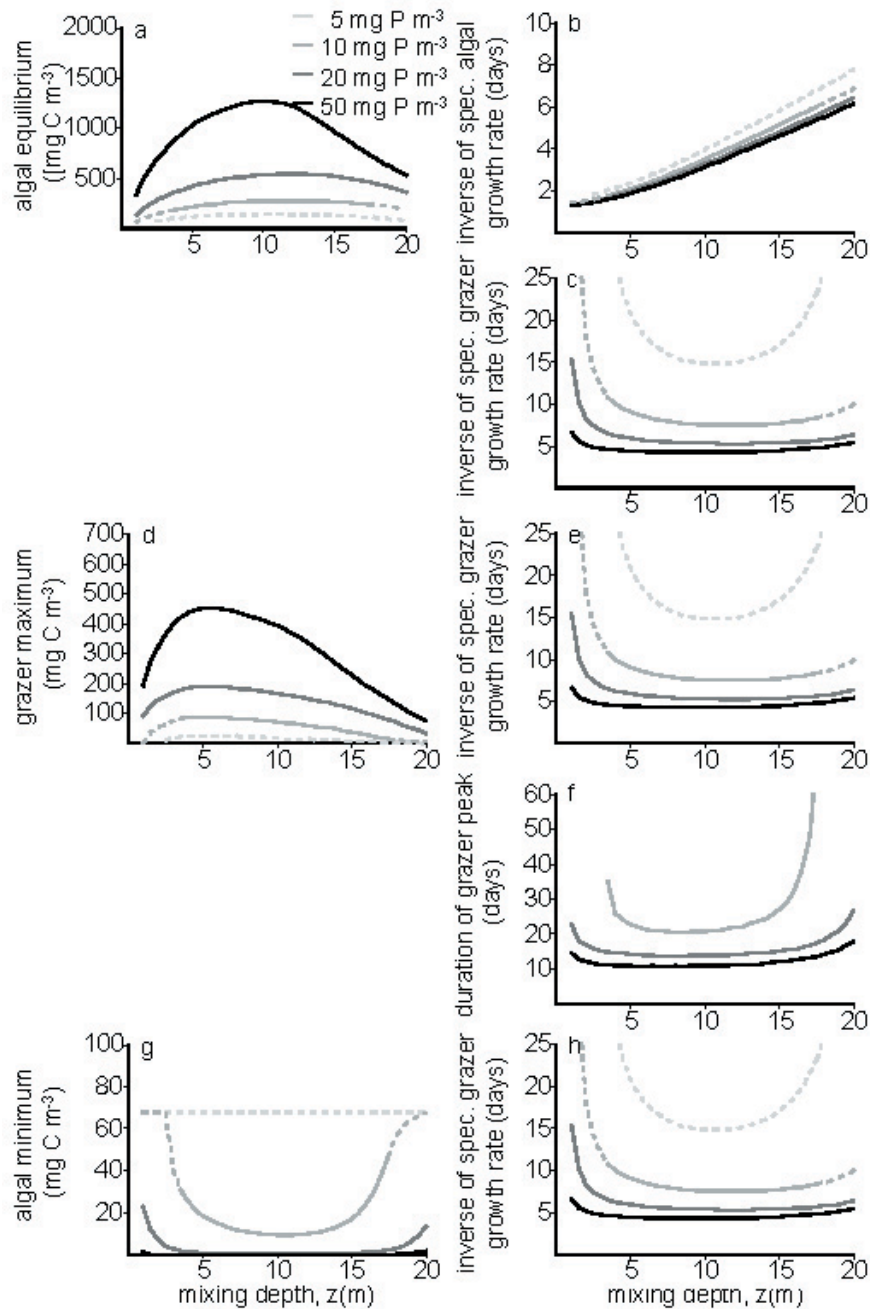


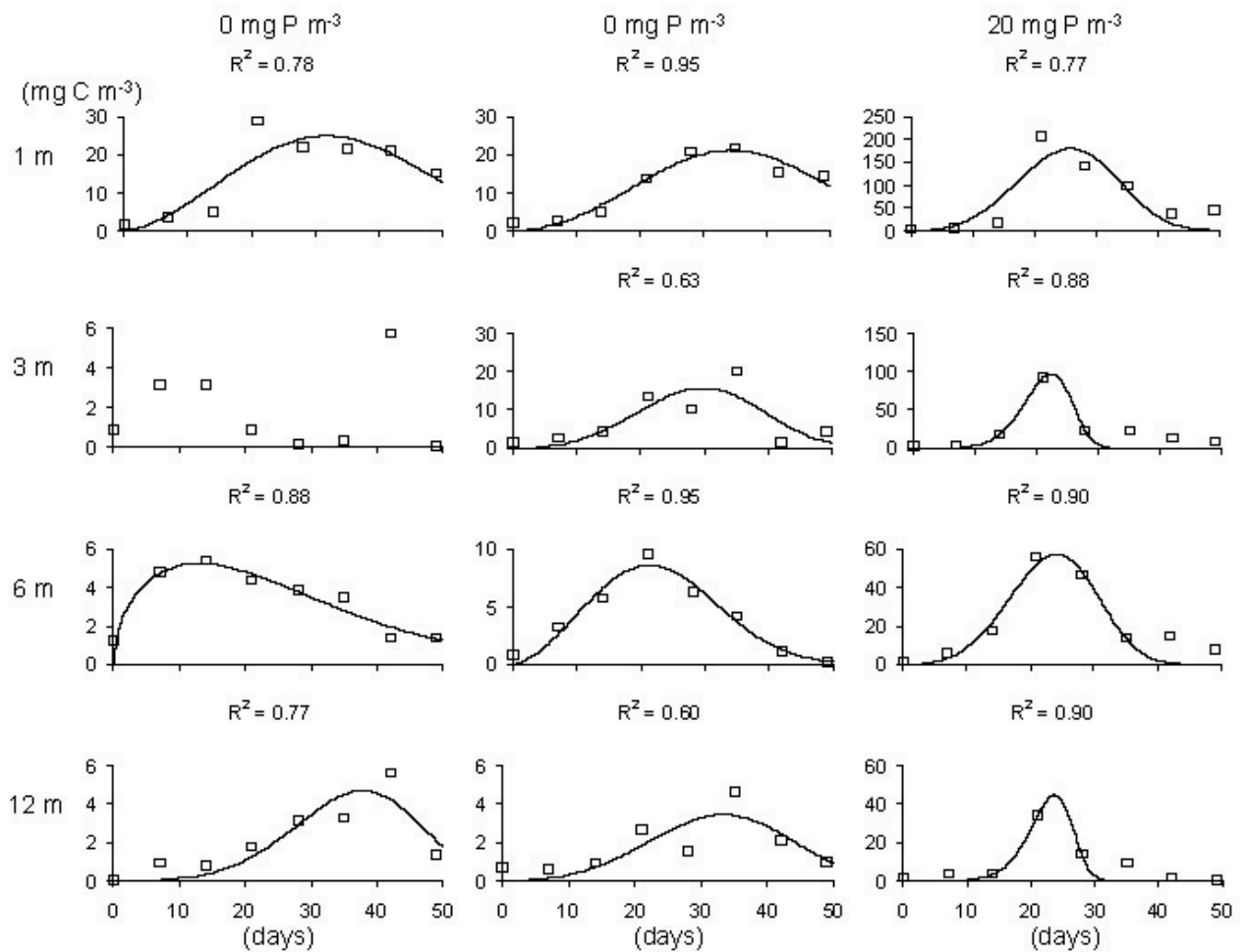
Fig. D1. Fixed stoichiometry model predictions. Effects of mixing depth (z) and initial dissolved phosphorus concentration (as indicated by legend) on properties of the asymptotic attractor and of boundary equilibria with one or both species missing, which represent analytical correlates of the transient oscillation properties shown in Appendix B. Panels are arranged exactly as in Fig. B1 to facilitate comparison: (a) equilibrium algal biomass in absence of grazers; (b) inverse of specific growth rate of an algal population invading an empty system; (c, e, h) inverse of specific growth rate of a grazer invading an algal monoculture at equilibrium; (d) grazer biomass at its maximum on limit cycle or at its stable equilibrium, whichever applies; (f) duration of grazer peak on limit cycle (when applicable); (g) algal biomass at its minimum on limit cycle or at its stable equilibrium, whichever applies. Dashed lines indicate that the algae-grazer system has a stable equilibrium. Parameter values are as in Table 2 with Q fixed at the Redfield ratio ($Q = 1/41 \text{ mg P mg C}^{-1}$).

Note the good qualitative congruence with the patterns in Fig. B1 (as summarized in Table 3), with the exception that the inverse of specific grazer growth (panels c, e, h) deviates from the corresponding panels c, e and h of Fig. B1 in that it decreases rather than increases from shallow to intermediate mixing depths.

The explanation for the latter discrepancy is as follows. In shallow systems, algae initially overshoot the equilibrium biomass they eventually attain in a grazer-free environment (equilibrium biomass is limited by total nutrients in the water column and it takes time for sinking losses to withdraw nutrients from the water column). Consequently, along the mixing depth gradient, the highest transient algal peak (Fig. B1a) occurs at a much shallower mixing depth than does the highest equilibrium algal biomass in absence of grazers (panel a). Since, with fixed stoichiometry, grazer growth rate depends solely on algal biomass, panel d must show the inverse pattern of panel a resulting in a minimum at intermediate mixing depths. The patterns in Fig. B1c, e, and h do therefore not correlate well with the corresponding patterns in panel c, e, h but are nevertheless robust against changes in initial conditions (as confirmed by simulation).

Online Appendix E.

Fits of Weibull functions to *Daphnia* population dynamics in the experimental enclosures



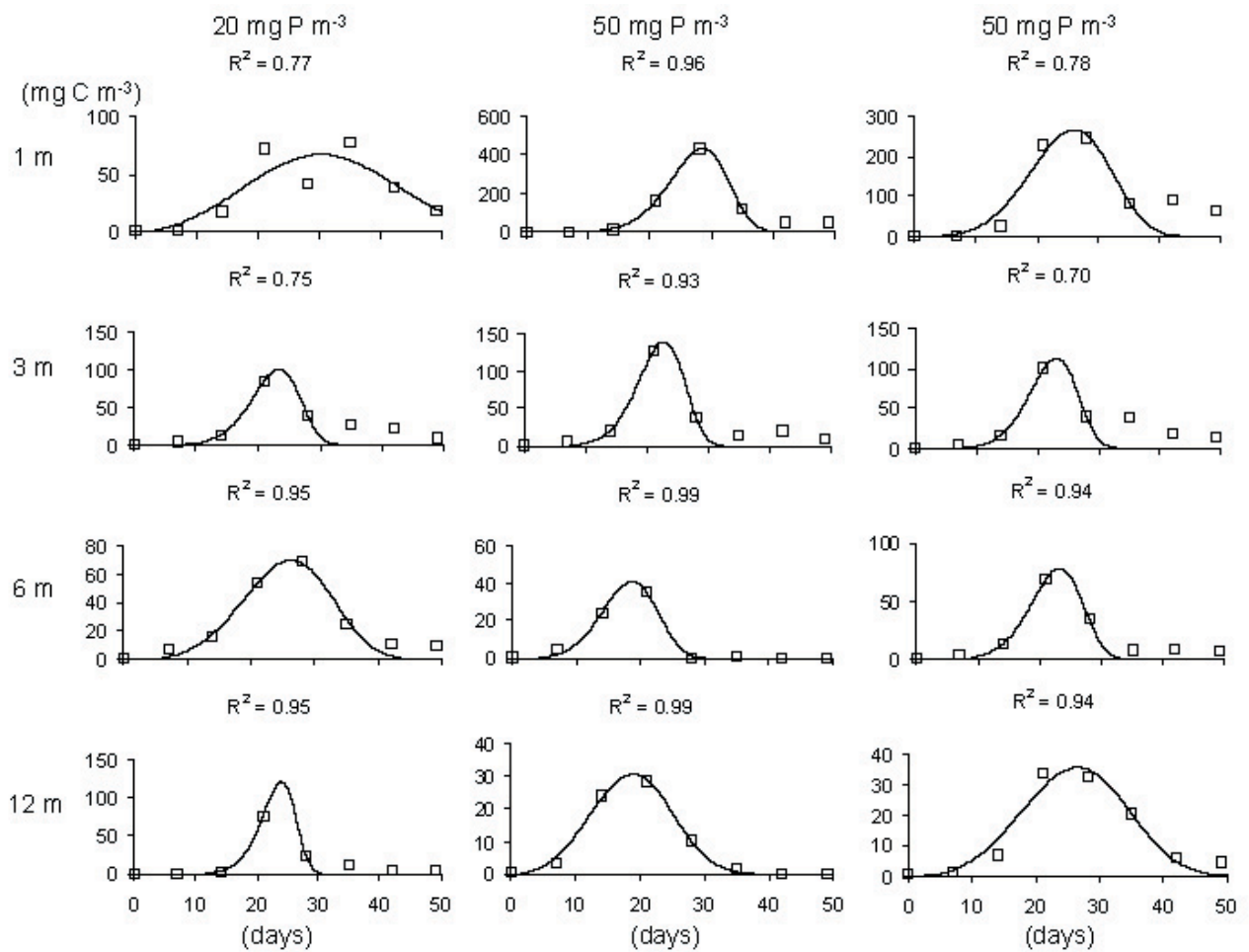


Fig. E1. Time courses of *Daphnia* biomass in all 24 experimental enclosures. Open squares are measurements, solid lines are fitted Weibull functions (eq. 1). Rows of panels are ordered according to enclosure depth, as indicated on the left. Columns of panels are ordered according to the initial phosphorus addition, as indicated at the top. Numbers on top of each panel show the R² values of the Weibull fits.

Online Appendix F.

Temporal dynamics of edible phytoplankton and *Daphnia* and of seston C:P ratio and TP concentration in the experimental enclosures

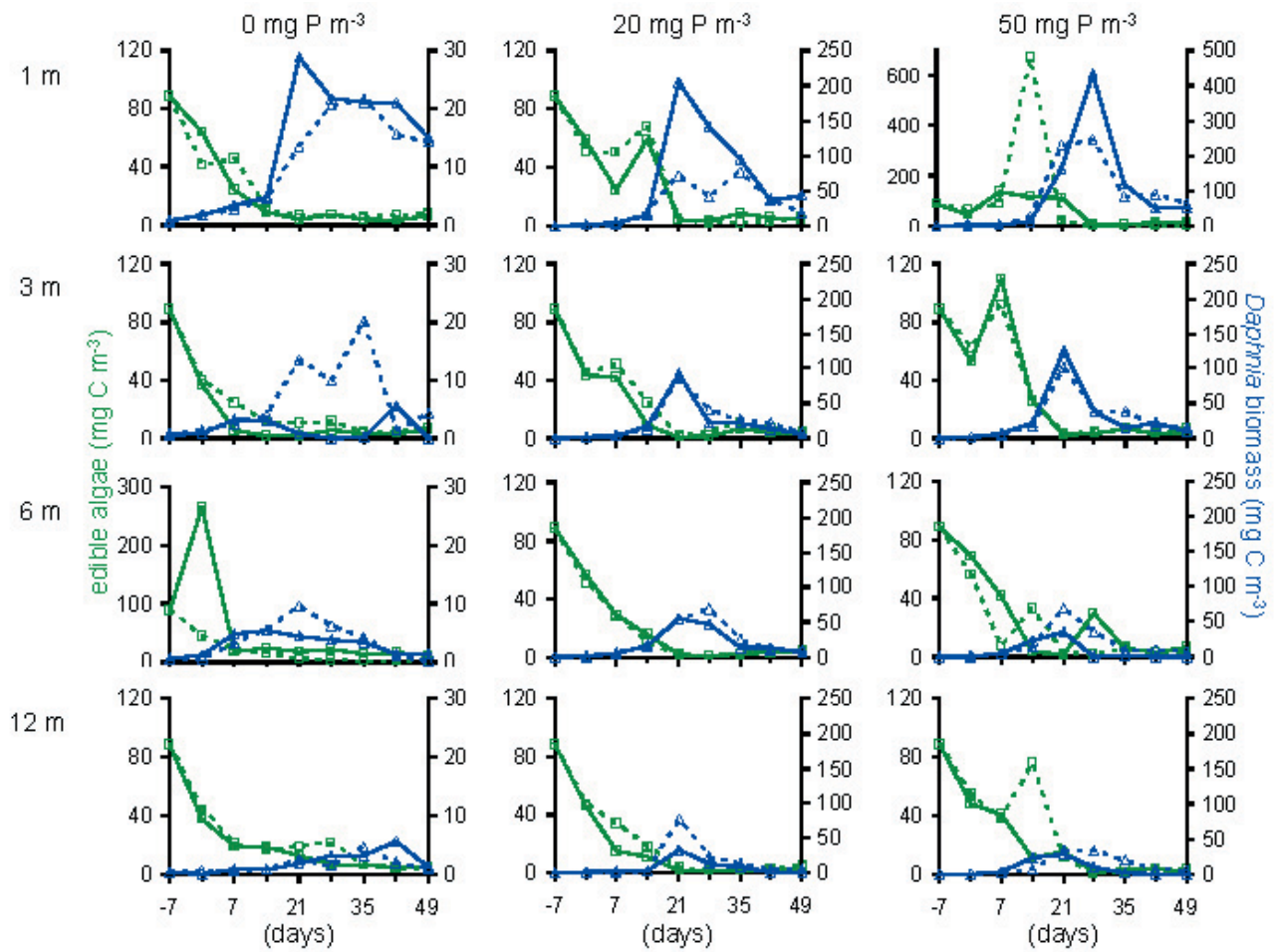


Fig. F1. Time courses of the biomasses of edible algae (green lines) and *Daphnia* biomass (blue lines) in all 24 experimental enclosures. Solid and dashed lines are for the two respective replicates. Rows of panels are ordered according to enclosure depth, as indicated on the left. Columns of panels are ordered according to the initial phosphorus addition, as indicated at the top. Note the differences in scale on the axes.

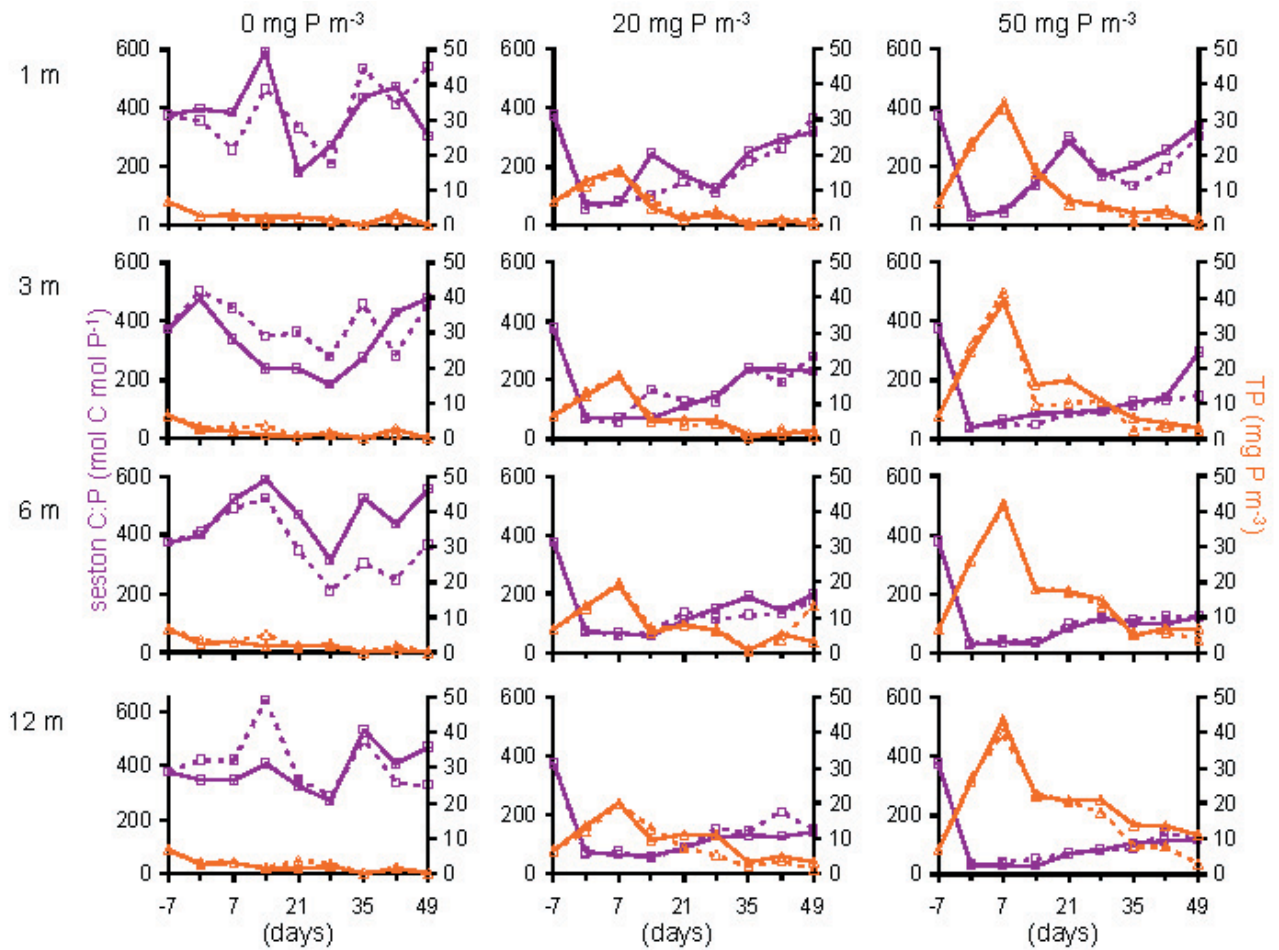


Fig. F2. Time courses of seston C:P ratios (purple lines) and TP concentration (orange lines) in all 24 experimental enclosures. Solid and dashed lines are for the two respective replicates. Rows of panels are ordered according to enclosure depth, as indicated on the left. Columns of panels are ordered according to the initial phosphorus addition, as indicated at the top. Note that phosphorus was added to the fertilized enclosures in two steps (on days 0 and 7), which explains the initial increase in TP in those treatments. TP was measured on 250 μm screened water samples and therefore does not include phosphorus stored in *Daphnia* biomass. The latter contributes (in addition to sedimentation losses) to the steep decrease in TP in the fertilized enclosures after day 7.

Chapter 4

Water temperature and mixing depth affect timing and magnitude of events during spring succession of the plankton

Stella Angela Berger,
Sebastian Diehl,
Herwig Stibor,
Gabriele Trommer,
Miriam Ruhenstroth,
Angelika Wild,
Achim Weigert,
Christoph Gerald Jäger,
and Maren Striebel

Oecologia 150: 643-654

Abstract

In many lakes the most conspicuous seasonal events are the phytoplankton spring bloom and the subsequent clear-water phase, a period of low phytoplankton biomass that is frequently caused by mesozooplankton (*Daphnia*) grazing. In Central European lakes, the timing of the clear water phase is linked to large-scale climatic forcing, with warmer winters being followed by an earlier onset of the clear water phase. Mild winters may favor an early build-up of *Daphnia* populations both directly through increased surface temperatures and indirectly by reducing light limitation and enhancing algal production, all being a consequence of earlier thermal stratification. We conducted a field experiment to disentangle the separate impacts of stratification depth (affecting light supply) and temperature on the magnitude and timing of successional events in the plankton. We followed the dynamics of the phytoplankton spring bloom, the clear water phase, and the spring peak in *Daphnia* abundance in response to our experimental manipulations. Deeper mixing delayed the timing of all spring seasonal events and reduced the magnitudes of the phytoplankton bloom and the subsequent *Daphnia* peak. Colder temperatures retarded the timing of the clear water phase and the subsequent *Daphnia* peak, whereas the timing of the phytoplankton peak was unrelated to temperature. Most effects of mixing depth (light) and temperature manipulations were independent, effects of mixing depth being more prevalent than effects of temperature. Because mixing depth governs both the light climate and the temperature regime in the mixed surface layer, we propose that climate-driven changes in the timing and depth of water column stratification may have far-reaching consequences for plankton dynamics and should receive increased attention.

Introduction

The impacts of global climate change on earth's ecosystems are the subject of an increasing number of studies in terrestrial and aquatic habitats [reviewed in Hays et al. (2005) and Harrington et al. (1999)]. Global warming has been found to correlate with changes in organisms' distributions and in the timing of seasonal events (Hughes 2000, Parmesan and Yohe 2003, Root et al. 2003). For example, the onset of spring is advancing in many terrestrial ecosystems (Parmesan and Yohe 2003). Similarly, seasonal abundance shifts of short-lived organisms such as marine copepods occur earlier during warm years and are tightly coupled with sea surface temperatures (Mackas et al. 1998, Greve et al. 2002). While there are many examples of strong statistical relationships between climate variability and ecological patterns, the nature of the underlying mechanisms is often uncertain (Stenseth and Mysterud 2002). Climate impacts on the distribution and phenology of biota may not only act directly through individual physiology, but also indirectly through species interactions. Disentangling the interplay of climatic drivers with density-dependent processes is therefore a major challenge, which calls for the increased use of proper experimental approaches (Stenseth and Mysterud 2002).

In many temperate lakes the most conspicuous events during seasonal succession of the plankton community are the phytoplankton spring bloom and the subsequent clear-water phase, a period of low phytoplankton biomass. Although the decline of a phytoplankton spring bloom can sometimes be explained by the exhaustion of a pool of limiting nutrients (O'Brien 1974, Huppert et al. 2002), the clearwater phase is usually attributed to intense grazing from a growing population of crustacean zooplankton (Lampert et al. 1986, Sarnelle 1993, Winder and Schindler 2004a). In Central European lakes, the timing of the clear-water phase is empirically linked to large-scale climatic forcing, with warmer winters being followed by an earlier onset of the clear-water phase (Straile 2000, 2002, Scheffer et al. 2001). This synchronizing effect of large-scale climate patterns on the timing of the clear-water phase has been observed across lakes varying in morphometry and nutrient state (Straile and Adrian 2000, Straile 2002). In the particularly well-researched case of Lake Constance, Straile (2000) documented a cascade of meteorological, hydrological and ecological processes linking the winter index of the North Atlantic Oscillation (NAO) to events in the seasonal succession of the plankton occurring up to almost six months later. Based on a time series spanning 16 years of data, the temporal sequence of events was as follows. Mild (= high NAO) winters were followed by high water temperatures and high population growth rates of *Daphnia* (the major grazing zooplankton) in April and May. Thus, a critical daphnid biomass necessary to suppress phytoplankton was reached earlier during high NAO years, resulting in an earlier and longer-lasting clear-water phase but also in an earlier summer decline of *Daphnia*.

Because algal biomass in Lake Constance during early spring (prior to the seasonal increase in *Daphnia*) was, at best, only weakly related to the NAO winter index, Straile (2000) suggested that the influence of winter climate on *Daphnia* dynamics in April/May was most likely a direct effect of water temperature on *Daphnia* growth and was not mediated through changes in algal food abundance. Individual metabolism and growth of *Daphnia* are indeed highly dependent on temperature (Lampert 1977, Orcutt and Porter 1983, Davidowicz and Loose 1992, Reichwaldt et al. 2005). Still, a lack of a relationship between winter climate and algal density does not rule out the possibility that a significant part of the effects of winter climate on *Daphnia* population growth in spring is mediated through food supply. Sustained growth of a

consumer requires sustained *production* of food, but food production needs not be correlated with food *abundance* if, e.g., the additional production is harvested by a simultaneously growing grazer population.

It seems plausible that in deep lakes such as Lake Constance specific algal production is positively affected by mild winters and early warming in spring, as has been reported from other temperate lakes and oceans (Weyhenmeyer et al. 1999, Winder and Schindler 2004a, Richardson and Schoeman 2004). In most deep, temperate lakes phytoplankton production in late winter and early spring is limited by light availability, because under the prevailing non-stratified conditions individual algal cells spend most of the time below the euphotic zone (Reynolds 1984, Huisman and Weissing 1999, Diehl 2002). It is therefore commonly assumed that the timing of the spring phytoplankton bloom in deep lakes depends on the onset of water column stratification (Sommer et al. 1986, Reynolds 1989). In a detailed time series analysis of data from Lake Constance Gaedke et al. (1998a, b) did indeed find that substantial algal development in spring only occurred when algae were largely safe from being mixed below a depth of 20 m. Similarly, Winder and Schindler (2004) found that the timing of the phytoplankton spring bloom in Lake Washington correlated with the onset of stratification. This is consistent with data showing a strong negative dependence of specific algal production on depth of the mixed water column (Diehl et al. 2002, 2005, Ptacnik et al. 2003). The onset of water column stratification in spring, in turn, depends on regional weather conditions such as air temperature and wind speed. Relatively high temperatures and low wind speeds during winter and early spring promote an early onset of stratification (Gaedke et al. 1998a, b, Winder and Schindler 2004a) thus alleviating light limitation and boosting phytoplankton production.

In summary, there are two non-exclusive mechanisms by which mild winters might favor an early build-up of *Daphnia* biomass in deep lakes, (i) enhanced algal production and (ii) increased metabolic rate. Ultimately, both are consequences of an earlier stratification of the water column alleviating light limitation and preventing heat loss to deeper strata. Thus, successful prediction of climate effects on seasonal succession in the plankton requires a detailed understanding of the separate contributions of mixing depth-dependent light climate and temperature to the production and loss rates of phytoplankton and zooplankton.

Because increased light supply and increased water temperature inevitably co-vary with reduced mixing depth, their separate contributions to the spring dynamics of the plankton cannot be assessed without experimentation. We therefore conducted a field enclosure experiment in which we manipulated mixing depth and water temperature largely independently and investigated their effects on the magnitude and timing of three major events during spring succession of the plankton: (i) the peak of the phytoplankton spring bloom, (ii) the beginning of the clear-water phase, and (iii) the spring peak of the *Daphnia* population. We hypothesized that mixing depth should have strong direct effects on algae (by mediating light-dependent production) but not on *Daphnia*. In contrast, we expected *Daphnia* grazing and growth rates to depend strongly on temperature, but phytoplankton production only weakly so. These direct effects of light and temperature should propagate across the plant-herbivore interface. We therefore expected the peak densities of both phytoplankton and *Daphnia* to correlate negatively with mixing depth (because of reduced algal production at lower light levels), but increased temperature should shift the timing of these peaks and the beginning of the clear-water phase forward (because increased *Daphnia* grazing should deplete algae earlier).

Material and Methods

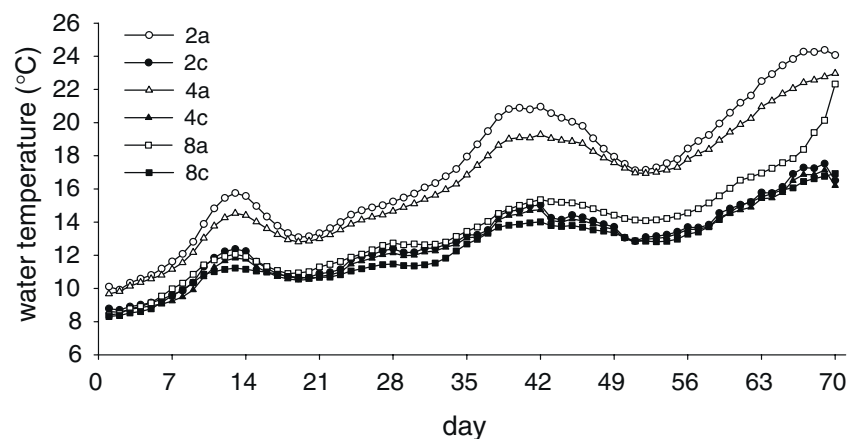
Study site and experimental design

The enclosure experiment was run in a 3x2 factorial design: three enclosure depths (2, 4, and 8 m) were cross-classified with two temperature treatments ('ambient' and 'cold'), with two replicates per treatment. Enclosures (cylindrical bags of transparent Tricoron, RKW Wasserburg, Germany) had a diameter of 0.95 m, were heat-sealed at the bottom and open to the atmosphere. We suspended them from a raft anchored at a water depth of 16 m in lake Brunnsee (47°56'N, 12°26' E), close to the University of Munich's Limnological Research Station at Seon. Lake Brunnsee (area 5.8 ha, max. depth 19 m) is fed by silica- and nitrate-rich groundwater with a low total phosphorus content (usually below 10 µg P L⁻¹).

We maintained well-mixed conditions inside the enclosures by intermittently (5 min on, 35 min off) blowing compressed air through tubing to the bottom of each enclosure. The mixing was highly effective, i.e., vertical temperature gradients *within* enclosures were negligible. However, because the lake usually stratifies in late spring at a depth of 3-4 m, temperature differences *between* enclosures developed over time in the 'ambient' treatments: temperatures there were highest in the 2 m enclosures and lowest in the 8 m enclosures (Fig. 1), mimicking a natural situation where depth and temperature of the mixed layer are inversely related. We surrounded all enclosures of the 'cold' treatment by a large, 12 m deep bag. The water inside this bag was kept well-mixed, creating a water bath of homogeneous, reduced temperature for the 'cold' enclosures. The procedure was highly effective, i.e. temperatures in the 'cold' enclosures were independent of mixing depth and were considerably lower than in the 2 and 4 m 'ambient' treatments (Fig. 1).

We surrounded each enclosure with black silage film in order to enhance background light extinction, making the enclosures optically deeper (see Diehl et al. 2002). Depth-averaged light attenuation coefficients were 0.65 m⁻¹, 0.73 m⁻¹, and 0.83 m⁻¹ in the 2, 4, and 8 m enclosures, respectively, compared to 0.28 m⁻¹ (calculated from 0-8 m) in the lake. The vertical light gradients in the 2, 4, and 8 m enclosures therefore corresponded to light gradients down to approximate depths of 4.6, 10.3, and 23.6 m, respectively, in natural lake water, thus mimicking a much wider range of stratification depths characteristic of larger and deeper lakes.

Fig. 1. Averaged daily water temperature (°C) of the two replicates of each enclosure treatment versus time (day 1 = April 21, day 70 = June 28). 2, 4, 8 = mixing depth (in meters), a = ambient temperatures (open symbols); c = cold temperatures (filled symbols). Data points are running means of three consecutive measurements.



We ran the experiment for 10 weeks from 21 April to 28 June 2005. On 20 April, we filled all enclosures with lake water sieved through a 50- μm gauze, which excluded crustacean zooplankton but preserved the natural phytoplankton spring community consisting mostly of small diatoms and cryptomonads (*Cyclotella* spp. and *Rhodomonas minuta*, with 60% and 13%, respectively, of total algal biovolume). We enriched all enclosures with 14.3 $\mu\text{g L}^{-1}$ phosphorus (as KH_2PO_4) to an initial total phosphorus content of about 25 $\mu\text{g L}^{-1}$ in order to stimulate a more pronounced algal spring bloom. To simulate spring recruitment from an egg bank in the sediment, we added small inocula of *Daphnia hyalina* (which is the naturally occurring *Daphnia* species in the lake) to all enclosures weekly over the first four weeks of the experiment. The *Daphnia* were descendants of three clones that had been isolated from the lake and been cultured separately at 20°C on a diet of *Scenedesmus*. Prior to stocking, the *Daphnia* were acclimated to 13°C for one night in a climate chamber. After transport to the lake, we mixed the clonal populations carefully in a 200 L tub and added appropriate aliquots to each treatment. Approximate stocking densities were 1.2 individuals L^{-1} on April 21, 0.6 ind. L^{-1} on April 26, 0.15 ind. L^{-1} on May 3, and 0.3 ind. L^{-1} on May 11. Subsequent density counts suggest that initial mortality was approximately 90% leading to an emergence rate between 0.002 and 0.017 ind. L^{-1} per day, which is close to observations by Càceres (1998).

Sampling program

In all enclosures, water temperature was recorded every 30 minutes by a sensor located 15 cm below the water surface and connected to a data logger (SE-309, Conrad Elektronik, Germany) on the raft. Additionally, we recorded vertical temperature profiles with a multi-probe (LT1/T, WTW-Weilheim, Germany) in 1 m steps several times a week in the outer water bath and once weekly in each enclosure to monitor the mixing regime. At bi-weekly intervals, we measured vertical profiles of photosynthetically active radiation (PAR) in 1 m steps with a spherical quantum sensor (LI-139SA, Licor, Lincoln, Nebraska, USA). Parallel to each underwater reading we took a reading of incident PAR (flat quantum sensor LI-190SA) just above the water surface. For each enclosure, we then calculated the depth-averaged intensity of PAR as a percentage of incident PAR (as described in Diehl et al. 2005) and the depth-averaged light attenuation coefficient (as described in Diehl et al. 2002).

Once per week, we took a 2 L water sample from just below the water surface in each enclosure. Measurements of vertical Chl *a* profiles with a fluorescence probe confirmed that the samples were representative of the perfectly mixed water columns. The samples were filtered through a 250- μm mesh to remove mesozooplankton and were immediately analyzed for alkalinity. To determine particulate organic carbon (POC) and chlorophyll *a* (Chl *a*) concentrations, we filtered aliquots of 100-300 ml onto glass fiber filters (Whatman GFF, precombusted for POC). Chl *a* was determined in a fluorometer (TD 700, Turner Design, Sunnyvale, California, USA) after extraction in acetone. Seston POC content was determined by infrared-spectroscopy (C-Mat, Ströhlein, Korschbroich, Germany).

Once per week, we sampled zooplankton by means of vertical hauls with a 55 μm mesh net, taken from the bottom to the surface in each enclosure. Zooplankton samples were immediately fixed with cold sugar formalin (250 g sugar in 1L formalin) to a final concentration of 4 %. To estimate the abundances of *D. hyalina*, all individuals of a haul were counted under a dissecting microscope at 25 x magnification.

Data processing and statistics

In all enclosures, we observed similar temporal dynamics of the plankton. Phytoplankton densities increased from a starting value of $2 \mu\text{g Chl } a \text{ L}^{-1}$ to a peak several weeks into the experiment and subsequently declined to densities below the starting value. *Daphnia* densities showed the same ‘boom and bust’ pattern, but with a time delay of several weeks compared to phytoplankton. Thus, we observed three distinct successional events: a phytoplankton peak, a phytoplankton decline (= clear-water phase), and a *Daphnia* peak. We characterized these events by their magnitude (= peak height) and their timing (= date when a peak was reached or the clear-water phase started). We defined a peak as the highest density observed in a given enclosure during the experiment. The beginning of the clear-water phase was defined as the first sampling date (following a peak) when the Chl *a* concentration had declined below $2 \mu\text{g L}^{-1}$.

Our ability to characterize the timing and magnitude of successional events was limited by our weekly sampling resolution. To obtain a continuous temporal resolution we fitted the following Weibull function to the dynamics of Chl *a* and *D. hyalina* in each enclosure

$$N(t) = c + m \left(\frac{b}{a} \right) \left(\frac{t}{a} \right)^{b-1} e^{-(t/a)^b}, \quad (1)$$

where $N(t)$ is either Chl *a* concentration ($\mu\text{g L}^{-1}$) or *Daphnia* density (ind. L^{-1}), a , b , c , and m are fitted constants, and t is time (in days) since the start of the experiment. We used eq. 1 because it can describe unimodal distributions with both symmetric and asymmetric peaks (see examples in Supplementary electronic material Fig. 1). Because *Daphnia* densities were zero at the start and approached very low values at the end of the experiment, c was dropped from the model for *Daphnia* dynamics. The maxima of the fitted Weibull functions yielded estimates of the timing and height of density peaks. The beginning of the clear-water phase was estimated as the time when the fitted Chl *a* function dropped below $2 \mu\text{g L}^{-1}$.

To statistically test for effects of mixing depth and temperature on the magnitude and timing of successional events, we performed two-way ANOVA with enclosure depth and temperature treatment (‘ambient’ vs. ‘cold’) as fixed factors. As response variables we used both the directly measured values (with weekly temporal resolution) and the values derived from the fitted Weibull functions (with daily temporal resolution). All statistical analyses were performed with SPSS 13.0. If necessary, data were ln transformed to stabilize variances.

Results

The temperature treatment was successful. Water temperatures in the ‘ambient’ 2 and 4 m treatments differed on average by less than 1°C from each other and were considerably higher than in the ‘cold’ treatments; all ‘cold’ treatments were, in turn, very similar to one another, the ‘ambient’ 8 m treatment being on most days only slightly warmer (Fig. 1). As the lake warmed up during the course of the experiment, water temperatures increased over time in all enclosures, starting at 8.3°C (2-8 m ‘cold’ and 8 m ‘ambient’) and 10.1°C (2-4 m ‘ambient’) on 21 April and reaching 16.5 ± 0.2°C (2-8 m ‘cold’), 22.3°C (8 m ‘ambient’), 23.0°C (4 m ‘ambient’), and 24.1°C (2 m ‘ambient’) on 28 June (Fig. 1).

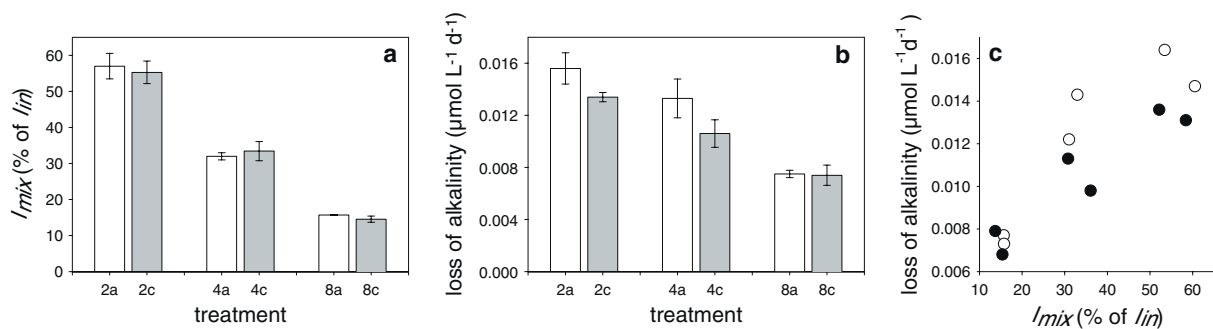


Fig. 2. **a** Average light intensity of PAR (I_{mix} in % of incident PAR, I_{in}), and **b** loss of alkalinity ($\text{mmol L}^{-1}\text{ day}^{-1}$) versus experimental treatment. Open bars indicate ‘ambient’ temperature treatments, filled bars ‘cold’ temperature treatments, and 2, 4, 8 represent the mixing depths (in meters). Error bars represent standard errors. **c** Average light intensity versus loss of alkalinity, open circles indicate ‘ambient’ and filled circles ‘cold’ temperature treatments.

The mixing depth treatments were similarly successful. Average light intensity in the water column was strongly negatively related to enclosure depth throughout the experiment but was independent of temperature treatment (Fig. 2a; ANOVA, effects of mixing depth: $p < 0.001$, effects of temperature treatment and depth x temperature interaction: $p > 0.77$; $R^2 = 0.98$). Alkalinity measurements indicate that lower light availability led to decreased algal production in deeper enclosures. In hard-water lakes such as Lake Brunnssee (alkalinity $\approx 3.5\text{ mmol L}^{-1}$), primary production causes precipitation of dissolved calcium carbonate at a rate roughly proportionate to carbon fixation (Wetzel 1983). This decalcification is reflected in a proportionate loss of alkalinity. Although this balance calculation ignores heterotrophic processes and fluxes of inorganic carbon among water and air, primary production over a certain period can be roughly approximated from the loss of alkalinity over that period (see Diehl et al. 2002). The average loss of alkalinity per day (calculated as the slope of a linear regression of alkalinity vs. time) was negatively affected by mixing depth and was lower in ‘cold’ than in ‘ambient’ treatments (Fig. 2b; ANOVA, effects of mixing depth: $p < 0.001$, effects of temperature treatment: $p = 0.023$, depth x temperature interaction: $p = 0.22$; $R^2 = 0.95$). Alkalinity losses were strongly positively related to average light intensity (Pearson Correlation 0.87, $p < 0.001$), suggesting that algal production was light limited (Fig. 2c). Moreover, temperature treatment affected alkalinity losses only in the 2 and 4 m enclosures but not in the 8 m enclosures (Fig. 2b, c), probably because actual water temperatures hardly differed among the 8 m ‘cold’ and 8 m ‘ambient’ treatments (Fig. 1). A stepwise multiple regression indicated indeed that light and temperature had additive effects on algal production. The relationship of alkalinity losses (AL , in $\text{mmol L}^{-1}\text{ day}^{-1}$) to average light intensity (I_{mix} , in percent of

incident PAR) and mean temperature during the experiment (T , in $^{\circ}\text{C}$) was best described by the equation $AL = -0.003 + 0.00013 I_{mix} + 0.00067 T$ ($R^2 = 0.89$), the term $I_{mix} \times T$ being excluded from the model.

We analysed treatment responses of both Chl a and POC as proxies of phytoplankton biomass. The concentrations of Chl a and POC were highly correlated throughout the experiment (Pearson $r = 0.75$; $p < 0.001$; $n = 108$) and responded very similarly to the treatments. We therefore only show and discuss the Chl a results below.

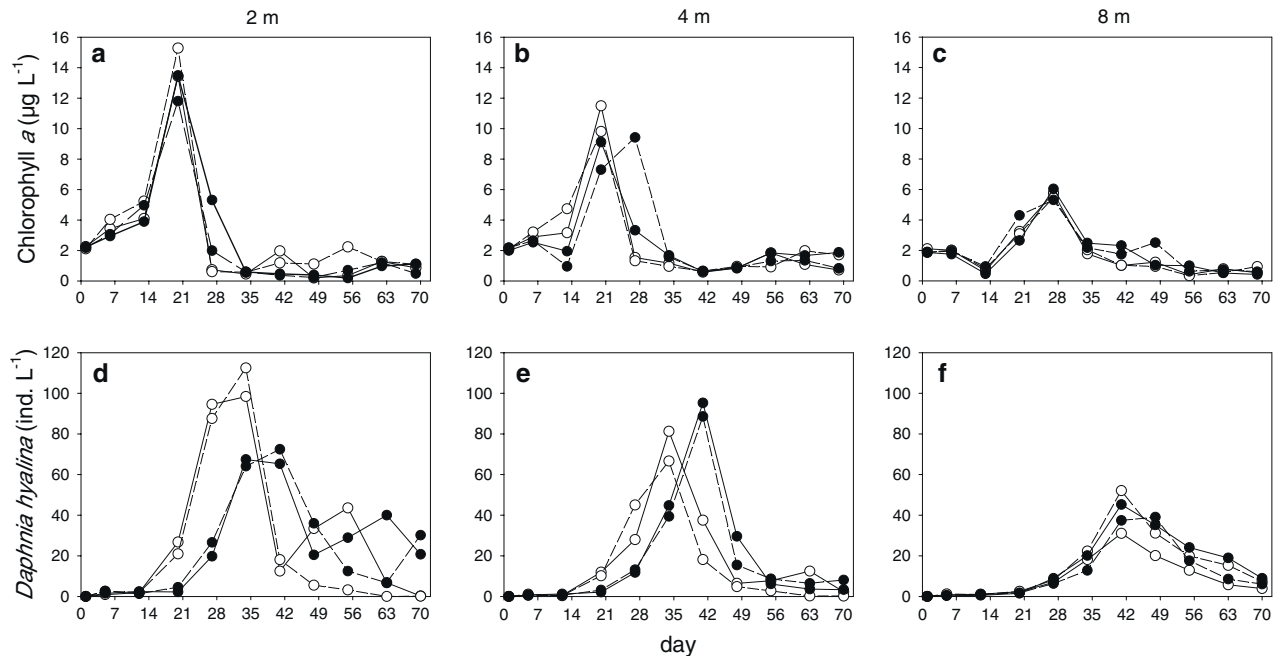


Fig. 3. a-c Phytoplankton biomass concentration (chlorophyll a , $\mu\text{g L}^{-1}$) and **3 d-f**, *Daphnia hyalina* abundance (ind. L^{-1}) versus time (day 1 = April 21, day 70 = June 28). Open circles indicate 'ambient' temperature treatments, filled circles 'cold' temperature treatments. 2, 4, and 8 m mixing depths are shown in the left, middle and right panels, respectively. Dashed and solid lines distinguish the two replicates of each treatment.

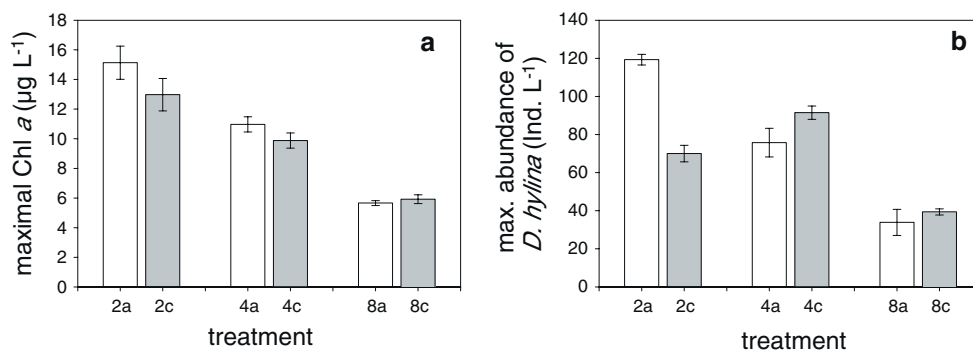


Fig. 4. Peak densities of **a** phytoplankton peak (chlorophyll a maximum, $\mu\text{g L}^{-1}$), and **b** *Daphnia hyalina* (ind. L^{-1}) versus experimental treatment. Peak densities were estimated from Weibull functions fitted to the data (see *Material and Methods*). Open bars indicate 'ambient' temperature treatments, filled bars 'cold' temperature treatments, and 2, 4, 8 represent the mixing depths (in meters). Error bars represent standard errors.

In all treatments we observed the same progression of seasonal events: a phytoplankton bloom was followed by a clear-water phase, a peak in *Daphnia* density, and, finally, a decline of the *Daphnia* population to low densities (Fig. 3). To statistically analyse treatment effects on the magnitude and timing of these events, we used both the directly measured values (Fig. 3) and the values derived from the fitted Weibull functions, which allowed a finer temporal resolution (Fig. 4, 5). Because the results and statistical outcomes were very similar for both types of response variables, we do not refer to them separately in the following.

As expected, peak densities of phytoplankton and *Daphnia* were strongly negatively affected by mixing depth (Fig. 3, 4, Table 1), suggesting that *Daphnia* population growth depended strongly on the availability of light for phytoplankton production. In line with this, *Daphnia* peak densities were positively correlated with the average loss of alkalinity (Pearson $r = 0.80$ and $r = 0.85$ for measured and Weibull fitted peak densities, respectively, $p < 0.002$, $n = 12$) and with peak concentrations of Chl *a* (Pearson $r = 0.81$ and $r = 0.85$ for measured and Weibull fitted peak densities, respectively, $p < 0.002$, $n = 12$). In contrast, temperature treatment had no consistent effects on peak densities. While the heights of the Chl *a* peaks were independent of temperature treatment, *Daphnia* peak densities were considerably lower in ‘cold’ than in ‘ambient’ enclosures at a mixing depth of 2 m, but not at 4 and 8 m (Fig. 3, 4, Table 1).

In accordance with expectations, both the clear-water phase and the *Daphnia* population peak occurred earlier in ‘ambient’ than in ‘cold’ enclosures (Fig. 3, 5b, c, Table 1), suggesting that increased temperature speeded up the timing of these successional events. In contrast to expectations, the timing of the first successional event, i.e., the peak of the phytoplankton bloom, was independent of temperature treatment (Fig. 3, 5a, Table 1). Most strikingly, however, the timing of all three successional events was negatively affected by mixing depth. The peak of the phytoplankton bloom, the beginning of the clear-water phase, and the peak of the *Daphnia* population all occurred earlier in shallow than in deep enclosures (Fig. 3, 5, Table 1). This strongly suggests that higher light availability speeded up the progression of successional events.

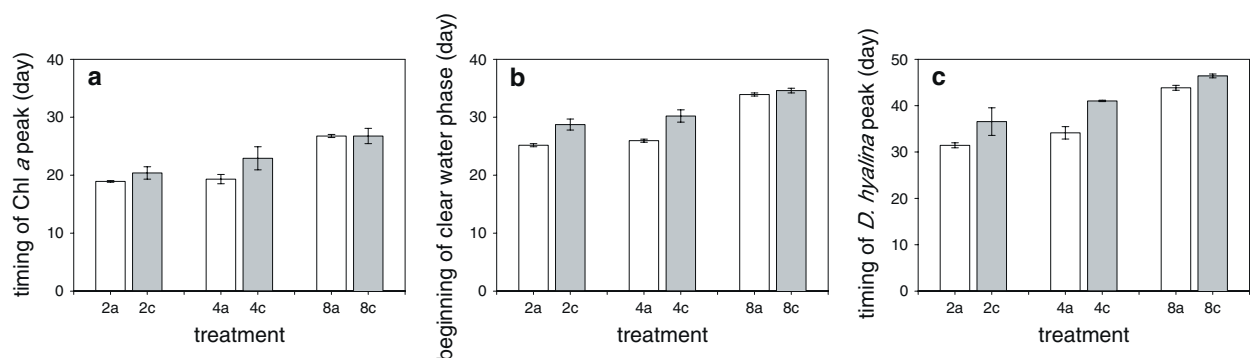


Fig. 5 **a** Timing of the phytoplankton peak (chlorophyll *a* maximum), **b** beginning of the clear-water phase (chlorophyll *a* < 2 $\mu\text{g L}^{-1}$), and **c** timing of the *D. hyalina* peak (abundance maximum) versus treatment. The timing of events was estimated from Weibull functions fitted to the data (see *Material and Methods*). Open bars indicate ‘ambient’ temperature treatments, filled bars ‘cold’ temperature treatments, and 2, 4, 8 represent the mixing depths (in meters). Error bars represent standard errors.

Table 1. Summary of ANOVAs of the effects of mixing depth and temperature treatment on the intensity and timing of phytoplankton and *Daphnia* density peaks (maximal Chl a in lg l⁻¹ and maximal abundance in individual l⁻¹), and the beginning of the clear-water phase (day)

Dependent variable	Treatment effects (<i>P</i> values)			Overall model <i>R</i> ²
	Depth	Temperature	Depth × temperature	
Phytoplankton peak				
Measured	<0.001	0.122	0.424	0.98
Fitted	<0.001	0.188	0.287	0.98
<i>Daphnia hyalina</i> peak				
Measured	0.002	0.647	0.096	0.90
Fitted	<0.001	0.506	0.017	0.95
Timing of phytoplankton peak				
Measured	0.007	0.356	0.422	0.83
Fitted	0.002	0.117	0.343	0.89
Timing of clear-water phase				
Measured	0.001	0.001	0.216	0.94
Fitted	<0.001	0.002	0.062	0.97
Timing of <i>Daphnia hyalina</i> peak				
Measured	0.031	0.030	0.630	0.79
Fitted	0.001	0.005	0.354	0.94
Difference in timing of phytoplankton and <i>Daphnia hyalina</i> peak				
Measured	0.196	0.091	0.959	0.58
Fitted	0.027	0.007	0.178	0.85

Peaks and timing were estimated from weekly measurements ('measured') or fitted with a Weibull function ('fitted') (see Materials and methods). Significant *P* values are indicated in bold

Discussion

Our enclosure experiment corroborates several of our previously stated hypotheses: (1) deeper mixing reduced the intensities of the phytoplankton bloom and the subsequent *Daphnia* peak; (2) colder temperatures retarded the timing of the clear-water phase and the subsequent *Daphnia* peak. Our first hypothesis is based on the consideration that sustained population growth rate of *Daphnia* requires sustained algal production. Algal production, in turn, depends on light supply, which is inversely related to mixing depth (Fig. 2a). Previous enclosure experiments have indeed revealed a strong negative influence of mixed water column depth on the specific production of phytoplankton (Diehl et al. 2002, 2005, Ptacnik et al. 2003). To our knowledge, there are so far no published experimental studies relating the production and biomass of zooplankton to mixing depth. In addition to the experiment reported here, we have conducted similar experiments in Lake Brunnsee in different seasons (Haas 2002, Haupt 2004) and in a North Atlantic marine system (Kunz 2005), all of which revealed strong negative effects of mixing depth on the biomass of crustacean zooplankton. Moreover, we found a strong negative relationship of crustacean biomass to mixed layer depth in a comparative study of thermally stratified North German lakes (Berger et al. 2006). Together, these studies suggest that mixing depth is an important, so far overlooked, environmental factor determining the abundance of zooplankton in deep lakes.

Our second hypothesis is based on the well-established, positive influence of water temperature on individual growth rate of *Daphnia* (Lampert 1977, Ocrutt and Porter 1983, Davidowicz and Loose 1992, Reichwaldt et al. 2005). Because the spring clear-water phase usually coincides with intense grazing from a growing *Daphnia* population (Lampert et al. 1986, Sarnelle 1993), high temperatures would be expected to foster an earlier onset of the clear-water phase via the faster build-up of significant grazer densities. Observational data have indeed reported an earlier build-up of *Daphnia* densities and an earlier onset of the clear-water phase following warmer winters (Straile 2000, 2002, Scheffer et al. 2001). Interestingly, we did not find a relationship of crustacean biomass to water temperature in our comparative lake study, which analysed this relationship across seasonally averaged summer data (Berger et al. 2006). The latter suggests that temperature may affect the dynamics of crustacean zooplankton more strongly in spring (when the water is still relatively cold and high quality food is temporally abundant) than in summer (when growth rates are often limited by the availability of high quality algal food and by predation from planktivorous fish) (Sommer et al. 1986).

In our comparative lake survey, the epilimnetic concentration of algal biomass during summer was negatively related to mixing depth and weakly positively related to water temperature (Berger et al. 2006). We therefore asked whether the plankton communities in our enclosures settled to such a pattern towards the end of spring succession, when phytoplankton densities had stabilized. Early summer phytoplankton biomass (averaged over the last three weeks of the experiment) was indeed negatively related to mixing depth, but was unrelated to temperature (Fig. 3; ANOVA, effects of mixing depth: $p < 0.007$, effects of temperature treatment: $p = 0.59$, depth x temperature interaction: $p = 0.343$; $R^2 = 0.83$). We did not perform a similar analysis on the *Daphnia* data, because *Daphnia* populations in several enclosures were still in transient dynamics towards the end of the experiment.

Notably, the timing of successional events was not only affected by temperature but also by mixing depth, with shallower mixing fostering an earlier onset of the spring phytoplankton bloom, an earlier

onset of the clear-water phase, and an earlier occurrence of the *Daphnia* peak. These effects of mixing depth on successional events could be plausibly explained by the following scenario. (1) Higher algal growth led to initially higher algal biomass in shallower enclosures. (2) Higher food densities fostered faster *Daphnia* population growth in shallower enclosures. (3) The resultant higher *Daphnia* densities and grazing rates led to an earlier depletion of algal biomass (i.e., an earlier clearwater phase) in shallower enclosures. (4) As a consequence, *Daphnia* populations eventually experienced severe food limitation and started to decline earlier (= earlier *Daphnia* peak) in shallower enclosures.

This scenario is consistent with the data from the ‘cold’ enclosures, where temperature differences among depth treatments were negligible. Accordingly, any differences in the timing of successional events in the ‘cold’ enclosures are most plausibly attributed to mixing depth-mediated differences in algal production.. Consistent with step 1, phytoplankton biomass increased initially faster in shallower ‘cold’ enclosures (day 21: appr. 12, 8, and 4 $\mu\text{g Chl } a \text{ L}^{-1}$ in the 2, 4, and 8 m enclosures, respectively; Fig. 3a-c). Consistent with step 2, *Daphnia* biomass subsequently followed this pattern (day 28: appr. 20, 10, and 5 *Daphnia* L^{-1} ; day 35: appr. 60, 40, and 15 *Daphnia* L^{-1} in the 2, 4, and 8 m enclosures, respectively; Fig. 3d-f). Consistent with steps 3 and 4, shallower ‘cold’ enclosures entered the clearwater phase and reached the *Daphnia* peak earlier (Fig. 5b, c). Step 2 requires that algal biomass was not in the fully saturating range of *Daphnia*’s functional response, because otherwise *Daphnia* populations should have increased at identical rates in all depth treatments. Peak densities of seston biomass were around 0.8, 0.5, and 0.3 mg C/L in the 2, 4, and 8 m enclosures, respectively (data not shown). At these food densities, the ingestion rate of *D. galeata* (a similar sized species as *D. hyalina*) is at 85, 75, and 65%, respectively, of its maximum following data of Muck and Lampert (1984) and at 45, 35, and 25% of its maximum following data of Lynch et al. (1986) and Urabe and Watanabe (1991) [see McCauley et al. (1996) and Rinke and Vijverberg (2005) for details], suggesting that even peak algal densities did not saturate *Daphnia*’s functional response during our experiment.

In retrospect, effects of mixing depth on the timing of successional events are not surprising. Increased growth rates usually speed up population dynamics in simple resource-consumer models. Specifically, algal biomass in a dynamic light-nutrient-phytoplankton model approaches equilibrium much faster in shallow than in deep mixed water columns owing to higher transient growth rates at higher light supply (see Fig. 5 in Diehl et al. 2005). We were surprised however that the effects of mixing depth on the timing of successional events were more prevalent than effects of temperature, despite the rather strong temperature differences among treatments. Again, this suggests that climate-driven changes in the timing and depth of stratification may have at least as far-reaching consequences for plankton dynamics as have changes in temperature.

It should be noted, however, that treatment effects on the timing of successional events were relatively small in absolute terms, given the rather large treatment ranges especially with respect to mixing depth (recall that the black enclosures mimicked a much larger range of optical than physical depths). The timing of the clear-water phase in the shallowest, warmest enclosures differed by no more than 9 days from the deepest and coldest enclosures (treatments ‘2a’ and ‘8c’ in Fig. 5b), which is a relatively minor difference compared to the year-to-year variability observed in natural lakes. For example, the difference between the earliest and latest occurrence of the clear-water phase in Lake Constance was 45 days in the period 1979 and 1994 (Straile 2000). This discrepancy may in part be explained by the relatively late

start of our experiment and the relatively high initial water temperatures (both being consequences of a late ice-out followed by a period of rapid warming of Lake Brunnsee in 2005), leaving a limited scope for the development of treatment differences. In particular, one might expect larger temperature effects on the growth of *Daphnia* in the range 5-10°C (Orcutt and Porter 1983), which was only marginally covered in our experiment. Furthermore, although the temperature differences between ‘ambient’ and ‘cold’ treatments were large compared to current climate change scenarios (IPCC 2001), they were only moderate compared to the observed year-to-year temperature variation in temperate lakes. Moreover, the timing of seasonal events in most real lakes should be influenced by more complex biotic interactions than were possible in our experimental plankton communities. For example, Lampert and Schober (1978) observed that the *Daphnia* population in Lake Constance remained low in early spring in spite of high fecundity and suggested that *Daphnia* population growth and, consequently, the onset of the clear-water phase were retarded by predation from *Cyclops vicinus* until the latter diapaused in May.

Shifts in phenology and the timing of seasonal events in response to global climate change have been described from a multitude of terrestrial, marine, and freshwater habitats (see introduction). Because different species may show independent responses to climate variability, there is growing concern that climate change may de-synchronize the life cycles of resources and their consumers, disrupting the flow of energy through food webs (Thomas et al. 2001, Visser and Holleman 2001, Edwards and Richardson 2004). The importance of a seasonal match between food availability and nutritional demands of developing consumers has long been recognized in fisheries biology (Cushing 1974). Recently, this ‘match-mismatch’ concept has been applied to the plankton dynamics of Lake Washington under global warming, where increased temperatures coincided with decreased synchrony in the seasonal development of phytoplankton and *Daphnia*, and thus possibly with a decreased transfer efficiency of primary production to higher trophic levels (Winder and Schindler 2004b). We caution, however, that the ‘match-mismatch’ concept may be most applicable to strictly donor-controlled systems. It is well documented that *Daphnia* populations can control phytoplankton biomass (Sarnelle 1992, 2003, Murdoch et al. 1998). It therefore seems plausible to assume that the spring dynamics of phytoplankton and *Daphnia*, and thus the timing of their respective peak densities, are mutually interdependent. Our data support this view. Decreasing mixing depth (= increasing average light supply) and increasing temperature both *decreased* the time difference between the successive peaks in phytoplankton and *Daphnia* densities (Fig. 6, Table 1), which is in line with the observation that increased (light-dependent) algal production and increased (temperature-dependent) *Daphnia* growth both speed up succession dynamics in coupled *Daphnia*-phytoplankton models (Diehl, unpublished results).

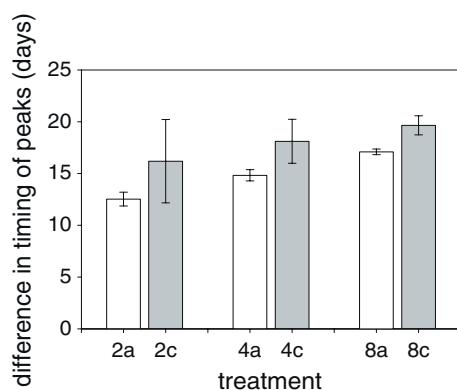


Fig. 6 Difference in timing of the peak densities of phytoplankton and *D. hyalina* versus treatment. The timing of events was estimated from Weibull functions fitted to the data (see *Material and Methods*). Open bars indicate ‘ambient’ temperature treatments, filled bars ‘cold’ temperature treatments, and 2, 4, 8 represent the mixing depths (in meters). Error bars represent standard errors.

In summary, our experiment revealed strong effects of mixing depth-dependent light supply, but not of temperature, on an algal spring bloom and a subsequent *Daphnia* population peak, and that temperature and mixing depth had separate and largely independent effects on the timing of these successional events including the onset of the clear-water phase. Mixing depth and temperature are highly correlated in real lakes (Mazumder and Taylor 1994, Berger et al. 2006). We therefore emphasize that these patterns could only be detected through experimentation. Furthermore, because mixing depth governs both the light climate and the temperature regime in the mixed surface layer, we propose that climate-driven changes in the timing and depth of water column stratification may have particularly far-reaching consequences for plankton dynamics and should receive increased attention.

Acknowledgements

We are grateful to Margit Feissel, Mechthild Kredler, and Sabine Giessler for help with culturing algae and *Daphnia*. We thank three anonymous reviewers for comments on the manuscript. The research was supported by grant DI 745/5 from Deutsche Forschungsgemeinschaft (DFG) within the priority program ‘Aquashift’.

General Discussion and Research Outlook

The influence of mixing intensity: theoretical expectations and observations in natural communities

The most central result emerging from the model analyses in chapter 1 is the recognition of the overwhelming importance of the transport of recycled nutrients from the bottom to the surface and, consequently, of the severe nutrient limitation of algal growth at low mixing intensities. Also, sinking algae taxa would be expected to form a subsurface maximum at low mixing intensities. Consistent with the latter, the field experiment described in chapter 2 showed that pennate diatoms, which dominated plankton communities in nearly all enclosures towards the end of the experiment, initially occupied deeper water strata in the unmixed enclosures, as expected for fast sinking algae taxa. In contrast, most of the initially dominant motile algae were found near the surface in the unmixed enclosures. Presumably, this was the depth where they could attain the highest production, as predicted by Klausmeier and Litchman (2001) for nutrient rich conditions (*see* Figs. 2 & 3 of chapter 2). It seems plausible that pennate diatoms, which are known to be tolerant against low light conditions (Litchman 1998; Flöder et al. 2002), intercepted the nutrient flux from the sediment to the surface in deeper water layers. Consequently, with decreasing nutrient concentration in the upper strata, motile taxa should have become increasingly nutrient limited, which would explain their eventual displacement. In highly eutrophic environments, where the nutrient flux from deeper strata to the surface is less important compared to external inputs, a persistent dominance of buoyant cyanobacteria has been observed under conditions of weak mixing (Visser et al. 1996; Huisman et al. 2004). These buoyant cyanobacteria can then strongly shade deeper strata and thus diminish the possibilities for vertical niche partitioning and for coexistence with sinking taxa, in contrast to our experimental results.

Possible algal behavioral responses to opposing vertical resources gradients

In low turbulence environments motile taxa cannot only avoid sinking losses but they can also respond behaviorally to the trade-off between light and nutrient availability and move to an ‘optimal depth’ in the water column, where their specific growth rate is equally limited by light and nutrients and therefore is maximal (Klausmeier and Litchman 2001). During the diurnal cycle this ‘optimal depth’ may change. Depending on environmental conditions, one scenario for such a change in ‘optimal depth’ during the diurnal cycle could be as follows: At low light intensity in the morning primary production is limited by light and the ‘optimal depth’ is near/at the surface. With increasing light intensity primary production becomes less and less limited by light and, consequently, relatively more limited by nutrients and the ‘optimal depth’ moves down between morning and noon towards depths with higher nutrient concentrations. In the afternoon, when the light intensity decreases again, the ‘optimal depth’ moves upward again. During night photosynthesis is not possible. Thus, if the yield of enhanced production exceeds the costs of movement, algae should move down again in the night and take up and store nutrients to alleviate a possible nutrient limitation during the following day. If algal cells can store nutrients very efficiently, one could also imagine a scenario yielding a ‘classical’ diurnal vertical migration, with an occurrence of algae in deep, nutrient rich strata during night and in well-lit upper strata during day (Pick and Lean 1984; Jones 1988; Knapp et al. 2003).

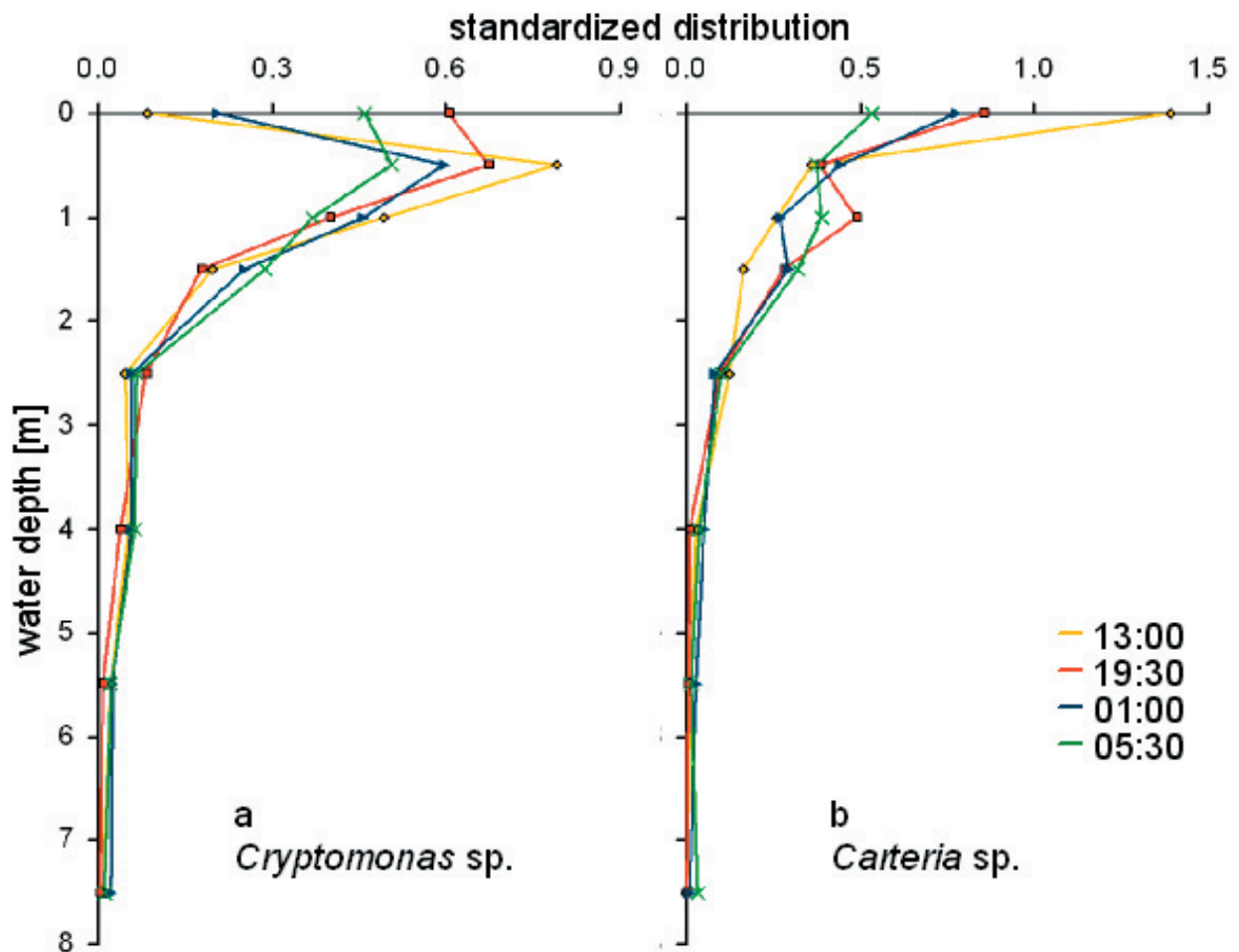


Fig. 1. Diurnal patterns of the vertical distribution of (a) *Cryptomonas sp.* sampled on 01/02 Sep. 2005 and (b) *Carteria sp.* sampled on 25/26 Aug. 2005 in steps of 0.5 to 2m in an 8 m enclosure during the experiment described in chapter 2. Line colors indicate different sampling times as defined in the legend. For a more detailed description of the methods see Schmidt (2006). Shown are standardized distributions, i.e. the integrated distributions add up to 1.

Both of these different patterns of diurnal vertical migration (i.e. either one or two migration cycles in 24 hours) were observed in different algal taxa during additional surveys in the experiment described in chapter 2. *Cryptomonas sp.* (Fig. 1a) showed a more bimodal movement rhythm (two abundance peaks at the surface at dawn and dusk), whereas *Carteria sp.* (Fig. 1b) showed a unimodal rhythm (one abundance peak at the surface at noon). These two different types of diurnal vertical migrations would theoretically require two different types of algal nutrient use physiologies. A unimodal movement rhythm requires good storage possibilities for nutrients and an efficient use of stored nutrients under good light conditions, resulting in a highly flexible carbon to nutrient stoichiometry. In contrast, algae with a limited nutrient storage capacity should always move to the ‘optimal depth’, yielding a bimodal movement rhythm and a less variable carbon to nutrient stoichiometry. Such a fixed stoichiometry has been observed by Katschakis et al. (2005) for flagellates, which they interpreted as a result of mixotrophy (= capability of organisms to balance carbon and nutrient sequestration through autotrophy as well as heterotrophy). However, the taxon *Cryptomonas sp.* examined by them belongs to the same genus as the one that showed the bimodal rhythm in my experiment (Fig. 1a). Additional research on algal diurnal vertical migration and its underlying physiological conditions is required to clarify this issue.

Possible effects of producer stoichiometry on grazers in incompletely mixed systems

The potential importance of algal carbon to nutrient stoichiometry for grazer dynamics in completely mixed systems was described in detail in chapter 3. What is to be expected in incompletely mixed water columns, where algal stoichiometry is likely to show a pronounced vertical gradient (c.f. Fig. 1 of chapter 1)? At low to intermediate turbulence my model predicts the establishment of opposing gradients of food quality (algal C:P ratio) and food quantity in the absence of grazers. A recent study has shown that pelagic grazers of the genus *Daphnia* can sense vertical gradients in foraging profitability and move along them towards the depth offering optimal food conditions (Schatz and McCauley 2007). Evidence for such a habitat selection of *Daphnia* has also been observed by Reichwaldt and Abrusan (2007) within a water column, in which algal taxa of different food quality were differently distributed.

Daphnia commonly perform diel vertical migrations. It has been suggested that vertically migrating *Daphnia* suffer from reduced temperatures and reduced food concentrations in deep water layers and pay energetic costs for the migration, but benefit from reduced predation by visual predators (Orcutt and Porter 1983; Stich and Lampert 1984; Dawidowicz and Loose 1992; Loose and Dawidowicz 1994; McKee and Ebert 1996; Giebelhausen and Lampert 2001). In the context of a vertically changing algal C:P ratio speculations about a further possible benefit of *Daphnia*'s diurnal vertical migration seem reasonable. Vertically migrating *Daphnia* could feed on phosphorus rich food during day in deep water layers and on carbon rich food during night at the surface. Each of these spatially separated diets might be deficient in one or more elements, but the daily integrated diet might be more balanced. The ability of *D. magna* to integrate over two complementary food sources on a daily timescale has already been documented by Sterner and Schwalbach (2001). In their experiment, only algal phosphorus content was varied while carbon density was the same in both types of diet. In contrast, food sources should differ in carbon density and phosphorus content in vertical gradients, as expected at low to intermediate mixing. *Daphnia*'s population response to opposing availability of food carbon and phosphorus in alternate habitats would therefore be an interesting subject for future research.

Light, nutrients, algal stoichiometry and alternative food web pathways

The relative supplies with light and nutrients may not only affect algal stoichiometry and algal-grazer interactions, but entire food webs. In aquatic food webs there is usually an additional pathway linking primary producers and higher trophic levels, i.e. the microbial loop. This microbial loop is based on bacteria, which compete with algae for nutrients but use carbohydrates [dissolved organic carbon (DOC)] released by algae as a food source. Bacteria can be fed upon by mixotrophic algae and microzooplankton (e.g. ciliates, flagellates). The top predator guild of this loop is mesozooplankton (e.g. rotifers, cladocerans, copepods), which feed mainly on algae and have only limited capacities to feed on microzooplankton and/or bacteria, depending on predator to prey size ratios. Bacteria are superior competitors for phosphorus than algae, giving them an advantage under nutrient poor conditions (Rhee 1972; Currie and Kalff 1984; Jansson 1993; Joint et al. 2002). This competitive advantage of bacteria can, under conditions of high light and low phosphorus supply, even be enhanced by increasing DOC release by algae with a high C:P ratio (Obernosterer and Herndl 1995; Sterner et al. 1997; Danger et al. 2007a; Danger et al. 2007b). Under such conditions bacteria can be a good nutrient source for mixotrophic algae or a good carbon

source for microzooplankton (Nygaard and Tobiesen 1993; Stibor and Sommer 2003).

Setting these results into a context of ecological stoichiometry, Elser et al. (2003) suggested that, at low phosphorus supply algae are limited by nutrients and mesozooplankton is either limited by low food quality (high algal C:P ratio) at high light supply or by low food quantity at low light supply. The competitive advantage of bacteria at low phosphorus supply should result in high bacterial production, which, in turn, should increase microzooplankton biomass. If microzooplankton is small enough to be eaten by mesozooplankton, microzooplankton can be an alternative food source to low quality (high C:P) algae. Mesozooplankton might benefit from this alternative pathway and reach higher population densities than without the microbial loop. If microzooplankton cannot be eaten by mesozooplankton, low population densities of mesozooplankton and high population densities of microzooplankton would be expected. In the latter case a shift of mesozooplankton organisms towards taxa that are able to feed on larger prey (e.g. from cladocerans to copepods) may also be possible. In contrast, at high phosphorus supply algal production should be high, at least at high light intensity. Algal food quality and quantity should then support a high mesozooplankton biomass. Under such conditions bacterial production should be relatively low compared to algal production and, consequently, the bacterial loop should be rather weakly developed. At present, many characteristics of these different pathways of pelagic food webs are more educated speculation than certain knowledge. This topic therefore provides many interesting future research perspectives.

Environmental factors and global change

In this dissertation I have shown various and profound influences of environmental factors on pelagic communities. Some of these factors, e.g. the nutrient status and eutrophication of lakes, have been relevant to policy makers and society for at least the last 25 years. In the actual debate on global climate change physical environmental factors have been set into new focus (Behrenfeld et al. 2006; Falkowski and Oliver 2007). These physical factors can be highly variable. Mixed water column depth, for example, can vary from a few meters in small lakes to several hundred meters in the ocean (Soto 2002; Kunz and Diehl 2003; Schmittner 2005). Mixing intensity may range from about $10^{-2} \text{ m}^2 \text{ day}^{-1}$ at strong stratification up to $10^3 \text{ m}^2 \text{ day}^{-1}$ during intense mixing events (MacIntyre et al. 1999, Peeters et al. 2007b). Regional and seasonal differences in the mixing regimes of lakes and oceans are, in turn, determined by temperature, wind, and precipitation and, consequently, highly influenced by weather and climate. While the direction and magnitude of future changes in physical water column structure is still somewhat uncertain, there is increasing evidence that one consequence of global warming may be more shallow stratification and increased water column stability (Sarmiento et al. 1998; Lehman 2000; George and Hewitt 2006; Coats et al. 2006). Clearly, environmental factors have potentially far reaching implications not only for ecosystem processes (primary production, sinking export, nutrient recycling etc.), but also for community processes such as food web dynamics and seasonal succession (chapter 4). Further investigations of the influences of physical environmental factors on pelagic systems should therefore generate a better understanding of both the systems themselves and the consequences of global climate change on ecosystem functions such as the cycling of nutrients and the distribution of carbon among the atmosphere, the ocean, soils, and the biosphere.

References

- Andersen, T. 1997. Pelagic nutrient cycles: herbivores as sources and sinks. Springer.
- Andersen, T., J. J. Elser, and D. O. Hessen. 2004. Stoichiometry and population dynamics. *Ecology Letters* 7:884-900.
- Andersen, T. and D. O. Hessen. 1991. Carbon, nitrogen, and phosphorus-content of fresh-water zooplankton. *Limnology and Oceanography* 36:807-814.
- Antia, A. N. 2005. Solubilization of particles in sediment traps: revising the stoichiometry of mixed layer export. *Biogeosciences* 2:189-204.
- Behrenfeld, M. J., R. T. O'Malley, D. A. Siegel, C. R. McClain, J. L. Sarmiento, G. C. Feldman, A. J. Milligan, P. G. Falkowski, R. M. Letelier, and E. S. Boss. 2006. Climate-driven trends in contemporary ocean productivity. *Nature* 444:752-755.
- Berger, S. A., S. Diehl, T. J. Kunz, D. Albrecht, A. M. Oucible, and S. Ritzer. 2006. Light supply, plankton biomass, and seston stoichiometry in a gradient of lake mixing depths. *Limnology and Oceanography* 51:1898-1905.
- Berger, S. A., S. Diehl, H. Stibor, G. Trommer, M. Ruhlenstroth, A. Wild, A. Weigert, C. G. Jäger, and M. Striebel. 2007. Water temperature and mixing depth affect timing and magnitude of events during spring succession of the plankton. *Oecologia* 150:643-654.
- Bertilsson, S., O. Berglund, D. M. Karl, and S. W. Chisholm. 2003. Elemental composition of marine *Prochlorococcus* and *Synechococcus*: Implications for the ecological stoichiometry of the sea. *Limnology and Oceanography* 48:1721-1731.
- Briand, F. and E. McCauley. 1978. Cybernetic mechanisms in lake plankton systems - how to control undesirable algae. *Nature* 273: 228-230.
- Burns, C. W. 1968. Relationship between body size of filter-feeding Cladocera and maximum size of particle ingested. *Limnology and Oceanography* 13: 675-678.
- Càceres, C. E. 1998. Interspecific variation in the abundance, production, and emergence of *Daphnia* diapausing eggs. *Ecology* 79:1699-1710.
- Christian, J. R. 2005. Biogeochemical cycling in the oligotrophic ocean: Redfield and non-Redfield models. *Limnology and Oceanography* 50:646-657.
- Clegg, M. R., S. C. Maberly, and R. I. Jones. 2007. Behavioral response as a predictor of seasonal depth distribution and vertical niche separation in freshwater phytoplanktonic flagellates. *Limnology and Oceanography* 52:441-455.
- Cloern, J. E. 2007. Habitat connectivity and ecosystem productivity: Implications from a simple model. *American Naturalist* 169:E21-E33.
- Coats, R., J. Perez-Losada, G. Schladow, R. Richards, and C. Goldman. 2006. The warming of Lake Tahoe. *Climatic Change* 76:121-148.
- Condie, S. A. and M. Bormans. 1997. The influence of density stratification on particle settling, dispersion and population growth. *Journal of Theoretical Biology* 187:65-75.
- Cuker, B. E. 1987. Field experiment on the influences of suspended clay and P on the plankton of a small lake. *Limnology and Oceanography* 32:840-847.
- Currie, D. J. and J. Kalff. 1984. Can bacteria outcompete phytoplankton for phosphorus - a chemostat test. *Microbial Ecology* 10:205-216.
- Cushing, J. M., B. Dennis, R. A. Desharnais, and R. F. Costantino. 1998. Moving toward an unstable equilibrium: saddle nodes in population systems. *Journal of Animal Ecology* 67: 298-306.

- Danger, M., J. Leflaive, C. Oumarou, L. Ten Hage, and G. Lacroix. 2007a. Control of phytoplankton-bacteria interactions by stoichiometric constraints. *Oikos* 116:1079-1086.
- Danger, M., C. Oumarou, D. Benest, and G. Lacroix. 2007b. Bacteria can control stoichiometry and nutrient limitation of phytoplankton. *Functional Ecology* 21:202-210.
- Dawidowicz, P. and C. J. Loose. 1992. Metabolic costs during predator-induced diel vertical migration of *Daphnia*. *Limnology and Oceanography* 37:1589-1595.
- DeAngelis, D. L. and J. C. Waterhouse. 1987. Equilibrium and nonequilibrium concepts in ecological models. *Ecological Monographs* 57: 1-21.
- De Senerpont Domis, L. N., W. M. Mooij, S. Hülsmann, E. H. van Nes, and M. Scheffer. 2007. Can overwintering versus diapausing strategy in *Daphnia* determine match-mismatch events in zooplankton-algae interactions? *Oecologia* 150: 682-698.
- Diehl, S. 2002. Phytoplankton, light, and nutrients in a gradient of mixing depths: Theory. *Ecology* 83:386-398.
- Diehl, S. 2007. Paradoxes of enrichment: Effects of increased light versus nutrient supply on pelagic producer-grazer systems. *American Naturalist* 169:E173-E191.
- Diehl, S., S. Berger, R. Ptacnik, and A. Wild. 2002. Phytoplankton, light, and nutrients in a gradient of mixing depths: Field experiments. *Ecology* 83:399-411.
- Diehl, S., S. Berger, and R. Wöhrle. 2005. Flexible nutrient stoichiometry mediates environmental influences, on phytoplankton and its resources. *Ecology* 86:2931-2945.
- Edwards, M., and A. J. Richardson. 2004. The impact of climate change on the phenology of the plankton community and trophic mismatch. *Nature* 430:881-884.
- Elliott, J. A., A. E. Irish, and C. S. Reynolds. 2002. Predicting the spatial dominance of phytoplankton in a light limited and incompletely mixed eutrophic water column using the PROTECH model. *Freshwater Biology* 47:433-440.
- Elser, J. J. and N. B. George. 1993. The stoichiometry of n and p in the pelagic zone of Castle Lake, California. *Journal of Plankton Research* 15:977-992.
- Elser, J. J., M. Kyle, W. Makino, T. Yoshida, and J. Urabe. 2003. Ecological stoichiometry in the microbial food web: a test of the light:nutrient hypothesis. *Aquatic Microbial Ecology* 31:49-65.
- Falkowski, P. G. and M. J. Oliver. 2007. Mix and match: how climate selects phytoplankton. *Nature Reviews Microbiology* 5:813-819.
- Flöder, S., and U. Sommer. 1999. Diversity in planktonic communities: An experimental test of the intermediate disturbance hypothesis. *Limnology and Oceanography* 44: 1114-1119.
- Flöder, S., J. Urabe, and Z. Kawabata. 2002. The influence of fluctuating light intensities on species composition and diversity of natural phytoplankton communities. *Oecologia* 133:395-401.
- Fussmann, G. F., S. P. Ellner, K. W. Shertzer, and N. G. Hairston. 2000. Crossing the Hopf bifurcation in a live predator-prey system. *Science* 290: 1358-1360.
- Gaedke, U., D. Ollinger, E. Bäumler, and D. Straile. 1998a. The impact of interannual variability in hydrodynamic conditions on the plankton development in Lake Constance in spring and summer. *Archiv für Hydrobiologie Special Issues: Advances in Limnology* 53:565-585.
- Gaedke, U., D. Ollinger, P. Kirner, and E. Bäumler. 1998b. The influence of weather conditions on the seasonal plankton development in a large and deep lake (L. Constance). Pages 71-84 in George DG, Jones JG, Punochár JG, Reynolds CS, Sutcliffe DW (eds.) *Management of Lakes and Reservoirs during global climate change*. Kluwer Academic Publishers.
- Geider, R. J., H. L. MacIntyre, and T. M. Kana. 1998. A dynamic regulatory model of phytoplanktonic acclimation to light, nutrients, and temperature. *Limnology and Oceanography* 43:679-694.

- George, D. C. and D. P. Hewitt. 2006. The impact of year-to-year changes in the weather on the dynamics of *Daphnia* in a thermally stratified lake. *Aquatic Ecology* 40:33-47.
- Giebelhausen, B. and W. Lampert. 2001. Temperature reaction norms of *Daphnia magna*: the effect of food concentration. *Freshwater Biology* 46:281-289.
- Greve, W. U. Lange, F. Reiners, and J. Nast. 2001. Predicting the seasonality of North Sea zooplankton. *Senckenbergiana maritima* 31:263-268.
- Grover, J. P. 1997. *Resource Competition*. Chapman & Hall.
- Guildford, S. J., F. P. Healey, and R. E. Hecky. 1987. Depression of primary production by humic matter and suspended sediment in limnocorral experiments at Southern Indian Lake, Northern Manitoba. *Canadian Journal of Fisheries and Aquatic Sciences* 44:1408-1417.
- Gurney, W. S. C. and R. M. Nisbet. 1998. *Ecological dynamics*. Oxford University Press.
- Haas, K. 2002. Einfluss der Tiefe des Epilimnions auf experimentelle Phytoplanktonsysteme mit besonderem Augenmerk auf dem Zooplankton. Diplomarbeit. Ludwig-Maximilians-Universität München, Germany.
- Harrington, R., I. Woiwod, and T. Sparks. 1999. Climate change and trophic interaction. *Trends in Ecology & Evolution* 14:146-150.
- Haupt, F. 2004. Auswirkungen der Epilimniontiefe auf Phytoplankton-Daphnien-Interaktionen mit Schwerpunkt Zooplankton. Diplomarbeit. Ludwig-Maximilians-Universität München, Germany.
- Hastings, A. 2004. Transients: the key to long-term ecological understanding? *Trends in Ecology & Evolution* 19: 39-45.
- Hays, G. C., A. J. Richardson, and C. Robinson. 2005. Climate change and marine plankton. *Trends in Ecology & Evolution* 20:337-344.
- Hessen, D. O., G. I. Agren, T. R. Anderson, J. J. Elser, and P. C. De Ruiter. 2004. Carbon, sequestration in ecosystems: The role of stoichiometry. *Ecology* 85:1179-1192.
- Hillebrand, H., C. D. Durselen, D. Kirschtel, U. Pollingher, and T. Zohary. 1999. Biovolume calculation for pelagic and benthic microalgae. *Journal of Phycology* 35: 403-424.
- Hughes, L. 2000. Biological consequences of global warming: is the signal already apparent? *Trends in Ecology & Evolution* 15:56-61.
- Huisman, J. 1999. Population dynamics of light-limited phytoplankton: microcosm experiments. *Ecology* 80:202-210.
- Huisman, J. and F. J. Weissing. 1995. Competition for nutrients and light in a mixed water column - a theoretical-analysis. *American Naturalist* 146:536-564.
- Huisman, J., P. van Oostveen, and F. J. Weissing. 1999. Critical depth and critical turbulence: Two different mechanisms for the development of phytoplankton blooms. *Limnology and Oceanography* 44:1781-1787.
- Huisman, J. and F. J. Weissing. 2001. Fundamental unpredictability in multispecies competition. *American Naturalist* 157: 488-494.
- Huisman, J. and B. Sommeijer. 2002. Maximal sustainable sinking velocity of phytoplankton. *Marine Ecology-Progress Series* 244:39-48.
- Huisman, J., M. Arrayas, U. Ebert, and B. Sommeijer. 2002. How do sinking phytoplankton species manage to persist? *American Naturalist* 159:245-254.
- Huisman, J., J. Sharples, J. M. Stroom, P. M. Visser, W. E. A. Kardinaal, J. M. H. Verspagen, and B. Sommeijer. 2004. Changes in turbulent mixing shift competition for light between phytoplankton species. *Ecology* 85:2960-2970.

- Huisman, J., N. N. P. Thi, D. M. Karl, and B. Sommeijer. 2006. Reduced mixing generates oscillations and chaos in the oceanic deep chlorophyll maximum. *Nature* 439:322-325.
- Huppert, A., B. Blasius, and L. Stone. 2002. A model of phytoplankton blooms. *American Naturalist* 159:156-171.
- Hutchinson, G. E. 1961. The paradox of the plankton. *American Naturalist* 95: 137-145.
- IPCC. 2001. *Climate Change 2001: Synthesis Report*. Watson RT and the Core Writing Team (eds). Cambridge University Press.
- Jäger, C. G., S. Diehl, C. Matauschek, C. A. Klausmeier, and H. Stibor. 2008. Transient dynamics of pelagic producer-grazer systems in a gradient of nutrients and mixing depths. *Ecology* (in press).
- Jäger, C. G., S. Diehl, G. M. Schmidt. Influence of water column depth and mixing intensity on phytoplankton biomass and functional community composition. Submitted to *Limnology and Oceanography*.
- Jansson, M. 1993. Uptake, exchange, and excretion of orthophosphate in phosphate-starved *Scenedesmus-quadricauda* and *Pseudomonas* k7. *Limnology and Oceanography* 38:1162-1178.
- Joint, I., P. Henriksen, G. A. Fonnes, D. Bourne, T. F. Thingstad, and B. Riemann. 2002. Competition for inorganic nutrients between phytoplankton and bacterioplankton in nutrient manipulated mesocosms. *Aquatic Microbial Ecology* 29:145-159.
- Jones, R. I. 1988. Vertical-distribution and diel migration of flagellated phytoplankton in a small humic lake. *Hydrobiologia* 161:75-87.
- Katechakis, A., T. Haseneder, R. Kling, and H. Stibor. 2005. Mixotrophic versus photoautotrophic specialist algae as food for zooplankton: the light:nutrient hypothesis might not hold for mixotrophs. *Limnology and Oceanography* 50:1290-1299.
- Kirk, J. T. O. 1994. *Light and photosynthesis in aquatic ecosystems*. Second:
- Kirk, J. T. O. and P. A. Tyler. 1986. The spectral absorption and scattering properties of dissolved and particulate components in relation to the underwater light-field of some tropical Australian fresh-waters. *Freshwater Biology* 16:573-583.
- Klausmeier, C. A. and E. Litchman. 2001. Algal games: The vertical distribution of phytoplankton in poorly mixed water columns. *Limnology and Oceanography* 46:1998-2007.
- Knapp, C. W., F. deNoyelles, D. W. Graham, and S. Bergin. 2003. Physical and chemical conditions surrounding the diurnal vertical migration of *Cryptomonas* spp. (Cryptophyceae) in a seasonally stratified midwestern reservoir (USA). *Journal of Phycology* 39:855-861.
- Knoechel, R., L. B. Holtby. 1986. Construction and validation of a body-length-based model for the prediction of cladoceran community filtering rates. *Limnology and Oceanography* 31: 1-16.
- Kooijman, S. A. L. M. 1998. The Synthesizing Unit as model for the stoichiometric fusion and branching of metabolic fluxes. *Biophysical Chemistry* 73: 179-188.
- Kooijman, S. A. L. M. 2000. *Dynamic energy and mass budgets in biological systems*. 2nd edition. Cambridge University Press.
- Kunz, T. J. and S. Diehl. 2003. Phytoplankton, light and nutrients along a gradient of mixing depth: a field test of producer-resource theory. *Freshwater Biology* 48:1050-1063.
- Lampert, W. 1977. Studies on the carbon balance of *Daphnia pulex* De Geer as related to environmental conditions. III. Production and production efficiency. *Archiv für Hydrobiologie*. 48:336-360.
- Lampert, W., and U. Schober. 1978. Das regelmäßige Auftreten von Frühjahrs-Algenmaximum und "Klarwasserstadium" im Bodensee als Folge von klimatischen Bedingungen und Wechselwirkungen zwischen Phyto- und Zooplankton. *Archiv für Hydrobiologie* 82:364-386.

- Lampert, W., W. Fleckner, H. Rai, and B. E. Taylor. 1986. Phytoplankton control by grazing zooplankton - a study on the spring clear-water phase. *Limnology and Oceanography* 31:478-490.
- Lehman, P. W. 2000. The influence of climate on phytoplankton community biomass in San Francisco Bay Estuary. *Limnology and Oceanography* 45:580-590.
- Litchman, E. 1998. Population and community responses of phytoplankton to fluctuating light. *Oecologia* 117:247-257.
- Litchman, E. 2003. Competition and coexistence of phytoplankton under fluctuating light: experiments with two cyanobacteria. *Aquatic Microbial Ecology* 31:241-248.
- Loladze, I., Y. Kuang, and J. J. Elser. 2000. Stoichiometry in producer-grazer systems: Linking energy flow with element cycling. *Bulletin of Mathematical Biology* 62: 1137-1162.
- Loose, C. J. and P. Dawidowicz. 1994. Trade-offs in diel vertical migration by zooplankton - the costs of predator avoidance. *Ecology* 75:2255-2263.
- Lynch, M., L. J. Weider, and W. Lampert. 1986. Measurement of the carbon balance in *Daphnia*. *Limnology and Oceanography* 31: 17-33.
- MacIntyre, S., K. M. Flynn, R. Jellison, and J. R. Romero. 1999. Boundary mixing and nutrient fluxes in Mono Lake, California. *Limnology and Oceanography* 44:512-529.
- Mackas, D. L., R. Goldblatt, and A. G. Lewis. 1998. Interdecadal variation in developmental timing of *Neocalanus plumchrus* populations at Ocean Station P in the subarctic North Pacific. *Canadian Journal of Fisheries and Aquatic Sciences* 55:1878-1893.
- May, R. M. 1975. Biological populations obeying difference equations - stable points, stable cycles, and chaos. *Journal of Theoretical Biology* 51: 511-524.
- Mazumder, A., and W. D. Taylor. 1994. Thermal structure of lakes varying in size and water clarity. *Limnology and Oceanography* 39:968-976.
- McCann, K. S. 2000. The diversity-stability debate. *Nature* 405: 228-233.
- McCauley, E., R. M. Nisbet, A. M. deRoos, W. W. Murdoch, and W. S. C. Gurney. 1996. Structured population models of herbivorous zooplankton. *Ecological Monographs* 66: 479-501.
- McCauley, E., R. M. Nisbet, W. W. Murdoch, A. M. de Roos, and W. S. C. Gurney. 1999. Large-amplitude cycles of *Daphnia* and its algal prey in enriched environments. *Nature* 402: 653-656.
- McKee, D. and D. Ebert. 1996. The interactive effects of temperature, food level and maternal phenotype on offspring size in *Daphnia magna*. *Oecologia* 107:189-196.
- Montagnes, D. J. S., J. A. Berges, P. J. Harrison, and J. R. Taylor. 1994. Estimating carbon, nitrogen, protein, and chlorophyll-a from volume in marine-phytoplankton. *Limnology and Oceanography* 39: 1044-1060.
- Muck, P., and W. Lampert. 1984. An experimental study on the importance of food conditions for the relative abundance of calanoid copepods and cladocerans. *Archiv für Hydrobiologie Supplement* 66:157-179.
- Murdoch, W. W., R. M. Nisbet, E. McCauley, A. M. deRoos, and W. S. C. Gurney. 1998. Plankton abundance and dynamics across nutrient levels: Tests of hypotheses. *Ecology* 79:1339-1356.
- Murdoch, W. W., R. M. Nisbet, and C. J. Briggs. 2003. *Consumer-resource dynamics*. Princeton University Press, Princeton, New Jersey, USA.
- Nelson, W. A., E. McCauley, and F. J. Wrona. 2001. Multiple dynamics in a single predator-prey system: experimental effects of food quality. *Proceedings of the Royal Society of London Series B-Biological Sciences* 268: 1223-1230.
- Neubert, M. G. and H. Caswell. 1997. Alternatives to resilience for measuring the responses of ecological systems to perturbations. *Ecology* 78: 653-665.

- Neubert, M. G., T. Klanjscek, and H. Caswell. 2004. Reactivity and transient dynamics of predator-prey and food web models. *Ecological Modelling* 179: 29-38.
- Nisbet, R. M., E. McCauley, W. S. C. Gurney, W. W. Murdoch, and A. M. deRoos. 1997. Simple representations of biomass dynamics in structured populations. p. 61-79. *In*[eds.], H. G. Othmer, F. R. Adler, M. A. Lewis, and J. C. Daloan. *Case Studies in Mathematical Modeling – ecology, physiology, and cell biology*. Prentice Hall.
- Nygaard, K. and A. Tobiesen. 1993. Bacterivory in algae - a survival strategy during nutrient limitation. *Limnology and Oceanography* 38:273-279.
- O'Brien, W. J. 1974. The dynamics of nutrient limitation of phytoplankton algae: a model reconsidered. *Ecology* 55:135-141.
- O'Brien, K. R., G. N. Ivey, D. P. Hamilton, A. M. Waite, and P. M. Visser. 2003. Simple mixing criteria for the growth of negatively buoyant phytoplankton. *Limnology and Oceanography* 48:1326-1337.
- Obernosterer, I. and G. J. Herndl. 1995. Phytoplankton extracellular release and bacterial-growth - dependence on the inorganic N-P ratio. *Marine Ecology-Progress Series* 116:247-257.
- Orcutt, J. D. and K. G. Porter. 1983. Diel vertical migration by zooplankton - constant and fluctuating temperature effects on life-history parameters of *Daphnia*. *Limnology and Oceanography* 28:720-730.
- Park, S., S. Chandra, D. C. Müller-Navarra, and C. R. Goldman. 2004. Diel and vertical variability of seston food quality and quantity in a small subalpine oligomesotrophic lake. *Journal of Plankton Research* 26:1489-1498.
- Parmesan, C., and G. Yohe. 2003. A globally coherent fingerprint of climate change impacts across natural systems. *Nature* 421:37-42.
- Passarge, J., S. Hol, M. Escher, and J. Huisman. 2006. Competition for nutrients and light: Stable coexistence, alternative stable states, or competitive exclusion? *Ecological Monographs* 76:57-72.
- Peeters, F., A. Wuest, G. Piefke, and D. M. Imboden. 1996. Horizontal mixing in lakes. *Journal of Geophysical Research-Oceans* 101: 18361-18375.
- Peeters, F. D. Straile, A. Lorke, and D. M. Livingstone. 2007a. Earlier onset of the spring phytoplankton bloom in lakes of the temperate zone in a warmer climate. *Global Change Biology* 13: 1898-1909.
- Peeters, F., D. Straile, A. Lorke, and D. Ollinger. 2007b. Turbulent mixing and phytoplankton spring bloom development in a deep lake. *Limnology and Oceanography* 52:286-298.
- Peterson, M. L., S. G. Wakeham, C. Lee, M. A. Askea, and J. C. Miquel. 2005. Novel techniques for collection of sinking particles in the ocean and determining their settling rates. *Limnology and Oceanography-Methods* 3:520-532.
- Pick, F. R. and D. R. S. Lean. 1984. Diurnal movements of metalimnetic phytoplankton. *Journal of Phycology* 20:430-436.
- Ptacnik, R., S. Diehl, and S. Berger. 2003. Performance of sinking and nonsinking phytoplankton taxa in a gradient of mixing depths. *Limnology and Oceanography* 48:1903-1912.
- Polis, G. A., W. B. Anderson, and R. D. Holt. 1997. Toward an integration of landscape and food web ecology: The dynamics of spatially subsidized food webs. *Annual Review of Ecology and Systematics* 28:289-316.
- Reichwaldt, E. S., I. D. Wolf, and H. Stibor. 2005. Effects of fluctuating temperature regime experienced by *Daphnia* during diel vertical migration on *Daphnia* life history parameters. *Hydrobiologia* 543:199-205.
- Reichwaldt, E. S. and G. Abrusan. 2007. Influence of food quality on depth selection of *Daphnia pulicaria*. *Journal of Plankton Research* 29:839-849.

- Reiners, W. A. and K. L. Driese. 2001. The propagation of ecological influences through heterogeneous environmental space. *Bioscience* 51:939-950.
- Reynolds, C. S. 1984. *The ecology of freshwater phytoplankton*. Cambridge University Press.
- Reynolds, C. S. 1988. The concept of ecological succession applied to seasonal periodicity of freshwater phytoplankton. *Verhandlungen Internationale Vereinigung für theoretische und angewandte Limnologie* 23: 683-691.
- Reynolds, C. S. 1992. Dynamics, selection and composition of phytoplankton in relation to vertical structure in lakes. *Archiv für Hydrobiologie Beiheft* 35:13-31.
- Reynolds, C. S. 1989. Physical determinants of phytoplankton succession. In Sommer, U. (ed.) *Plankton ecology: Succession in plankton communities*. Springer. pp 9-56.
- Reynolds, C. S. 2006. *Ecology of Phytoplankton*. Cambridge University Press.
- Reynolds, C. S., S. W. Wiseman, B. M. Godfrey, and C. Butterwick. 1983. Some effects of artificial mixing on the dynamics of phytoplankton populations in large limnetic enclosures. *Journal of Plankton Research* 5:203-234.
- Reynolds, C. S., S. W. Wiseman, and M. J. O. Clarke. 1984. Growth-rate and loss-rate responses of phytoplankton to intermittent artificial mixing and their potential application to the control of planktonic algal biomass. *Journal of Applied Ecology* 21:11-39.
- Rhee, G. Y. 1972. Competition between an alga and an aquatic bacterium for phosphate. *Limnology and Oceanography* 17:505-&.
- Richardson, A. J., and D. S. Schoeman. 2004. Climate impact of plankton ecosystems in the Northeast Atlantic. *Science* 305:1609-1612.
- Riebesell, U., K. G. Schulz, R. G. J. Bellerby, M. Botros, P. Fritsche, M. Meyerhofer, C. Neill, G. Nondal, A. Oschlies, J. Wohlers, and E. Zollner. 2007. Enhanced biological carbon consumption in a high CO₂ ocean. *Nature* 450:545-U10.
- Riley, G. A., H. Stommel, and D. F. Bumpus. 1949. Quantitative ecology of the plankton of the western North Atlantic. *Bulletin of the Bingham Oceanographic collection Yale University* 12:1-169.
- Rinke, K., and J. Vijverberg. 2005. A model approach to evaluate the effect of temperature and food concentration on individual life-history and population dynamics of *Daphnia*. *Ecological Modelling* 186:326-344.
- Root, T. L., J. T. Price, K. R. Hall, S. H. Schneider, C. Rosenzweig, and J. A. Pounds. 2003. Fingerprints of global warming on wild animals and plants. *Nature* 421:57-60.
- Rothhaupt, K. O. 1991. Variations on the zooplankton menu - reply. *Limnology and Oceanography* 36:824-827.
- Sarmiento, J. L., T. M. C. Hughes, R. J. Stouffer, and S. Manabe. 1998. Simulated response of the ocean carbon cycle to anthropogenic climate warming. *Nature* 393:245-249.
- Sarnelle, O. 1992. Nutrient enrichment and grazer effects on phytoplankton in lakes. *Ecology* 73:551-560.
- Sarnelle, O. 1993. Herbivore effects on phytoplankton succession in a eutrophic lake. *Ecological Monographs* 63:129-149.
- Sarnelle, O. 2003. Nonlinear effects of an aquatic consumer: causes and consequences. *American Naturalist* 161:478-496.
- Schatz, G. S. and E. McCauley. 2007. Foraging behavior by *Daphnia* in stoichiometric gradients of food quality. *Oecologia* 153:1021-1030.
- Scheffer, M., S. Rinaldi, A. Gragnani, L. R. Mur, and E. H. van Nes. 1997a. On the dominance of filamentous cyanobacteria in shallow, turbid lakes. *Ecology* 78: 272-282.

- Scheffer, M., S. Rinaldi, Y. A. Kuznetsov, and E. H. vanNes. 1997b. Seasonal dynamics of *Daphnia* and algae explained as a periodically forced predator-prey system. *Oikos* 80: 519-532.
- Scheffer, M., D. Straile, E. H. van Nes, and H. Hosper. 2001. Climatic warming causes regime shifts in lake food webs. *Limnology and Oceanography* 46: 1780-1783.
- Scheffer, M., S. Rinaldi, J. Huisman, and F. J. Weissing. 2003. Why plankton communities have no equilibrium: solutions to the paradox. *Hydrobiologia* 491: 9-18.
- Schmidt, G. 2006. Biomasse und Vertikalverteilung beweglicher Phytoplankter in Wassersäulen unterschiedlicher Tiefe und Durchmischung. Diplomarbeit. Ludwig-Maximilians-Universität München, Germany.
- Schmittner, A. 2005. Decline of the marine ecosystem caused by a reduction in the Atlantic overturning circulation. *Nature* 434:628-633.
- Sherman, B. S., I. T. Webster, G. J. Jones, and R. L. Oliver. 1998. Transition between *Aulacoseira* and *Annabaena* dominance in turbid river weir pool. *Limnology and Oceanography* 43: 1902-1915.
- Smayda, T. J. 1969. Some measurements of sinking rate of fecal pellets. *Limnology and Oceanography* 14:621-625.
- Smith, R. E. H., and J. Kalff. 1983. Competition for phosphorus among co-occurring fresh-water phytoplankton. *Limnology and Oceanography* 28: 448-464.
- Sokal, R. R., and F. J. Rohlf. 1981. *Biometry*. 2nd ed. W. H. Freeman and Company.
- Sommer, U. 1985. Comparison between steady-state and non-steady state competition - experiments with natural phytoplankton. *Limnology and Oceanography* 30:335-346.
- Sommer, U. 1986. The periodicity of phytoplankton in Lake Constance (Bodensee) In comparison to other deep lakes of Central-Europe. *Hydrobiologia* 138: 1-7.
- Sommer, U. 1992. Phosphorus-limited *Daphnia* - intraspecific facilitation instead of competition. *Limnology and Oceanography* 37:966-973.
- Sommer, U., Z. M. Gliwicz, W. Lampert, and A. Duncan. 1986. The PEG-model of seasonal succession of planktonic events in fresh waters. *Archiv für Hydrobiologie* 106:433-471.
- Sommer, U., F. Sommer, B. Santer, C. Jamieson, M. Boersma, C. Becker, and T. Hansen. 2001. Complementary impact of copepods and cladocerans on phytoplankton. *Ecology Letters* 4: 545-550.
- Soto, D. 2002. Oligotrophic patterns in southern Chilean lakes: the relevance of nutrients and mixing depth. *Revista Chilena de Historia Natural* 75:377-393.
- Stenseth, N. C., and A. Mysterud. 2002. Climate, changing phenology, and other life history traits: nonlinearity and match-mismatch to the environment. *Proceedings of the National Academy of Sciences of the United States of America* 99:13379-13381.
- Sterner, R. W. and J. J. Elser. 2002. *Ecological Stoichiometry*. Princeton University Press.
- Sterner, R. W., J. J. Elser, E. J. Fee, S. J. Guildford, and T. H. Chrzanowski. 1997. The light:nutrient ratio in lakes: The balance of energy and materials affects ecosystem structure and process. *American Naturalist* 150:663-684.
- Sterner, R. W., D. D. Hagemeyer, and W. L. Smith. 1993. Phytoplankton nutrient limitation and food quality for *Daphnia*. *Limnology and Oceanography* 38:857-871.
- Sterner, R. W. and M. S. Schwalbach. 2001. Diel integration of food quality by *Daphnia*: luxury consumption by a freshwater planktonic herbivore. *Limnology and Oceanography* 46:410-416.
- Stibor, H. and J. Lüning. 1994. Predator-induced phenotypic variation in the pattern of growth and reproduction in *Daphnia-hyalina* (Crustacea, Cladocera). *Functional Ecology* 8: 97-101.
- Stibor, H. and U. Sommer. 2003. Mixotrophy of a photosynthetic flagellate viewed from an optimal foraging perspective. *Protist* 154:91-98.

- Stich, H. B. and W. Lampert. 1984. Growth and reproduction of migrating and non-migrating *Daphnia* species under simulated food and temperature conditions of diurnal vertical migration. *Oecologia* 61:192-196.
- Straile, D. 2000. Meteorological forcing of plankton dynamics in a large and deep continental European lake. *Oecologia* 122:44-50.
- Straile, D. 2002. North Atlantic Oscillation synchronizes food-web interactions in central European lakes. *Proceedings of the Royal Society of London Series B-Biological Sciences* 269:391-395.
- Straile, D., and R. Adrian. 2000. The North Atlantic Oscillation and plankton dynamics in two European lakes - two variations on a general theme. *Global Change Biology* 6: 663-670.
- Sverdrup, H. U. 1953. On conditions for the vernal blooming of phytoplankton. *Journal du Conseil Permanent International pour l'Exploration de la Mer* 18:287-295.
- Talling, J. F. 2003. Phytoplankton-zooplankton seasonal timing and the 'clear-water phase' in some English lakes. *Freshwater Biology* 48:39-52.
- Thomas, D. W., J. Blondel, P. Perret, M. M. Lambrechts, and J. R. Speakman. 2001. Energetic and fitness costs of mismatching resource supply and demand in seasonally breeding birds. *Science* 291:2598-2600.
- Urabe, J., and Y. Watanabe. 1991. Effect of food concentration on the assimilation efficiency and production efficiencies of *Daphnia galeata*. *Functional Ecology* 5:635-641.
- Urabe, J. and R. W. Sterner. 1996. Regulation of herbivore growth by the balance of light and nutrients. *Proceedings of the National Academy of Sciences of the United States of America* 93:8465-8469.
- Urabe, J., J. J. Elser, M. Kyle, T. Yoshida, T. Sekino, and Z. Kawabata. 2002. Herbivorous animals can mitigate unfavourable ratios of energy and material supplies by enhancing nutrient recycling. *Ecology Letters* 5:177-185.
- Utermöhl, H. 1958. Zur Vervollkommnung der quantitativen Phytoplanktonmethodik. *Mitteilungen der internationalen Vereinigung für theoretische und angewandte Limnologie* 9: 1-38.
- Vadstein, O. 2000. Heterotrophic, planktonic bacteria and cycling of phosphorus - Phosphorus requirements, competitive ability, and food web interactions. *Advances in Microbial Ecology* 16: 115-167.
- Visser, P. M., L. Massaut, J. Huisman, and L. R. Mur. 1996. Sedimentation losses of *Scenedesmus* in relation to mixing depth. *Archiv für Hydrobiologie* 136:289-308.
- Visser, M., and L. J. M. Holleman. 2001. Warmer springs disrupt the synchrony of oak and winter moth phenology. *Proceedings of the Royal Society of London Series B-Biological sciences* 268:289-294.
- Wetzel, R. G. 1983. *Limnology*. 2nd edition. Saunders.
- Weyhenmeyer, G., T. Blencker, and K. Petterson. 1999. Changes of the plankton spring outburst related to the North Atlantic Oscillation. *Limnology and Oceanography* 44:1788-1792.
- Winder, M. and D. E. Schindler. 2004a. Climatic effects on the phenology of lake processes. *Global Change Biology* 10: 1844-1856.
- Winder, M., and D. E. Schindler. 2004b. Climate change uncouples trophic interactions in a lake ecosystem. *Ecology* 85:56-62.

Danksagung

Ich möchte mich bei Sebastian Diehl für das Angebot und die Betreuung dieser Doktorarbeit bedanken. Ich danke Ihn für all die Freiheiten, die er mir gelassen hat, die vielseitigen Möglichkeiten die er mir aufgezeigt hat und für all die Unterstützung meiner Arbeit und meines Werdeganges. Ich habe die Zeit, die Arbeit, die Reisen und die Gespräche sehr genossen.

Ich möchte mich auch bei Herwig Stibor bedanken, dafür dass ich stets mit Fragen zu Ihm kommen konnte. Weiter möchte ich mich bei allen Mitarbeitern der Abteilung für Aquatische Ökologie in München für die gute Zusammenarbeit, die schöne Atmosphäre und den Spaß den wir die letzten Jahre zusammen hatten bedanken.

Ich danke auch allen Mitarbeitern und den Studenten des gesamten Lehrstuhls für Ökologie in München für die abteilungsübergreifende Hilfe und all die schöne Zeit die wir zusammen erlebt haben.

Vielen Dank auch an alle außerhalb der Uni München mit denen ich die letzten Jahre zusammenarbeiten durfte und an alle, die mir auf Kongressen, Workshops oder Sommer School gute Hinweise gaben. Vor allem danke ich natürlich meinen Koautoren von außerhalb Chris Klausmeier und Max Emans.

Zum Schluss möchte ich mich noch bei meiner Familie und meinen lieben Freunden (besonders bei Thomas Vonier für die Formatierung dieser Arbeit) bedanken, die mir eine gutes Umfeld boten und mir damit Kraft für meine Arbeit gaben.

Curriculum Vitae

Personal:

Name: Christoph Gerald Jäger
Date of birth: 28.12.1974, Munich, Germany
Marital status: single
Citizenship: German
Address: Guldeinstr. 40, 80339 Munich

School education:

September 1981-July 1985	Grundschule Kirchheim b. Munich
September 1985-July 1992	Gymnasium Kirchheim b. Munich
September 1992-July 1994	Ernst-Mach-Gymnasium Haar b. Munich
July 1994	Abitur

Civil Service

July 1994-September 1995	Civil Service (Zivildienst) at Blindeninstitutsstiftung in Munich
--------------------------	---

Professional education and experiences:

September 1995-July 1997
apprenticeship for landscape gardener (Gärtner der Fachrichtung Landschafts-, Garten- und Sportplatzbau) at Fa. May, Feldkirchen b. Munich

August 1997-September 1998
professional experience as landscape gardener at Fa. Schleizer, Munich, and at Baumschule Bösel, Munich

Academic education:

September 1998 - June 2004
studies in biology at Ludwigs-Maximilians-Universität Munich

Main subject:
ecology; minor subjects: systematic botany, geography, environmental management/nature conservation (Landnutzungsplanung/Naturschutz)

Diploma thesis:
The influence of mixing depth and mixing intensity on phytoplankton (translation of the German thesis title)

June 2004
Diploma in Biology

August 2004-present
PhD studies at Ludwigs-Maximilians-Universität Munich, Department Biology II, Aquatic Ecology, advisor: Prof. Dr. Sebastian Diehl

Publications:

- Berger, S. A., S. Diehl, H. Stibor, G. Trommer, M. Ruhlenstroth, A. Wild, A. Weigert, C. G. Jäger, and M. Striebel. 2007. Water temperature and mixing depth affect timing and magnitude of events during spring succession of the plankton. *Oecologia* 150: 643-654.
- Jäger, C. G., S. Diehl, C. Matauschek, C. A. Klausmeier, and H. Stibor. 2008. Transient dynamics of pelagic producer-grazer systems in a gradient of nutrients and mixing depths. *Ecology* (in press).
- Jäger, C. G., S. Diehl, G. M. Schmidt. Influence of water column depth and mixing intensity on phytoplankton biomass and functional community composition. *Limnology and Oceanography* (in revision).
- Jäger, C. G., S. Diehl, M. Emans. Physical determinants of phytoplankton production, algal stoichiometry, and vertical nutrient fluxes. Manuscript.